

306

TECHNICAL REPORT

BASIC RESEARCH IN AUTOMOBILE CRASHWORTHINESS— TESTING AND EVALUATION OF MODIFICATIONS FOR SIDE IMPACTS

By: Richard P. Mayor and Kenneth N. Naab

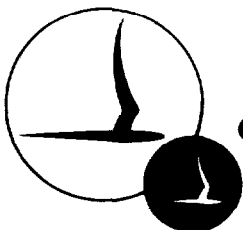
CAL No. YB-2684-V-3

Prepared For:

Department of Transportation
Federal Highway Administration
National Highway Safety Bureau
Washington, D. C. 20591

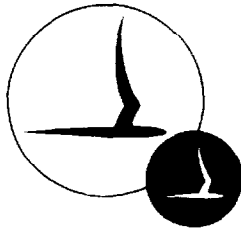
INTERIM TECHNICAL REPORT

Contract No. FH-11-6918
November 1969



CORNELL AERONAUTICAL LABORATORY, INC.

OF CORNELL UNIVERSITY, BUFFALO, N Y 14221



CORNELL AERONAUTICAL LABORATORY, INC.
4455 GENESEE STREET
BUFFALO, NEW YORK 14221
(716)-632-7500

INTERIM TECHNICAL REPORT
BASIC RESEARCH IN AUTOMOBILE CRASHWORTHINESS-
TESTING AND EVALUATION OF MODIFICATIONS FOR SIDE IMPACTS

By
RICHARD P. MAYOR
KENNETH N. NAAB
OF THE
TRANSPORTATION RESEARCH DEPARTMENT

CAL REPORT NO. YB-2684-V-3
CONTRACT NO. FH 11-6918

NOVEMBER 1969

Prepared for
DEPARTMENT OF TRANSPORTATION
FEDERAL HIGHWAY ADMINISTRATION
NATIONAL HIGHWAY SAFETY BUREAU
WASHINGTON D. C. 20591

FOREWORD

This report presents the results of the side impact studies as developed under the Basic Research in Crashworthiness Program. The objective of the overall program is to develop and test automobile structural configurations that will (1) reduce intrusions into the occupant compartment, (2) produce more nearly uniform crush characteristics, and (3) satisfy the strength and stiffness requirements of normal operating conditions. The results of the research will be used to explore the feasibility of an automobile crashworthiness standard to reduce penetration of the passenger compartment by outside objects and, at the same time, more efficiently utilize energy absorption principles.

The overall objectives are to be accomplished by making modifications on recent production automobiles. Three other concepts have been developed within the program. These are a forward structure modification, an engine deflection concept and a rear engine vehicle simulation.

The findings of the overall program are presented in the following series of reports:

"Basic Research in Automobile Crashworthiness - Testing and Evaluation of Forward Structure Modification Concept", CAL Report No. YB-2684-V-1;

"Basic Research in Automobile Crashworthiness - Testing and Evaluation of Engine Deflection Concept", CAL Report No. YB-2684-V-2,

"Basic Research in Automobile Crashworthiness - Testing and Evaluation of Modifications for Side Impacts", CAL Report No. YB-2684-V-3;

"Basic Research in Automobile Crashworthiness - Testing and Evaluation of Rear Engine Concept", CAL Report No. YB-2684-V-4;

"Basic Research in Automobile Crashworthiness -
Analytical Studies", CAL Report No. YB-2684-V-5;

"Basic Research in Automobile Crashworthiness -
Summary Report", CAL Report No. YB-2684-V-6.

The reported research was performed under Contract No. FH-11-6918 with the National Highway Safety Bureau, Federal Highway Administration, U. S. Department of Transportation. The opinions, findings and conclusions expressed in this report are those of the authors and not necessarily those of the National Highway Safety Bureau.

This report has been reviewed and is approved by:



Edwin A. Kidd, Head
Transportation Research Department

ACKNOWLEDGMENTS

The authors wish to acknowledge contributions of the following individuals, within CAL, to the research described in this report.

- Engineering Aspects
Dr. Patrick M. Miller and Mr. James E. Greene
- Vehicle Instrumentation and Testing
Messrs. James E. Greene, Norris E. Shoemaker,
Terry W. Reiman, Walter A. Stahl and Gerald Cory
- Photography
Messrs. Ralph L. Jones, Richard G. Matthies
and Raymond J. Kelly
- Data Reduction
Miss Barbara Coleman
- Vehicle Modification Design
Mr. Vincent F. Napierski
- Vehicle Fabrication and Construction
Members of the CAL Design and Shops Department,
especially Messrs. John Sadowski and Albert Benker

In addition, important suggestions were made by Mr. James E. Hofferberth, Contract Manager, National Highway Safety Bureau.

SUMMARY

The side structures of several frame-type automobiles were modified with the objective of achieving constant deceleration without excessive passenger compartment intrusion. A review of actual accident cases showed evidence of a lack of adequate door strength relative to the support posts; hence, the initial vehicle modification consisted of a strengthened door and related structure. Two other modified vehicles were tested which involved changes to the vehicle frame. Additional tests included an unmodified (base line) vehicle for comparison, a developmental vehicle for investigating the performance of a minor modification and to improve methods of data collection and interpretation, and a number of dynamic door and beam component tests.

All test vehicles were 1966 Fords impacted at a nominal velocity of 20 MPH into the CAL pole barrier -- a concrete filled, 12-3/4 O. D. pipe. The impact points were near the center line of the right front door.

Results of the tests showed the excessive compartment intrusion of present designs and demonstrated that improvement is possible with a moderate weight increase and without significantly higher peak decelerations. Additional side modifications are recommended which fully integrate the door reinforcing and frame modification concepts that were investigated in this study.

Appendices describe: (1) tests on a latch mechanism to permit strengthening of the door without interfering with its functional operations, and (2) a comparative study of the effects of accelerometer location and filtering.

TABLE OF CONTENTS

	<u>Page No.</u>
FOREWORD	11
ACKNOWLEDGMENTS	1v
SUMMARY	v
LIST OF FIGURES	viii
LIST OF TABLES	xiii
1. INTRODUCTION	1
2. CONCLUSIONS AND RECOMMENDATIONS	3
2.1 Conclusions	3
2.2 Recommendations	4
3. PRELIMINARY STUDY	6
4. TEST CONDITIONS	10
4.1 Impact Point	10
4.2 Impact Velocity	11
4.3 Pole vs. Car-to-Car	11
5. PERFORMANCE OF BASE LINE VEHICLE	12
5.1 Base Line No. 3 Crash Test	12
5.2 Test Results	12
6. DESIGN OBJECTIVES AND CONCEPTS	20
6.1 Design of Door Reinforcement (Mod. 3)	21
6.2 Design of Frame Structure (Mod. 3A)	25
7. MOD. 3 VEHICLE	29
7.1 Design Details	29
7.2 Test Results	34
7.3 Evaluation of Performance	41
8. D-2 DEVELOPMENTAL VEHICLE	45
8.1 Objectives	45
8.2 Test Results	45
8.3 Evaluation of Performance	55

TABLE OF CONTENTS (CONTINUED)

	<u>Page No.</u>
9. MOD. 3A(1) VEHICLE	60
9.1 Design Details	60
9.2 Test Results	64
9.3 Evaluation of Performance	70
10. MOD. 3A(2) VEHICLE	83
10.1 Design Changes Based on Mod. 3A(1) Results	83
10.2 Test Results	85
10.3 Evaluation of Performance	92
11. DISCUSSION OF RESULTS	101
12. REFERENCES	107
APPENDIX A: LATCH MECHANISM TEST	A-1
APPENDIX B: EVALUATION OF MULTIPLE DATA SENSORS	B-1
APPENDIX C: SUMMARIES OF TEST DATA AND RELATED INFORMATION	C-1

LIST OF FIGURES

<u>Figure No.</u>	<u>Description</u>	<u>Page No.</u>
3-1	Side Impacts Illustrating Relative Door and Door Post Damage	7
3-2	Side Impacts Illustrating Penetration in Pole Impacts	8
5-1	Base Line Test No. 3: Vehicle Acceleration Data	13
5-2	Base Line Test No. 3: Driver's Seat, Sideward Accelerometer Data	15
5-3	Base Line 3: Driver's Seat Acceleration vs. Displacement	16
5-4	Base Line Test No. 3: Side Pole Impact	17
5-5	Post Crash Profile of Base Line 3	19
6-1	Behavior of Simplified Base Line Structure	22
6-2	Behavior of Simplified Mod. 3 Structure	23
6-3	Effect of Support Restraint	24
6-4	Effect of Local Instability on Energy Absorption: I-Beam vs. Square Tube	26
6-5	Structural Configuration: Mod. 3A(1)	28
7-1	Hat Sections Prior to Installation	30
7-2	Hat Sections in Place on Mod. 3	30
7-3	Cross Section of Typical Hat	31
7-4	Clip Angle at "B" Post	32
7-5	Clip Angle at "A" Post	32
7-6	Strut Joining "B" Posts	33
7-7	Rods to Simulate Rear Door	33

LIST OF FIGURES (CONTINUED)

<u>Figure No.</u>	<u>Description</u>	<u>Page No.</u>
7-8	Mod. 3 Test: Vehicle Acceleration Data	35
7-9	Mod. 3 Test: Driver's Seat, Sideward Accelerometer Data	37
7-10	Compartment Reinforcing Strut Compressive Load	38
7-11	Mod. 3 Test, Side Pole Impact	39
7-12	Post Crash Profile of Side Impact Tests	40
7-13	Modified Door After Impact	42
7-14	Comparison of Mod. 3 and Base Line 3 Filtered Decelerations	43
8-1	D-2 Test: Vehicle Acceleration Data	47
8-2	D-2 Test: Driver's Seat, Sideward Accelerometer Data	48
8-3	Filtered (50 Hz) Acceleration Data, D-2 Test	50
8-4	Axial Load in Strut Between "B" Posts	51
8-5	Impact Pole Total Loads	52
8-6	Post-Crash Profile of D-2	53
8-7	D-2 Test, Side Impact with Pole	54
8-8	Post-Crash Profile of Side Impact Tests	56
8-9	Driver's Seat, Filtered Sideward Acceleration Data	57
8-10	Axial Force in Transverse Struts	58
9-1	Assumed Vertical Distribution of Pole Force	61
9-2	Forward and Rear Knees	62
9-3	Detail at "A" Post	63

LIST OF FIGURES (CONTINUED)

<u>Figure No.</u>	<u>Description</u>	<u>Page No.</u>
9-4	Modified Frame	63
9-5	Mod. 3A(1) Test: Vehicle Acceleration Data	65
9-6	Mod. 3A(1) Test: Driver's Seat Accelerometer Data	67
9-7	Mod. 3A(1): Driver's Seat Acceleration vs. Displacement	68
9-8	Impact Pole Loads	69
9-9	Post-Crash Profile of Mod. 3A(1)	71
9-10	Mod. 3A(1): Side Impact with Pole	72
9-11	Post-Crash Profile of Side Impact Tests	73
9-12	Comparison of Compartment Damage	75
9-13	Side Impacts: Comparison of Pole Forces	76
9-14	Comparison of Frame Acceleration (Nonimpact Side) 25 Hz Filter	77
9-15	Frame Damage - Overall	79
9-16	Deformed Shape of I-Beam Knee Stiffened with Web Plates	79
9-17	Frame Damage	80
9-18	Roll Bar After Impact	81
10-1	Horizontal Section Through Door	84
10-2	B-Post/Door Beam Detail	84
10-3	Mod. 3A(2) Test: Vehicle Acceleration Data	86
10-4	Mod. 3A(2) Test: Driver's Seat Accelerometer Data	88
10-5	Mod. 3A(2): Driver's Seat Acceleration vs. Displacement	89

LIST OF FIGURES (CONTINUED)

<u>Figure No.</u>	<u>Description</u>	<u>Page No.</u>
10-6	Impact Pole Loads	90
10-7	Top Profile Comparison of Mod. 3A(2) and Standard Vehicle	91
10-8	Mod. 3A(1), Side Impact with Pole	93
10-9	Post-Crash Profile of Side Impact Tests	94
10-10	Side Impact: Comparison of Pole Forces	96
10-11	Comparison of Passenger Compartment Accelerations, 25 Hz Filter	97
10-12	Mod. 3A(2): Frame Damage	98
10-13	Mod. 3A(2): Interior Damage	99
11-1	Comparison of Deceleration Responses with Idealized Waveform	104
A-1	Door Drop Test No. 1	A-3
A-2	Latching Device Test No. 1	A-5
A-3	Latching Device Test No. 2	A-6
A-4	Modified Door Impact Test	A-7
A-5	Dynamic Load-Deflection Behavior of Test No. 2 Door	A-9
B-1	Comparison of Acceleration Derived from Load Cell (Force) Data with Floorpan Accelerometer for Various Filters	B-3
B-2	Comparison of Acceleration Derived from Load Cell (Force) Data with Frame Accelerometer for Various Filters	B-4
B-3	Comparison of Acceleration Derived from Load Cell (Force) Data with B-Post Accelerometer for Various Filters	B-5

LIST OF FIGURES (CONTINUED)

<u>Figure No.</u>	<u>Description</u>	<u>Page No.</u>
B-4	Comparison of Acceleration Derived from Load Cell (Force) Data with Accelerometers Filtered at <u>25 Hz Cutoff</u>	B-8
B-5	Comparison of Acceleration Derived from Load Cell (Force) Data with Accelerometers Filtered at <u>10 Hz Cutoff</u>	B-10
B-6	Relative Displacement Between Frame and B-Post from Accelerometer Data	B-11

LIST OF TABLES

<u>Table No.</u>	<u>Description</u>	<u>Page No.</u>
11-1	Summary of Side Impact Test Results	102
B-1	Comparison of Peak g's Load Cell Data vs. Accelerometers at Various Locations with Various Filters	B-7

1. INTRODUCTION

The objective of modifying the side structure of a vehicle has been to obtain a uniform deceleration response in a collision without unacceptable intrusion into the passenger compartment. Permanent deformation, since all test vehicles were impacted against a rigid obstacle, is not undesirable per se, but the effectiveness of any modification requires that the deformation that does occur be used as efficiently as possible to limit the peak compartment deceleration. Passenger compartment intrusion is inherently bad since it can contribute to injuries in side collisions.

The underlying purpose of this research has been to explore the feasibility of reducing injuries and fatalities in lateral collisions. The relationship between those quantities such as deceleration, crush, etc., which can be directly measured during a crash test and the corresponding injury potential of the collision is tenuous and complex. Seating position, restraint devices and human tolerance data are all important variables. Such considerations, however, are not within the scope of this present study which primarily deals with vehicle structure. Some of these aspects of the overall problem were explored in a simplified computer study of car-to-car side collision, Reference 1.

Some differences between modifications to improve behavior in side collisions and those for frontal impacts should be noted. Passenger compartment intrusion is much more of a problem in side collisions; only a small space is available to protect the occupant on the impact side from the impacted object, and intrusion occurs in all but very low speed collisions. The limited space and the intrinsic weakness of conventional side structures of vehicles severely limit the modifications that can be considered.

This report presents the test results of two vehicle modifications for improved performance in lateral impacts -- one involving changes to the door and related structure using light gauge sheet metal and the second involving changes to the frame using structural I-beams and tubes. Also presented are results of a base line (unmodified) impact and a developmental crash test, the conclusions drawn from comparing the base line and modified vehicle tests, and results of component tests on doors.

2. CONCLUSIONS AND RECOMMENDATIONS

2.1 Conclusions

2.1.1 Present automotive design practice permits excessive passenger compartment intrusion in side impacts with narrow, fixed objects at low impact velocity. For a 20 MPH side collision into a fixed pole, permanent external penetration for a conventional (base line) vehicle was 24 inches. The roof, door, and floor structures offer inadequate resistance to side intrusions.

2.1.2 Discernable improvement in structural crashworthiness over a base line (unmodified) vehicle has been demonstrated with vehicle concepts involving modifications for side impact protection. Specifically, these design concepts were (1) a modified side structure incorporating door beams and (2) a more extensive modification including structural changes to both the vehicle frame and passenger compartment. Full-scale crash tests were performed which simulated a side collision into a fixed pole at 20 MPH.

2.1.3 For a moderate weight increase (approximately 20 pounds per door), intrusion resistance can be improved in side impacts at a door opening without causing significantly higher peak acceleration. This conclusion is based on the performance of the "Mod. 3" vehicle, which included door beams and a number of relatively minor design changes to the passenger compartment structure. Such an approach can improve performance somewhat by increasing lateral loads early in the collision. However, marked improvement in occupant protection in side impacts with fixed objects will require more extensive structural modification of present automobiles, including more substantial frame structures.

2.1.4 A structural concept combining modifications to the vehicle frame and passenger compartment showed significant improvement over the performance of the base line (unmodified) vehicle. This conclusion is based

on the performance of the "Mod. 3A(2)" vehicle, for which deformation of the side structure was substantially reduced in a nominal 20 MPH pole collision and the acceleration waveform was more uniform and closer to a 20 g mean value. Additional crashworthiness improvement is believed to be possible through further frame modification and a more complete integration of passenger compartment modification with existing vehicle structure.

2.1.5 Because of the limited acceptable crush distance available in side impacts, it is essential that substantial loads be developed as early as possible. This can be accomplished by the addition of structural members at the periphery of a vehicle, or by methods of transferring impact load to frame members. However, an effective structural design must also limit collapse loads to avoid unacceptably high accelerations which might cancel out any structural improvement in crashworthiness due to reduced intrusion. A uniform compartment acceleration response in the neighborhood of 20 g's appears to be a reasonable design goal for side impact performance.

2.2 Recommendations

2.2.1 Additional side structure modifications, aimed at more fully achieving the goals of this research, should be developed and tested. A combination of the passenger compartment and frame modifications already tested is suggested as a first step. Further modifications should more fully integrate added structural components with existing vehicle structure in order to demonstrate design practicability and limit weight increase.

2.2.2 Evaluation of side structure modifications in car-to-car impacts is recommended. In the present research program, side impact tests have been exclusively performed against a narrow, fixed object (stationary pole). This is believed to constitute a most stringent impact condition as well as being quite representative of real-world single vehicle

accident exposure. However, the implications of car-to-car side impact performance between conventional and modified vehicles should also be explored. This should include evaluating the effect of modifying the front structure of an impacting vehicle on the performance of conventional and modified side structure.

2.2.3 Side impact tests of structurally modified vehicles at an impact speed greater than 20 MPH are recommended. Test results indicate that higher speed tests would more dramatically demonstrate improvement in structural performance of modified vehicles in side impacts with fixed objects when compared with unmodified vehicle performance.

2.2.4 Rollover testing of vehicles with modified side structures is recommended. Results of the present program indicate that a roll bar structure designed to transfer load to the opposite side and to dissipate energy through controlled collapse is an attractive component for improving side impact structural performance. A roll-bar structure, as well as other side structure modifications, can likely be beneficial for improving crashworthiness in both side impact and rollover-type accidents. This dual-feature potential of side structure designs should be explored further.

2.2.5 The development and testing of a vehicle frame structure for providing effective collapse in both frontal and side impacts is recommended. It is believed that frame cross members which can be effectively utilized for transferring load and dissipating energy in side collisions could be integrated with a front structure designed to control collapse in frontal impacts.

3. PRELIMINARY STUDY

A survey of typical ACIR* cases involving lateral impacts with poles was undertaken. Subject to the limitations of dependence on photographs for information, the following conclusions pertinent to possible structural improvements were made.

- The strength of the door panel is incompatible with the strength of the supporting posts. Evidence for this observation lies in the many accidents where the impacted door is severely damaged with little apparent damage of the side post or the nonimpacted door. Figure 3-1 shows an accident illustrating this point.
- A preponderance of injuries can be ascribed to low intrusion resistance of the structure rather than high acceleration levels. The injuries include a large number in the pelvic region; head injuries are also common. Similar injury patterns were uncovered by States and States (Reference 2). Figure 3-2 illustrates penetration patterns in pole impacts.

Automotive Crash Injury Research program of Cornell Aeronautical Laboratory, Inc.

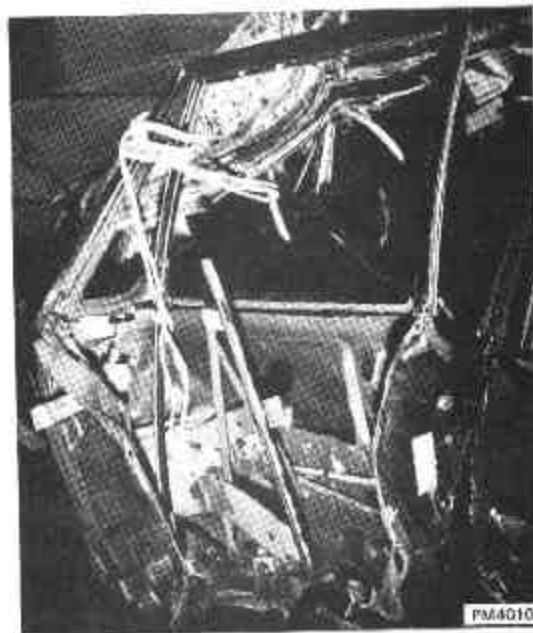


Figure 3-1 SIDE IMPACT ILLUSTRATING RELATIVE
DOOR AND DOOR POST DAMAGE



Figure 3-2 SIDE IMPACTS ILLUSTRATING PENETRATION
IN POLE IMPACTS

In addition to injury patterns, States and States present some conclusions on behavior of different vehicle structures, based on their clinical study of 48 lateral impact accidents. Those relevant to this study are:

- At present (1968), doors are sheet metal structures which collapse with little energy absorption. The door was the single structure most commonly causing injury.
- Chassis frame structure must be coordinated with door design. The introduction of perimeter frames, beginning in 1965, has been a major improvement.
- Some unit body frame vehicles are particularly vulnerable in side impact accidents.
- Door pillar (B-post) construction and anchorage is essential to prevent penetration of impacting vehicles which override the frame and floorpan of struck vehicles. Hard top models are particularly vulnerable. B-pillar anchorages in sedans of conventional construction may shear off at the floor level, in spite of their roof anchorage.

4. TEST CONDITIONS

Detailed information for each of the five side collisions that have been conducted is presented in subsequent sections of this report. The purpose here is to give the general conditions for all tests.

- All test vehicles were either unmodified (base line) or modified 1966 four-door Fords.
- Nominal impact velocity was 20 MPH.
- The impacted object was a 12-3/4 in. O. D., 1 inch wall thickness, concrete filled pipe.
- Nominal impact point was the center line of the front door, for all vehicles, this was very close to the longitudinal center of mass.
- Test vehicles were supported on casters attached to the frame. Impact velocity was achieved by towing with another vehicle.

The reasoning leading to these test conditions is discussed below.

4.1 Impact Point

Although actual side collisions frequently result in rotation, impact at or near the center of gravity is more severe in terms of vehicle damage. In terms of occupant injury a collision in which rotation of the vehicle occurs may result in more injury due to increased relative occupant-vehicle velocity in the second collision. Because this effect would be difficult to control and because it would obscure interpretation of purely structural behavior, it was decided to limit rotation by impacting as near to the center of gravity as possible.

4.2 Impact Velocity

The thickness of the Ford door (typical of standard American cars) is 12 inches at its widest point. Because of finite rise and decay times and the volume of crushed material, it is not possible to use the full 12 inches for constant force behavior. Using a typical efficiency of 60 percent (7.2 inches) it can be calculated that impacts with rigid objects can be sustained to 19 MPH without exceeding 20 g's. The velocity was rounded to 20 MPH, which was the nominal velocity for all side tests.

4.3 Pole vs. Car-to-Car

Although car-to-car side collisions are more common than those with fixed objects, all side test vehicles were impacted against a rigid pole. This test condition is particularly severe since a pole is usually non-deformable and all the energy must be absorbed by the impacting vehicle (see Figure 3-2). In a car-to-car side collision, however, residual motion of the colliding vehicles and sharing of deformation reduces the energy to be absorbed by the impacted vehicle. Furthermore, a pole impact generally results in a more concentrated loading than an intersection-type car-to-car collision.

Other reasons for choosing a pole impact configuration concern actual testing. For example, collision with a fixed object simplifies camera coverage, specifically, the underside camera can be used to observe frame deformation during impact. Also, a pole can easily be instrumented with load cells to obtain impact force data. In addition, if many tests are to be performed, the pole impact test is probably more economical than car-to-car testing since only half as many vehicles are required. Repeatability may also be more of a problem in large scale car-to-car testing since identical impacting vehicles would be required for convincing comparisons of impacted vehicle performance.

5. PERFORMANCE OF BASE LINE VEHICLE

5.1 Base Line No. 3 Crash Test

The purpose of the base line test was (1) to provide data for use in the design of the modified vehicles and (2) to provide a performance base for comparisons with the results of the modified vehicle tests. The base line test is particularly necessary for a lateral pole impact because no other source of data is available. As is explained in Section 8, the D-2 developmental vehicle involved only a very minor structural change. Since D-2 had more instrumentation than the base line vehicle, for some comparisons it is convenient to treat D-2 as a de facto base line test.

5.2 Test Results

The base line vehicle was crashed into the CAL pole barrier at a speed of approximately 21.5 MPH at a point about 6 inches aft of the right front door center. A summary of test conditions and related data is contained in Appendix C.

Driver's seat accelerations for the side (toward pole) and vertical directions are shown in Figure 5-1. The side trace has a maximum of 35 g's at .054 seconds, but this peak is not significant as far as a passenger is concerned due to its duration of only approximately .003 seconds. The significant peak of 25 g's occurred at .026 seconds. Similarly, for the vertical accelerations, the most important peak was 30 g's (upward) occurring at .034 seconds.

Based on trip switch data (+0.5 MPH estimated accuracy).

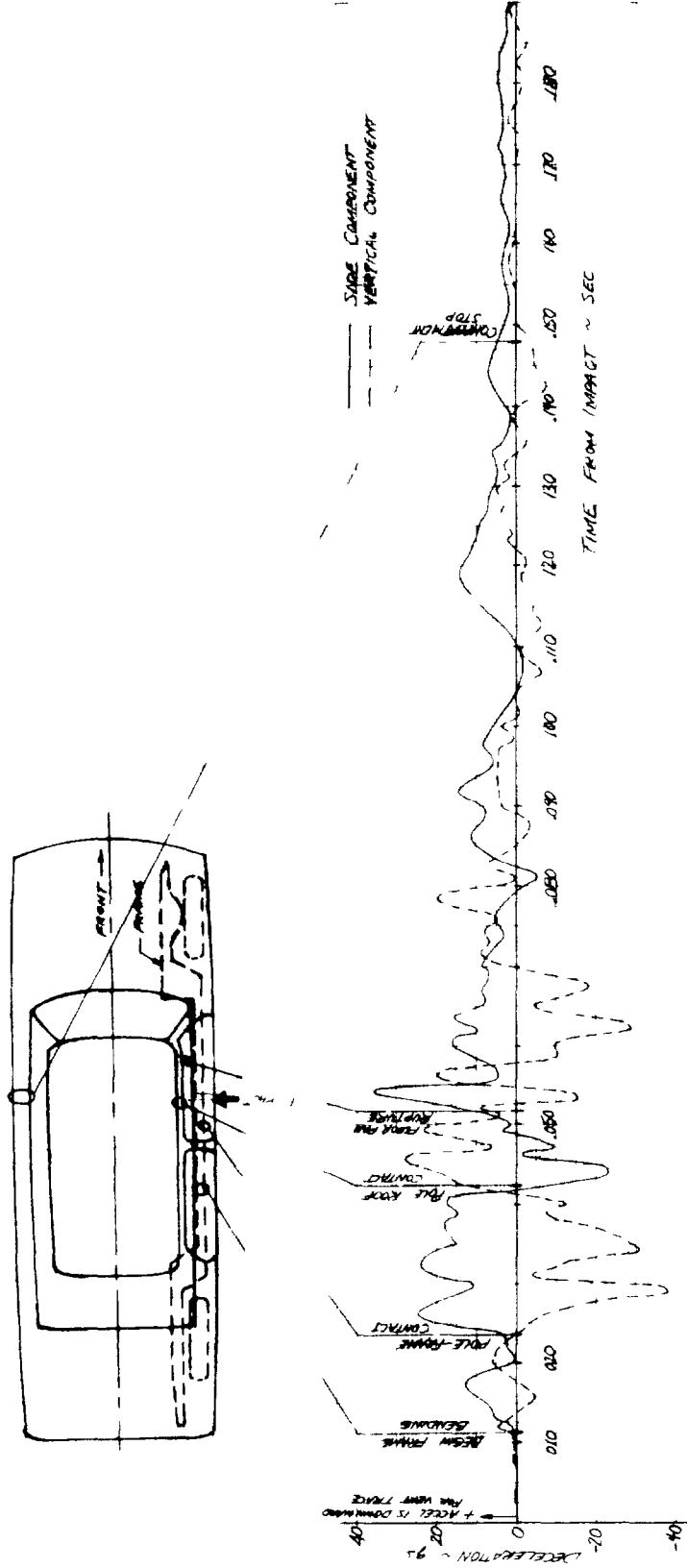


Figure 5-1 BASE LINE TEST NO. 3: VEHICLE ACCELERATION DATA

Driver's seat side acceleration data are replotted in Figure 5-2 along with a filtered version of the same trace. The filter has a cutoff frequency of 50 Hz and a roll-off frequency of 100 Hz. The filtered side accelerations showed a maximum of 20 g's at .036 seconds compared to the unfiltered maximum of 25 g's. In addition to the acceleration data in Figure 5-2, a velocity curve is shown, which was obtained by direct integration of the acceleration data. A graph of filtered acceleration of the floorpan at the driver's location versus computed displacement is shown in Figure 5-3. Acceleration of the vehicle in the fore-aft direction (longitudinal) showed no significant data and is not presented.

Sensor data from the package mounted on the drive shaft hump contained extraneous accelerations due to floorpan buckling and tilting during pole penetration. These data are less accurate than the driver location data and, hence, are not presented.

Photographs of the test vehicle after the collision are presented in Figure 5-4. Figures 5-4(c) and 5-4(d) show the upward displacement of the floorpan in the front and rear compartment areas and the fairly large bend in the front bench seat. Measured permanent deformation was approximately 24 inches.

The timing of specific events during the crash, relative to initial pole contact, was obtained from the film data and applied to Figure 5-1 along with a sketch of the vehicle. Contact of the pole with the main side frame was noted to occur at approximately .024 seconds.

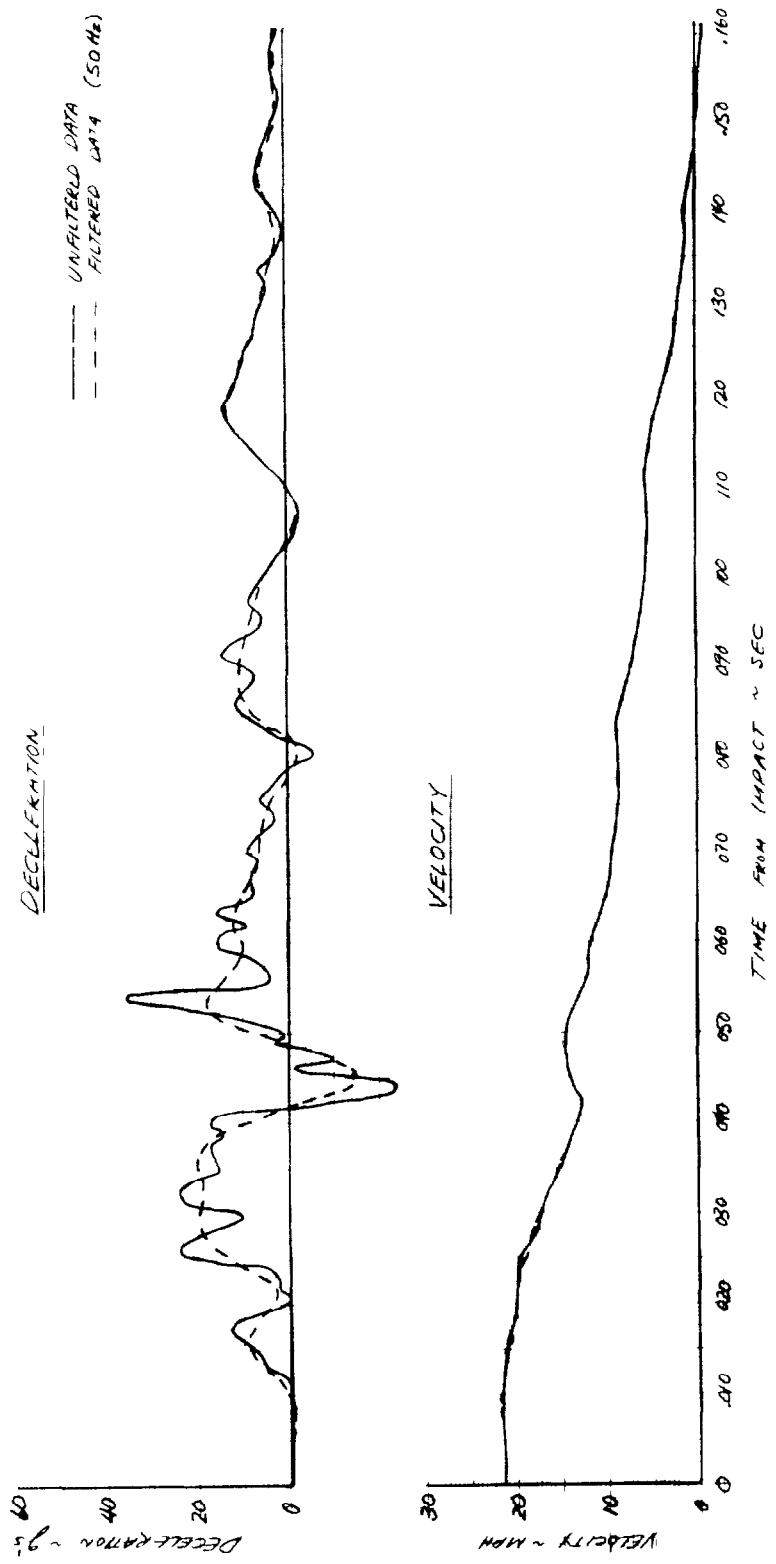


Figure 5-2 BASE LINE TEST NO. 3: DRIVER'S SEAT, SIDEWARD ACCELEROMETER DATA

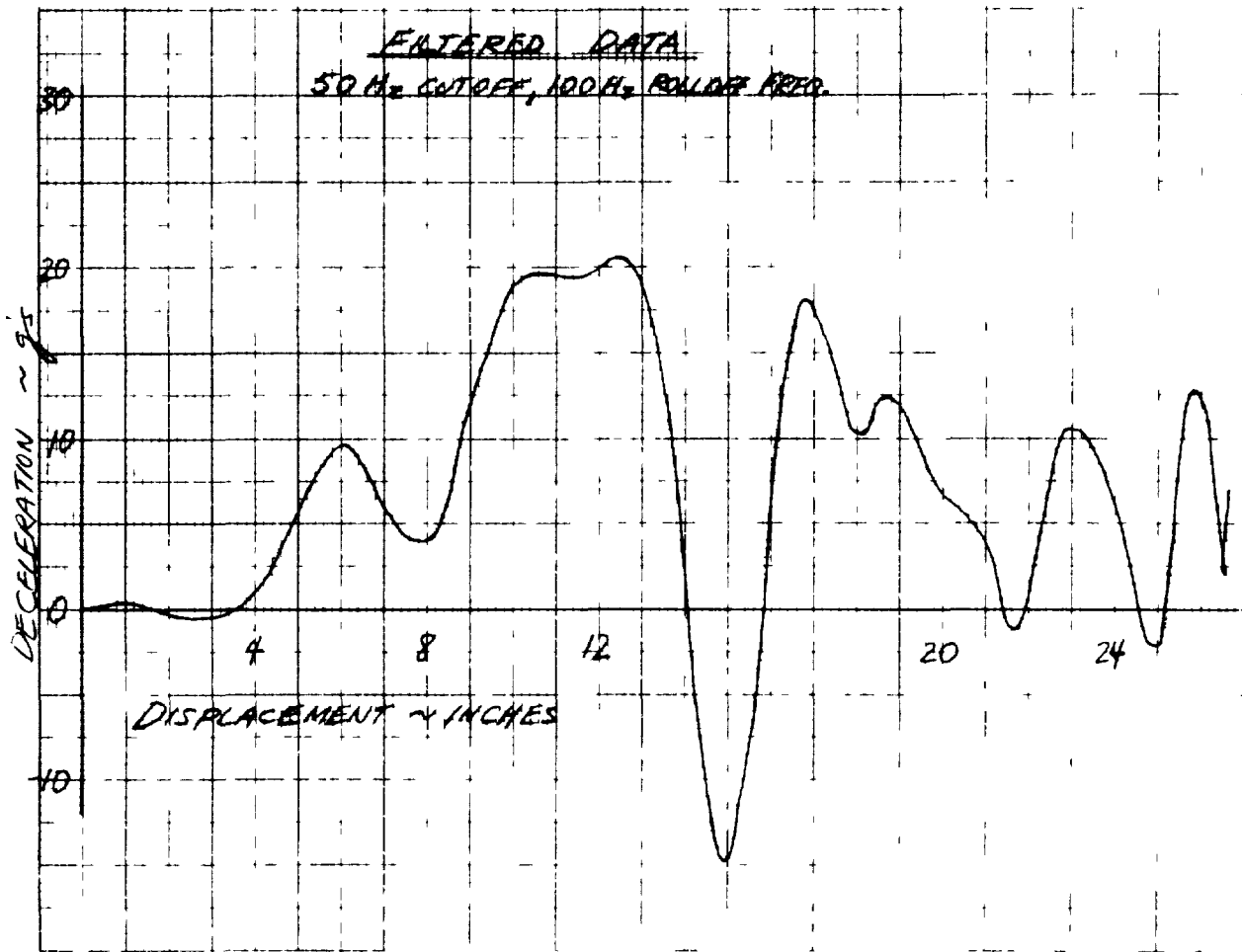
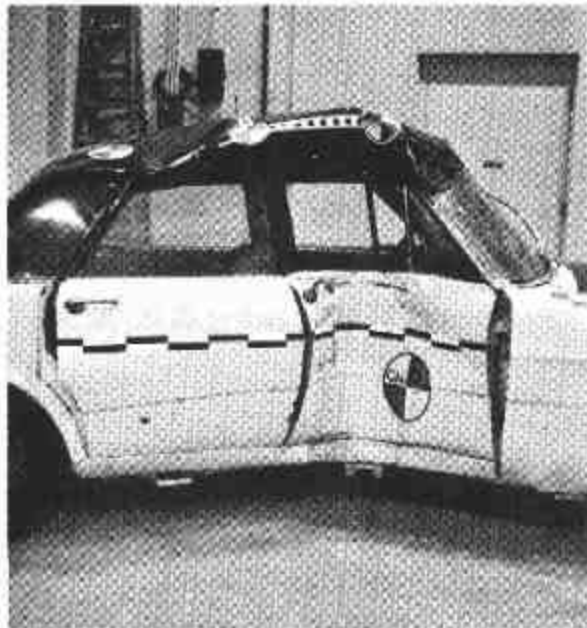
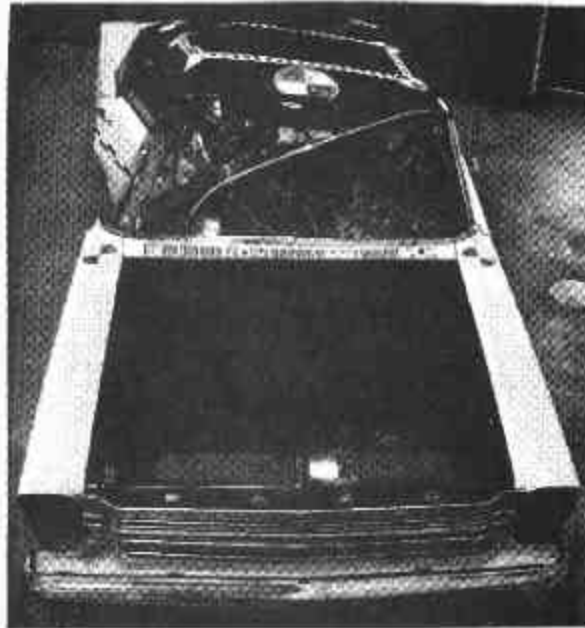


Figure 5-3 BASE LINE 3: DRIVER'S SEAT ACCELERATION VS. DISPLACEMENT



(A)



(B)



(C)



(D)

Figure 5-4 BASE LINE TEST No. 3: SIDE POLE IMPACT

The vehicle deformation and the external shape of the car were determined by measuring around the total periphery of the vehicle at a distance approximately 28 inches above the ground. These data are plotted to scale along with a standard car profile in Figure 5-5. An overall measure of vehicle structural rigidity and impact severity can be obtained from this type of comparison. Note the total body bending tendency.

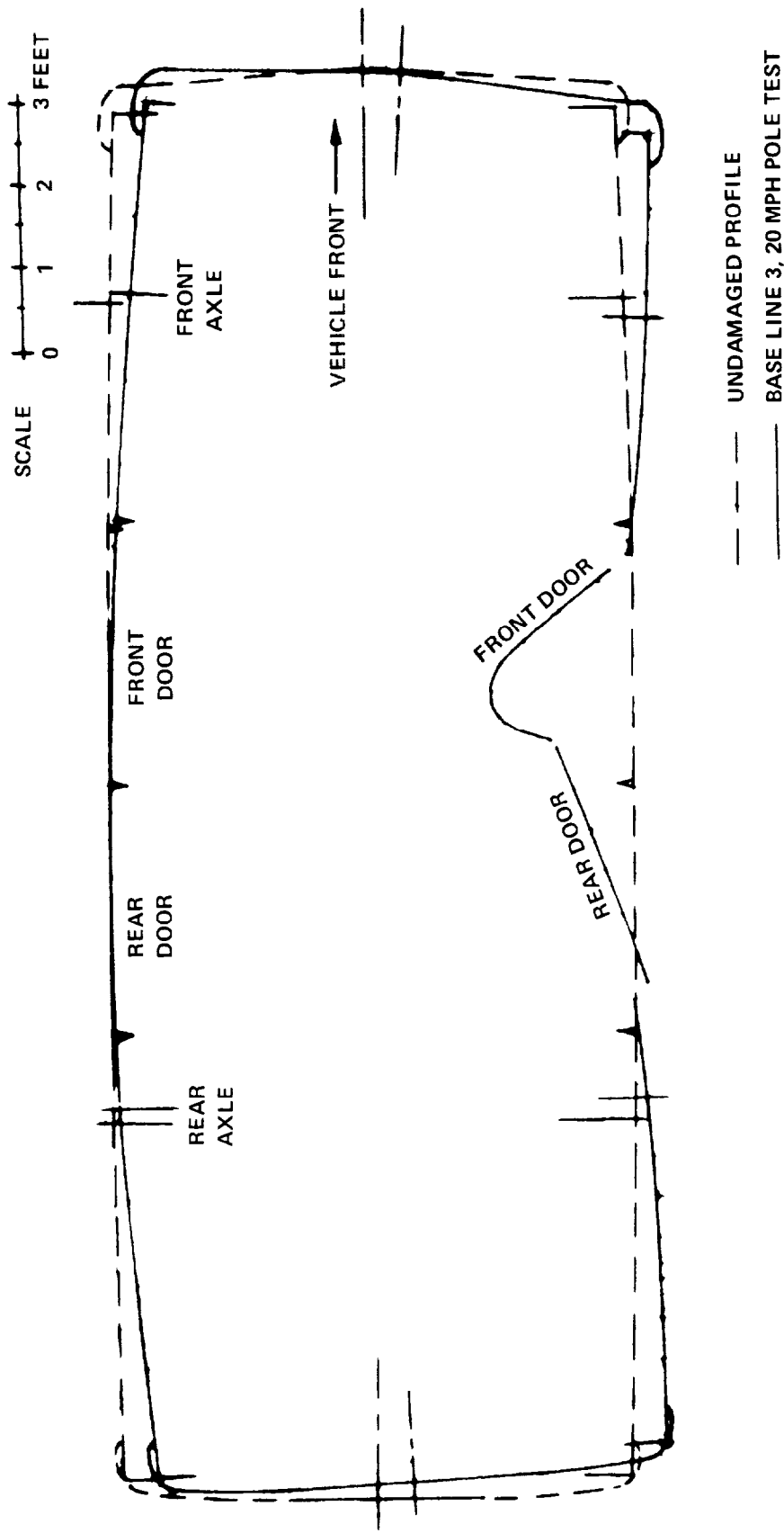


Figure 5-5 POST CRASH PROFILE OF BASE LINE 3

6. DESIGN OBJECTIVES AND CONCEPTS

The objectives of this research imposed limitations on the design and the extent to which the vehicles were modified. Since ultimate production cost was a consideration, automotive grade steel was considered for material where possible, and welding was the method of fabrication. An additional design condition was that the added structural members stay within the envelope of the original vehicle; this minimized changes to the appearance of the vehicle and limited a source of variation in the testing program.

Minimum weight of added structure was also a design criteria because weight is directly related to ultimate cost, vehicle performance and handling quality. Modifying existing vehicles has the effect of adding more weight than that which would be required if the modification were incorporated into the design of the vehicle from the beginning. This occurs because in construction of the modified vehicle it is frequently easier to parallel existing structure instead of attempting to integrate modifications.

All test vehicles were four-door 1966 Fords of typical frame-and-body construction. Four-door vehicles were chosen because it appeared more difficult to improve protection in side impacts and because modifications could be adapted to two-door cars.

Vehicle design for side impact protection can be separated into two distinct, but complementary, phases. These are (1) reinforcement of doors and adjacent supporting structure (primarily the A- and B-posts) to resist penetration and (2) strengthening the perimeter frame structure for improved load distribution and energy absorption capability. The latter area includes cross members between B-posts which, if located at roof level, also serve as added rollover protection. The objective of a design which incorporates both of these structural modifications is to reduce compartment intrusion in side impacts and, at the same time, limit compartment accelerations to acceptable levels (say 20 g's) by efficient use of collapse distance.

General structural concepts for each of these design phases are presented below. Specific design details are discussed in each of the sections which are mainly devoted to test results and evaluation of particular modified vehicles. The Mod. 3 vehicle addresses the door reinforcement problem. Improvement of frame structure is the primary design objective of the Mod. 3A sister vehicles, i.e., Mod. 3A(1) and Mod. 3A(2). A developmental test (designated D-2) was performed in order to assist in evaluating the Mod. 3 structural performance and to improve methods of data collection and interpretation.

6.1 Design of Door Reinforcement (Mod. 3)

The objective of Mod. 3 is to use the door as a beam, thus transferring load to the "A" and "B" posts. Figures 6-1 and 6-2 are simplified graphical comparisons of the base line structure and the associated deformation pattern with the modified structure and its anticipated deformation pattern.

A further objective is to obtain a cable-type action of the strengthened door as deflections increase in order to limit intrusion into the passenger compartment. The experimental and theoretical basis for the cable action is given in Appendix A, which describes tests of the strengthened door. Figure 6-3 shows that the cable action is dependent on the stiffness of the end restraints (i.e., the rigidity of the "A" and "B" posts).

A practicable and effective design should have the following features:

1. minimal weight increase,
2. no interference with window or locking mechanism,
3. limitation of penetration in side impacts where intrusion is often a source of injury,

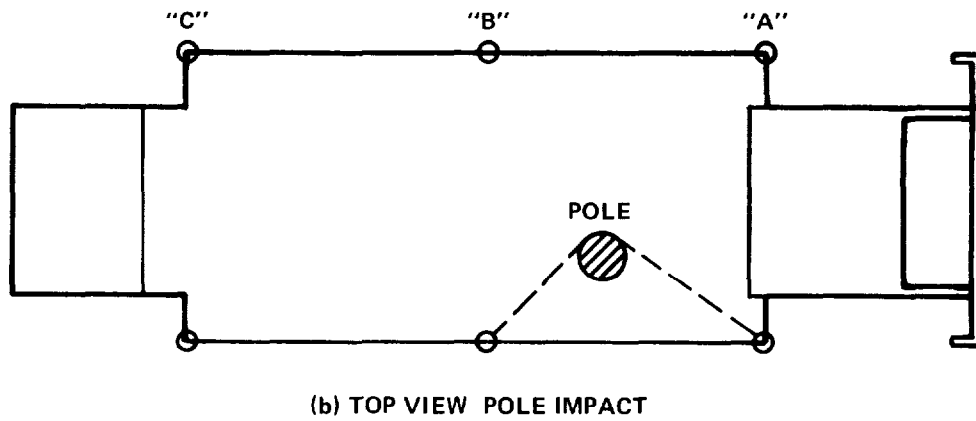
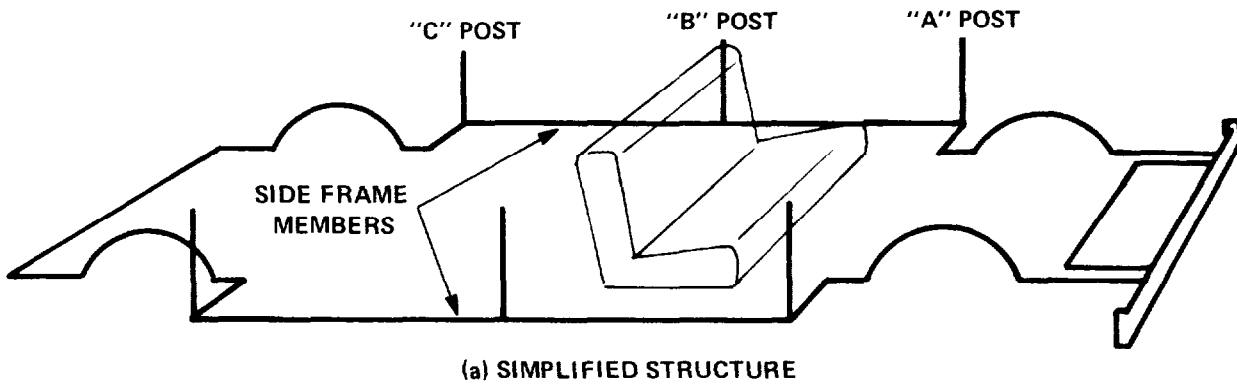
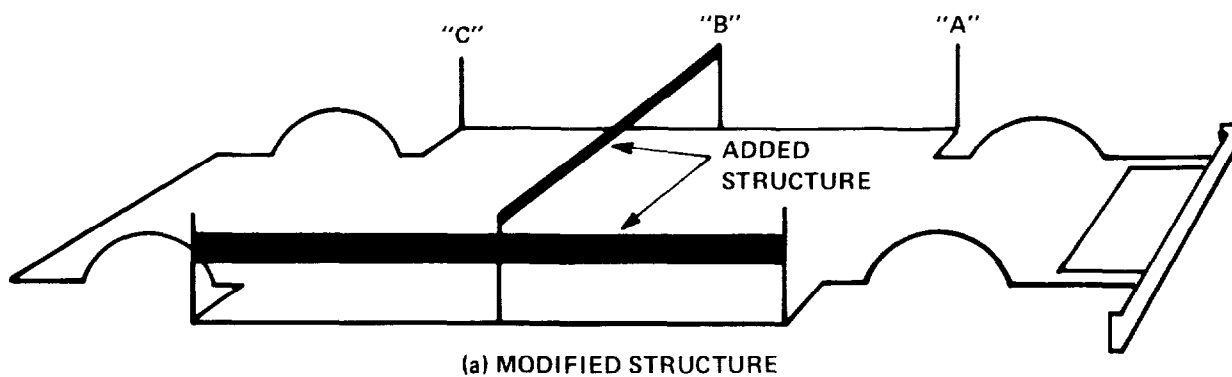
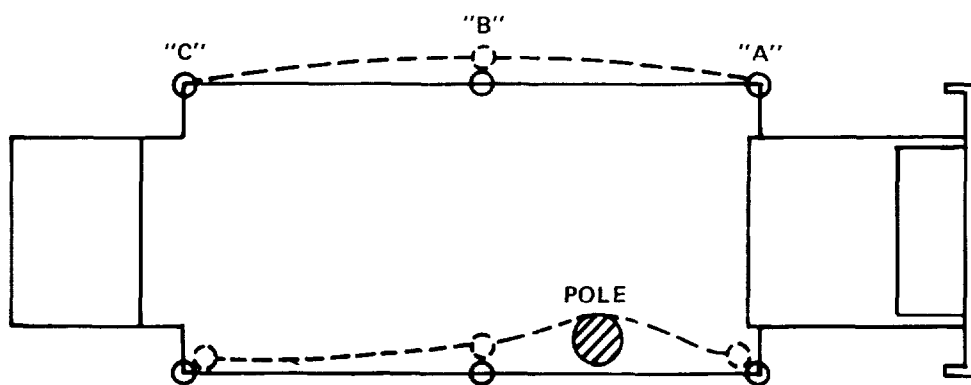


Figure 6-1 BEHAVIOR OF SIMPLIFIED BASE LINE STRUCTURE

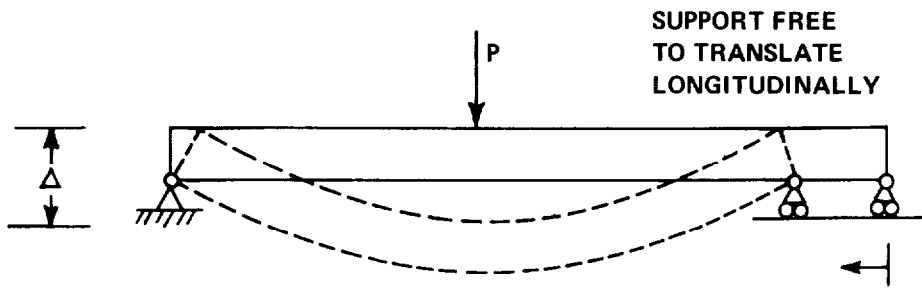


(a) MODIFIED STRUCTURE

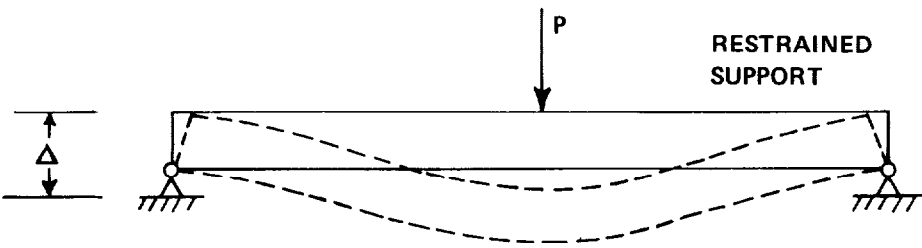


(b) TOP VIEW POLE IMPACT

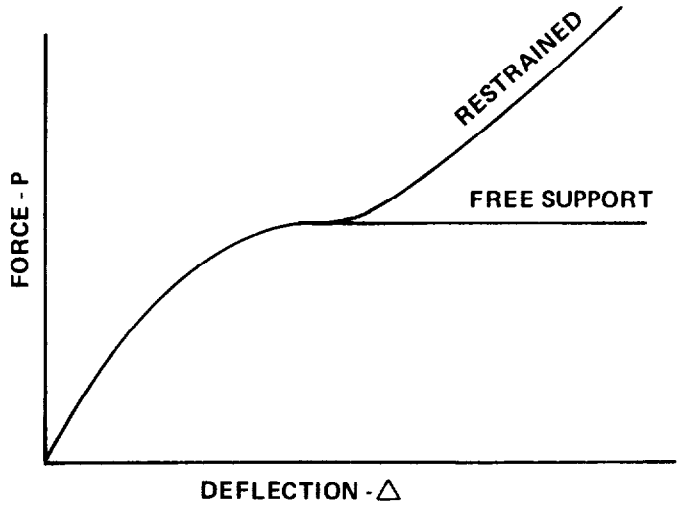
Figure 6-2 BEHAVIOR OF SIMPLIFIED MOD. 3 STRUCTURE



(a) BEAM WITHOUT END RESTRAINT



(b) CABLE ACTION. BEAM WITH RESTRAINED ENDS.



(c) EXPECTED FORCE-DEFLECTION CURVE

Figure 6-3 EFFECT OF SUPPORT RESTRAINT

4. uniform passenger compartment deceleration response of about 20 g's,
5. cable action between "A" and "B" posts after large deflections have occurred.

6.2 Design of Frame Structure (Mod. 3A)

Figure 6-4 compares normalized force-deflection curves of knee struts fabricated with a square tube and an I-beam, where web instability of the I-beam has been prevented by the addition of side plates. Since absorbed energy is equal to the area under the force-deflection curve, it is apparent that the performance of the stiffened I-beam is close to the maximum expectation. The square tube is shown for contrast since no convenient way has been devised to prevent buckling (i.e., local instability) of the side walls and the force-deflection curve is characteristic of this failure mode. The primary design objective was to incorporate the nearly ideal behavior of the I-beam into the vehicle frame to produce a reasonably uniform passenger compartment deceleration of about 20 g's.

The base line side test showed that deformation associated with a lateral pole impact is highly localized at the impact point. Since this is inefficient in terms of energy absorption, an additional objective of the design is to distribute the load to increase the participation of the structure away from the impact point, in particular, the nonimpact side and the heavy members in the vicinity of the engine.

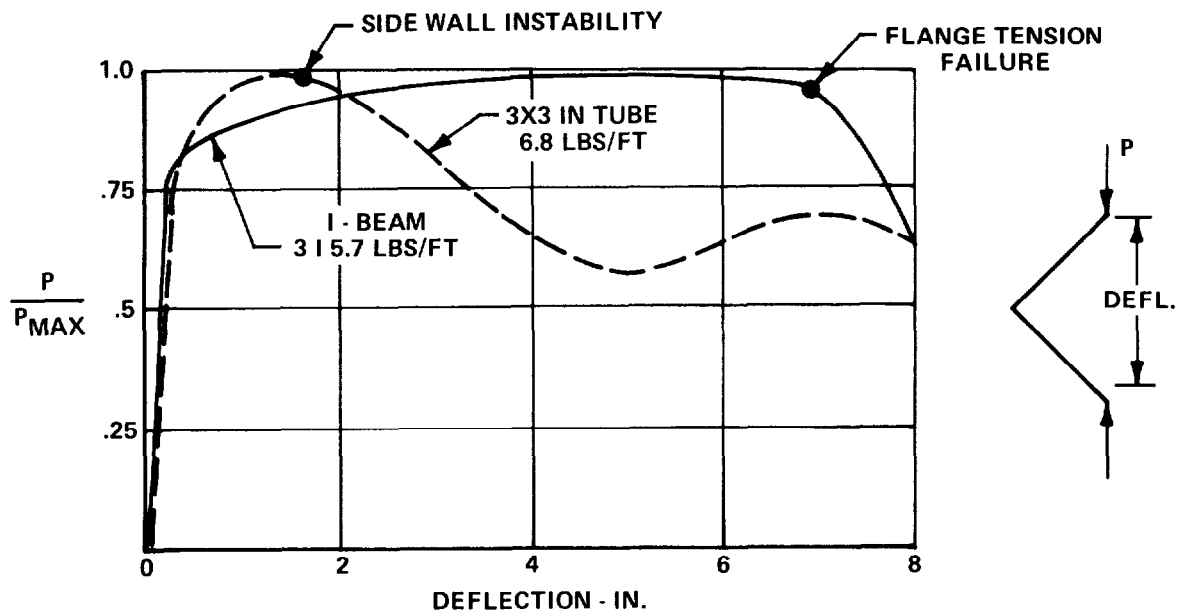


Figure 6-4 EFFECT OF LOCAL INSTABILITY ON ENERGY ABSORPTION: I-BEAM VS. SQUARE TUBE

The shaded members of Figure 6-5 comprise the basic structural concept utilized for the Mod. 3A vehicles. The existing thin wall rectangular side rails have been replaced by I-beams of approximately the same weight for increased bending strength in the horizontal plane. The side rails are connected by two knee-shaped cross members aligned along the center lines of the front and rear passenger doors. The purpose of the knees is to obtain the constant load behavior demonstrated by static component tests and to distribute load to the nonimpact side. In this modification, an I-beam between the "A" and "B" posts is included to simulate the increased strength of a Mod. 3 type reinforced door while avoiding the fabrication difficulties encountered in the Mod. 3 approach. Both the door beam and the side rail are rigidly framed to a vertical box beam which provides a substantially stronger "A" post to direct the impact force to the heavy existing members in the vicinity of the engine.

It has long been recognized that a roll bar is a desirable structural addition to maintain compartment integrity in rollovers. Also, in a side collision, a load path between the "B" posts serves to promote energy absorption at the nonimpact side. The arcuated roll bar of this modification constitutes an attempt to perform both the above functions as well as absorbing energy through bending during impact.

The structural sizes that are indicated in Figure 6-5 specifically apply to the Mod. 3A(1) vehicle, which is further described in Section 9. Mod. 3A(2) was partially constructed along with Mod. 3A(1), but incorporates minor changes that were deemed necessary based on the results of the Mod. 3A(1) test. These changes are discussed in Section 10.

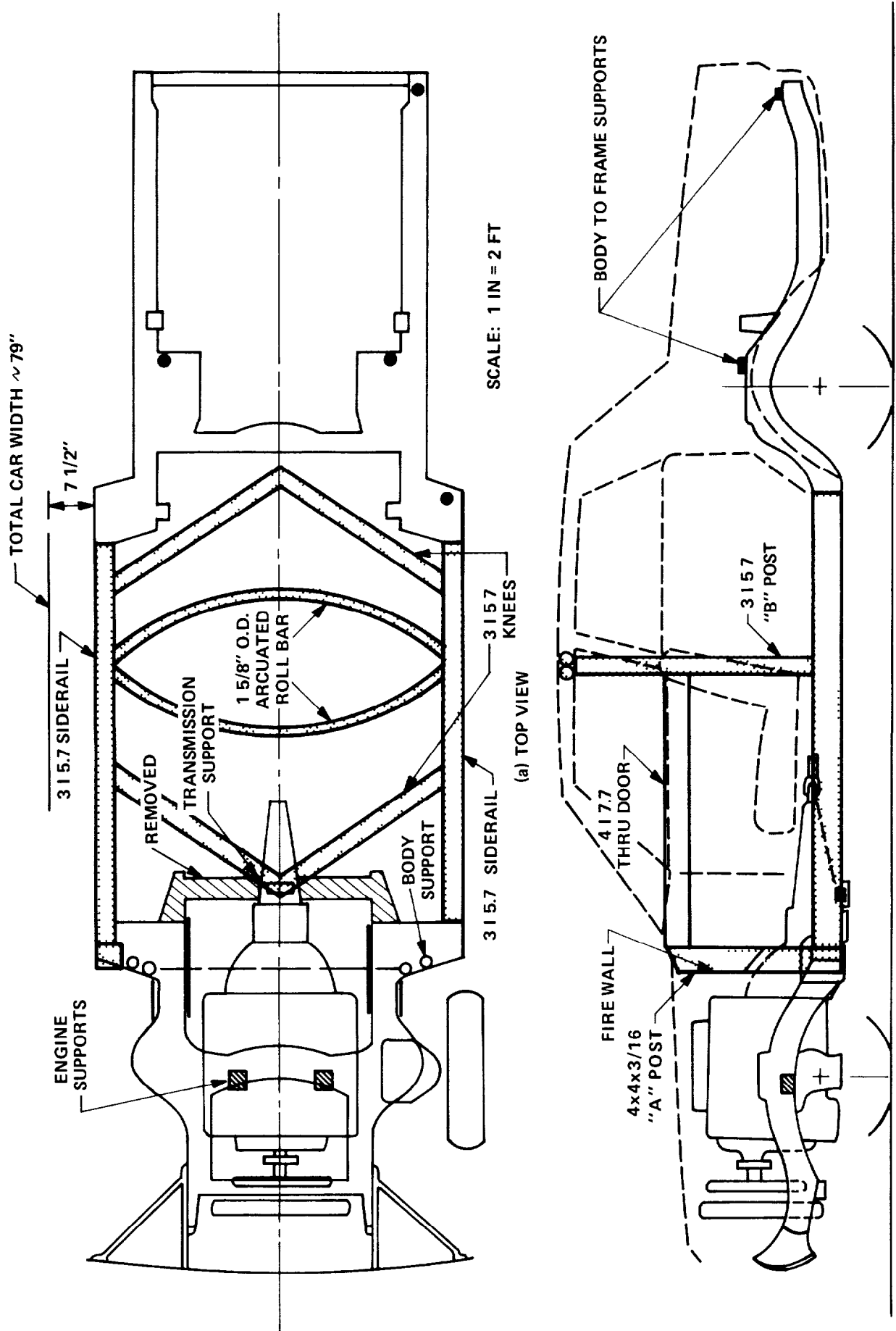


Figure 6-5 STRUCTURAL CONFIGURATION: MOD. 3A (1)

7. MOD. 3 VEHICLE

As discussed in Section 6, the objective of the Mod. 3 design is primarily to reduce intrusion into the passenger compartment in side impacts by reinforcing the door and adjacent supporting structure to produce uniform compartment deceleration of about 20 g's. The general design philosophy is discussed in Section 6.1. In the present section, design details are given, results of a 20 MPH side impact with a rigid pole are presented and the structural performance of the Mod. 3 vehicle is evaluated.

7.1 Design Details

Changing the flexural capacity of the door by the addition of internal beam structures subjects adjacent components to loads which are obviously much higher than for an unmodified door in a localized side impact. Consequently, many detailed changes were necessary to insure an integrated structural configuration.

Figures 7-1 and 7-2 show the hat section door beams before and after installation; the cross-sectional properties of a typical hat are given in Figure 7-3. Figures 7-4 and 7-5 illustrate various clip angles that were added, while Figure 7-6 shows a transverse strut between the "B" posts to distribute the load to the other side. The three rods visible in Figure 7-7 simulate the support to the "B" post that a modified rear door would provide and also permits camera coverage of the post in the test. Other details, which are not illustrated, involved addition of various gussets and straps to strengthen the existing door structure.

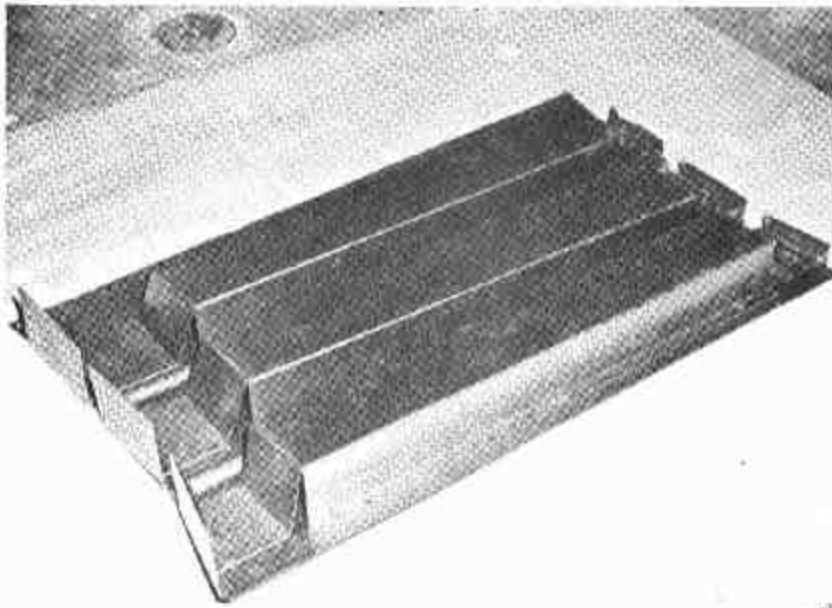


Figure 7-1 HAT SECTIONS PRIOR TO INSTALLATION

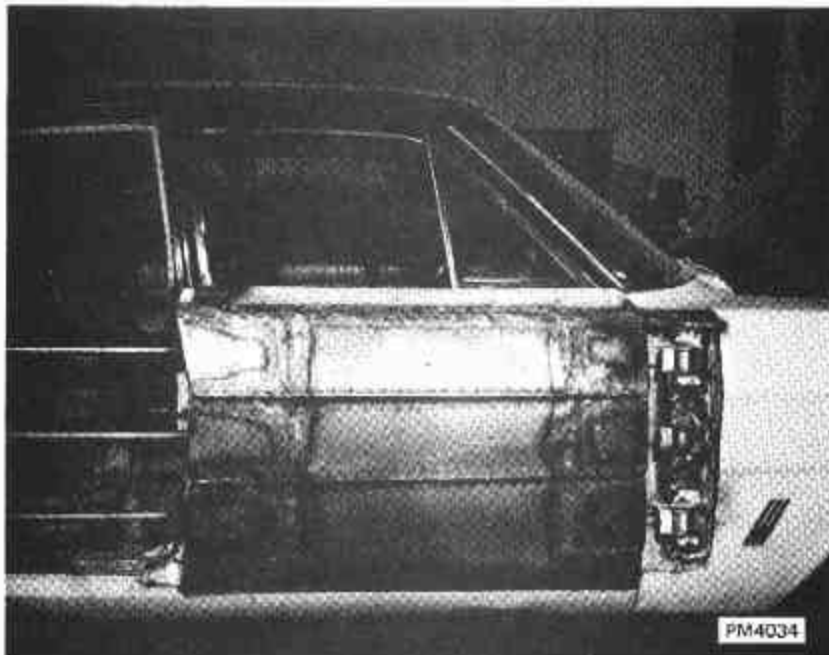


Figure 7-2 HAT SECTIONS IN PLACE ON MOD. 3

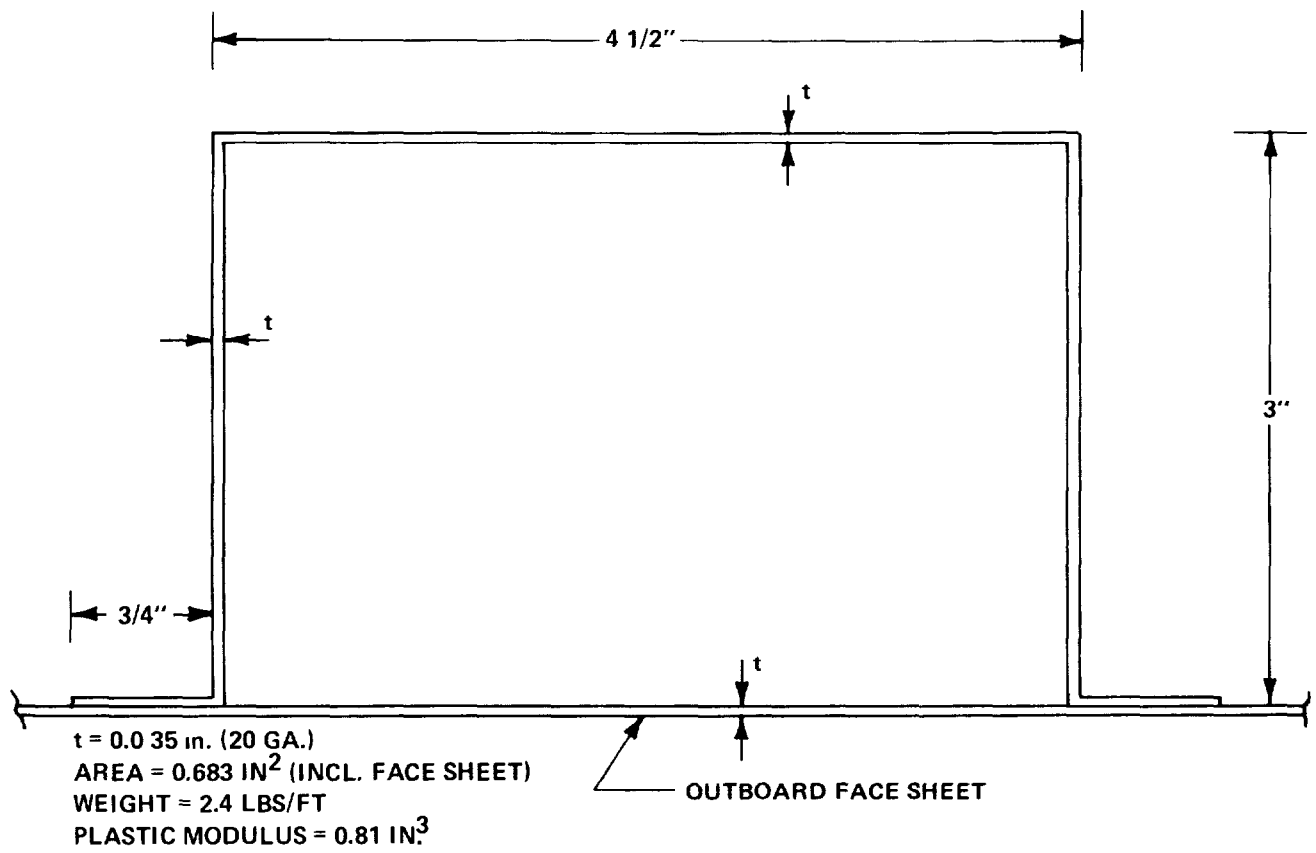


Figure 7-3 CROSS SECTION OF TYPICAL HAT

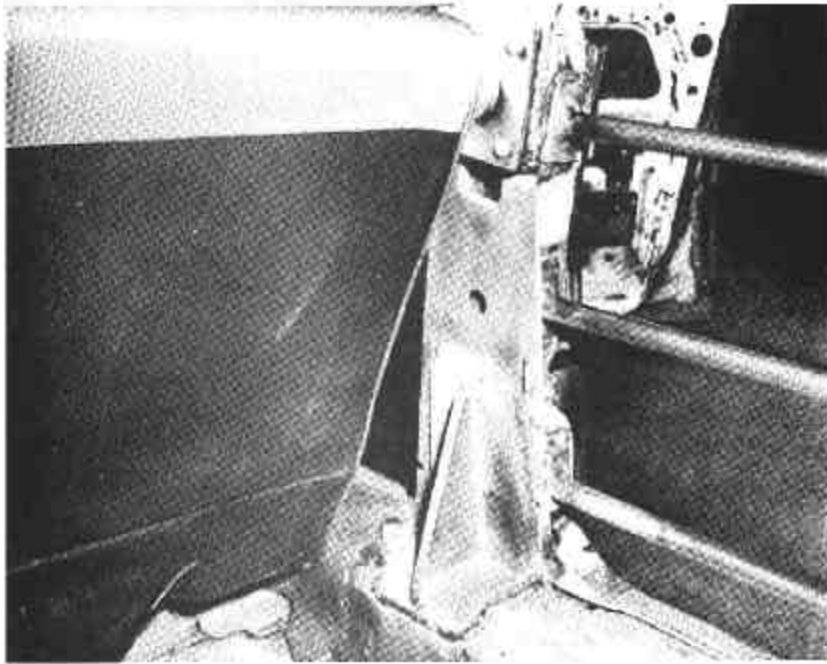


Figure 7-4 CLIP ANGLE AT "B" POST

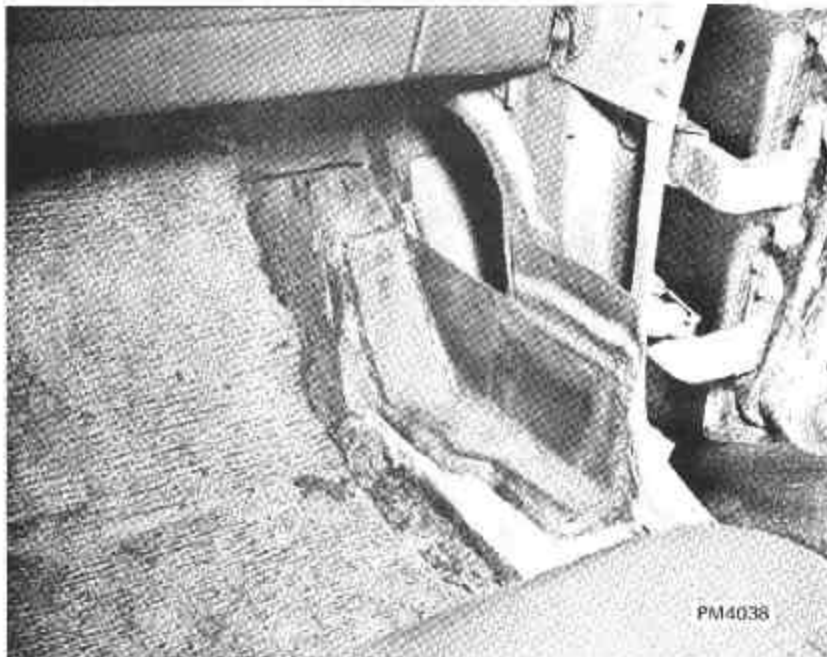


Figure 7-5 CLIP ANGLE AT "A" POST

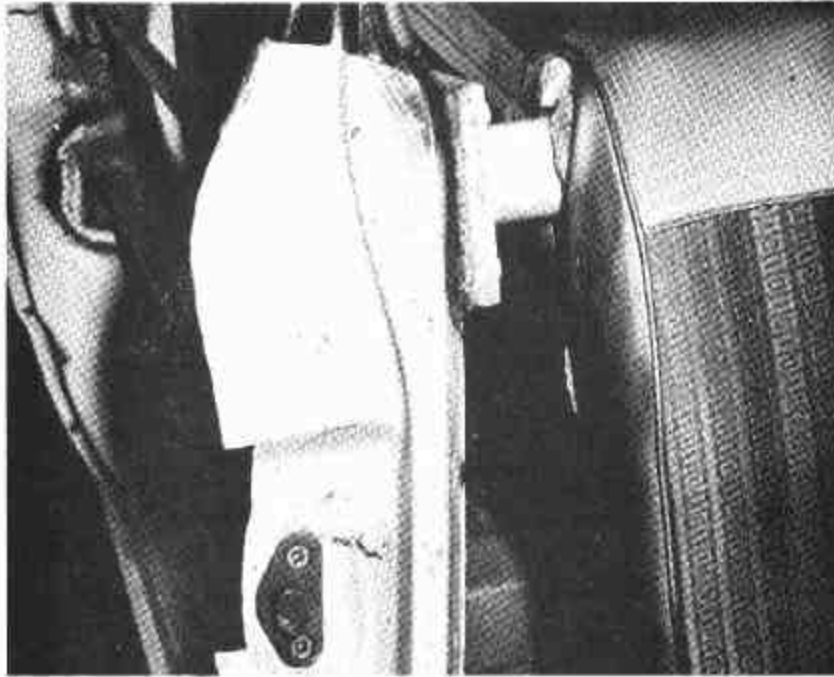


Figure 7-6 STRUT JOINING "B" POSTS

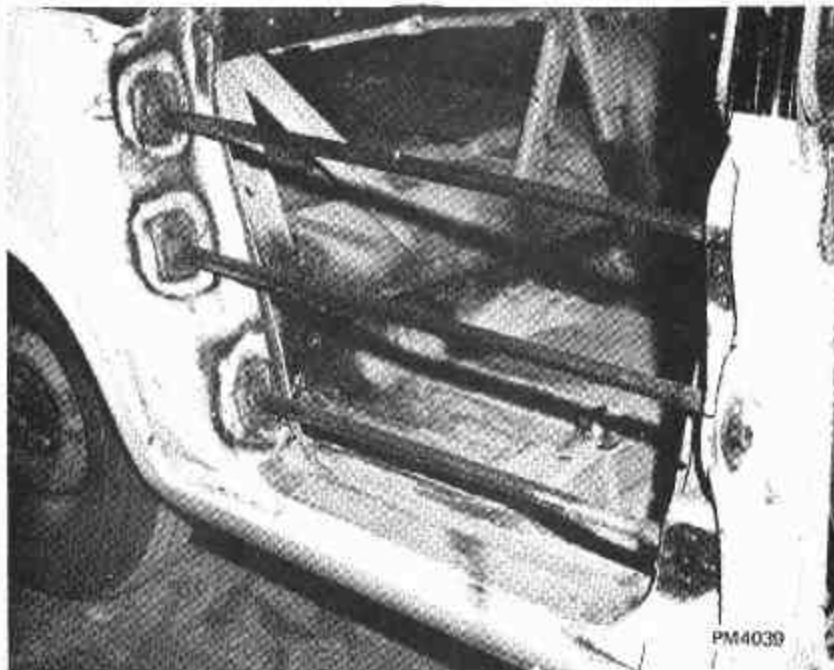


Figure 7-7 RODS TO SIMULATE REAR DOOR

A modified latching mechanism was intended for use on the Mod. 3 door for a positive connection between the door and "B" post. However, the latch failed to engage successfully in a dynamic component test performed prior to the full-scale crash test. The latch and component test are described in Appendix A. As a result of the failure, the Mod. 3 door latch was tack welded shut in an attempt to circumvent a similar failure in the full-scale test, since the latching mechanism was considered to be a relatively minor part of the overall structural concept. A redesigned latch was shown to operate successfully in a subsequent component test, which is also discussed in Appendix A.

7.2 Test Results

The Mod. 3 vehicle was impacted into the CAL pole barrier at a nominal speed of 20 MPH with impact intended for the center of the right front door. Actual impact velocity was determined to be approximately 17.4 MPH and impact occurred about 6 inches forward of the door center. The low impact velocity was caused by a defective fifth wheel which was used to measure the speed of the tow car. Other detailed test data and related information are contained in Appendix C.

Presented in Figure 7-8 are the side and vertical acceleration components measured in the passenger compartment under the driver's seating position. Side acceleration is toward the pole. A maximum side component deceleration of 25 g's occurred at .013 seconds. A spike of 46 g's (upward) is shown for the vertical component at .091 seconds, but this is not significant because of the small duration. A more meaningful peak in the vertical component was the 21 g's (upward) which occurred at .015 seconds.

Based on trip switch data (+0.5 MPH estimated accuracy).

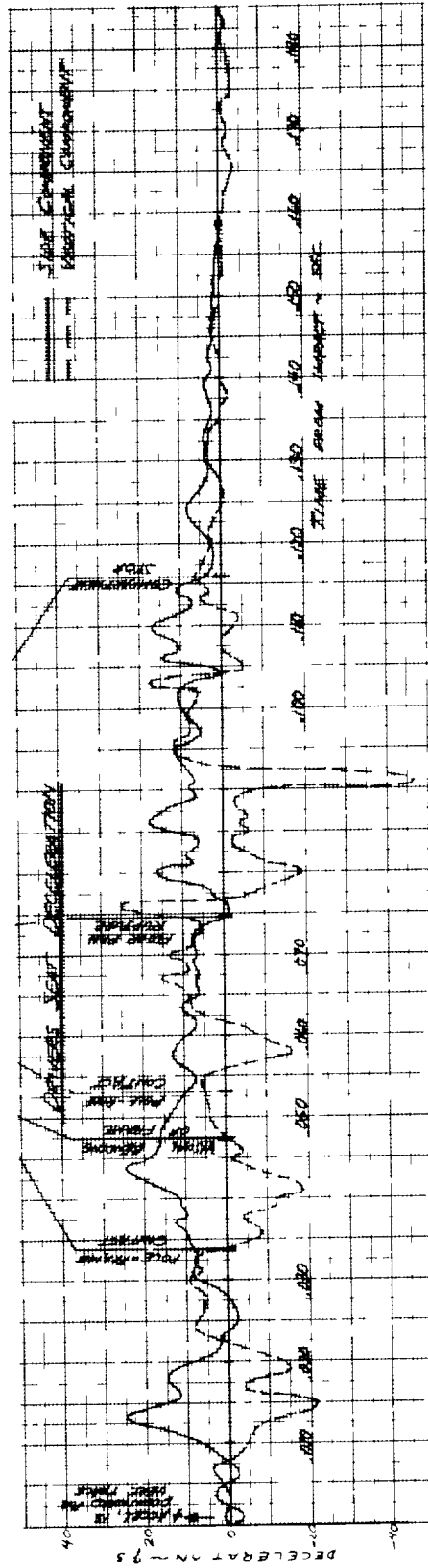
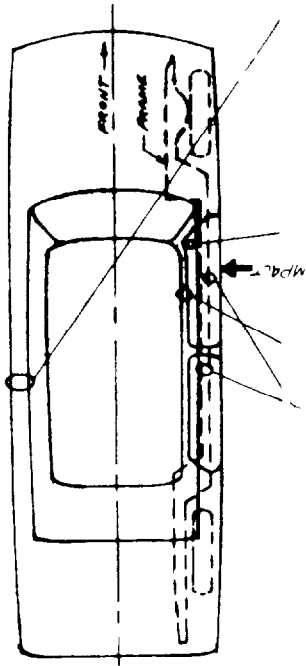


Figure 7-8 MOD. 3 TEST · VEHICLE ACCELERATION DATA

Accelerations from the passenger compartment sensors on the drive shaft hump showed oscillations similar to those of the driver's seat sensors. However, these sensors are believed to be less accurate due to their location in the compartment and are not presented.

Sideward deceleration data from the driver's seat location filtered at 50 Hz is presented in Figure 7-9. The filtered curve shows a maximum of 20 g's at .045 seconds which is a 4 g decrease from the unfiltered peak of 24 g's at approximately the same time. A velocity history obtained by integrating the acceleration data is also shown.

Mod. 3 contained a 2-1/4 inch O.D. pipe brace between the "B" posts in the passenger compartment. This lateral brace ran through the top section of the back of the front seat and was instrumented with two strain gauges to measure compressive strain. These gauges showed a maximum strain of approximately .017 inches/inch occurring at .040 seconds, which corresponds to a maximum compressive force of 8850 pounds. The resulting force versus time curve is shown in Figure 7-10.

Photographs of the Mod. 3 vehicle are shown in Figure 7-11, with a pretest photo of the impact side shown in Figure 7-11(a). The deformed profile can be seen in the top view shown in Figure 7-11(b).

Analysis of the high speed motion pictures of the crash produced the relative timing of several important events shown in Figure 7-8. Here, pole-to-frame contact occurred at .034 seconds and complete vehicle sideward motion stopped at .116 seconds.

The plan view profile of Mod. 3 was measured in the same manner as the base line test. This profile was superimposed over the undamaged car and base line profiles in Figure 7-12 for direct comparison. Note that Mod. 3 sustained 14 inches of permanent deformation compared with 24 inches for the base line test. Mod. 3 also exhibited less "pole wraparound" than the unmodified vehicle.

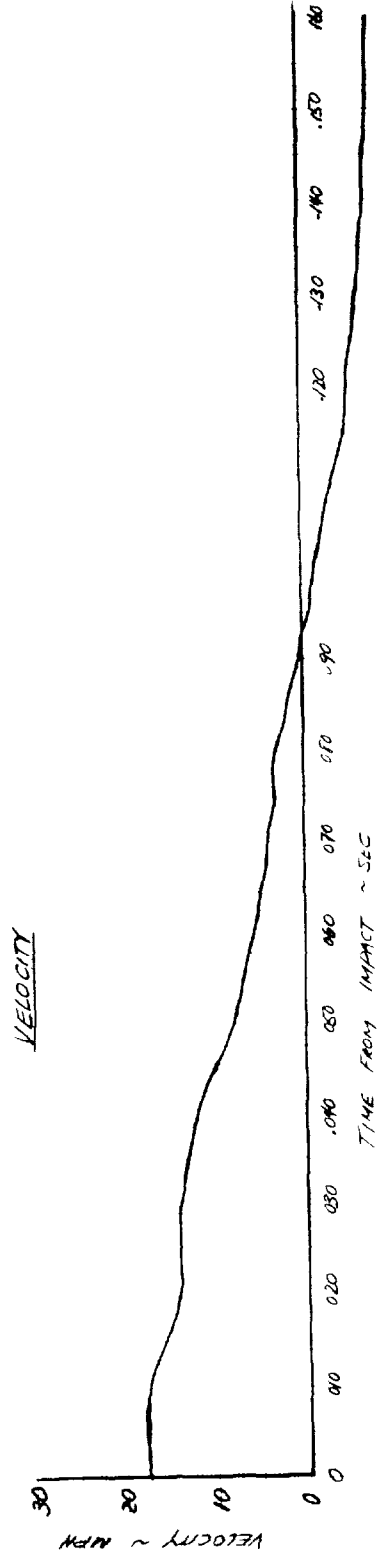
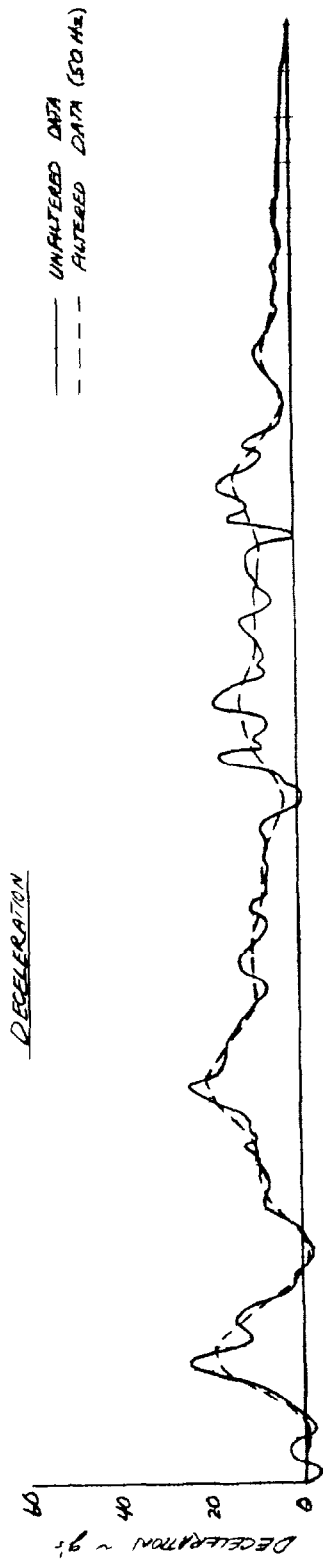


Figure 7-9 MOD. 3 TEST: DRIVER'S SEAT, SIDWARD ACCELEROMETER DATA

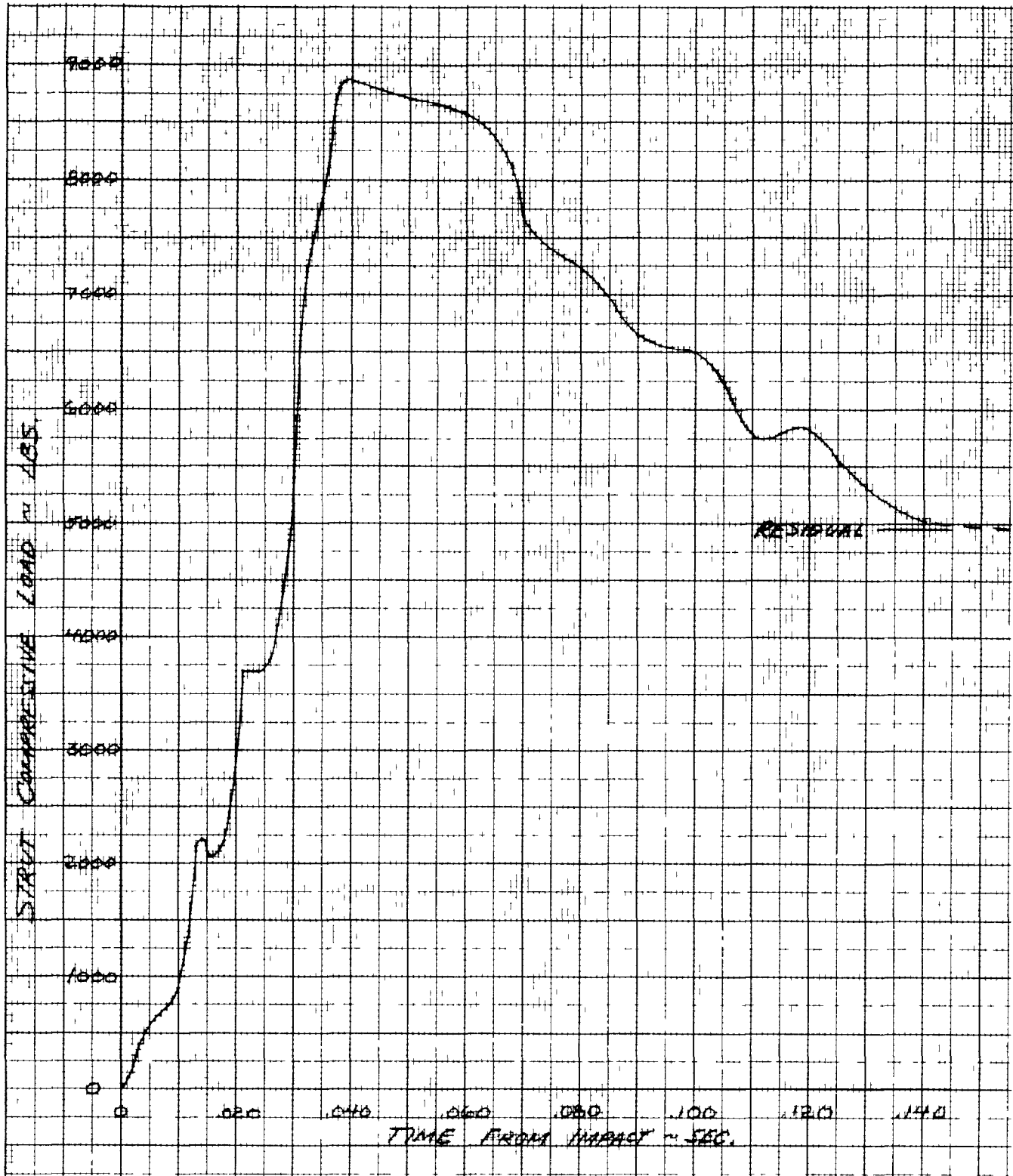
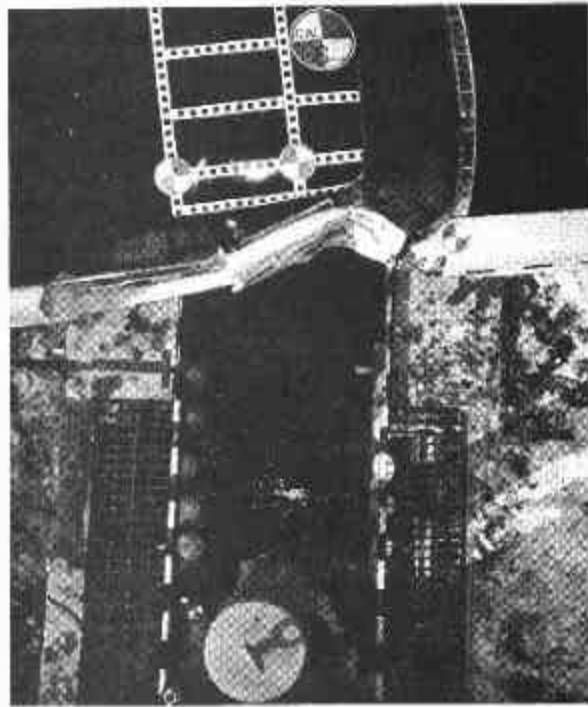


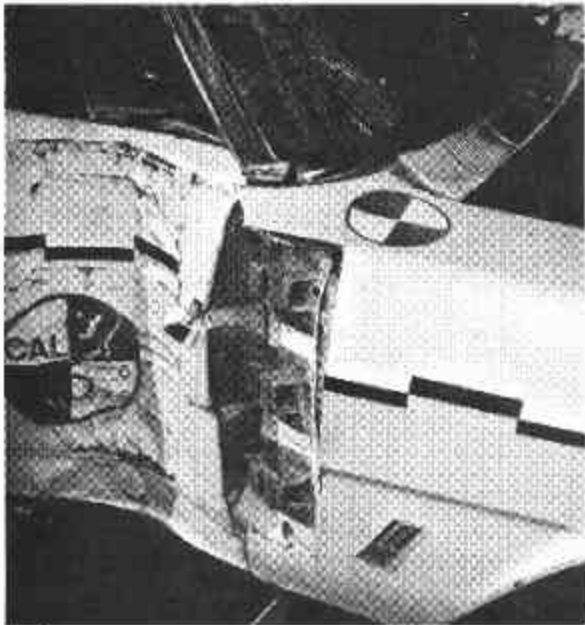
Figure 7-10 COMPARTMENT REINFORCING STRUT COMPRESSIVE LOAD



(A)



(B)



(C)



(D)

Figure 7-11 MOD. 3 TEST, SIDE POLE IMPACT

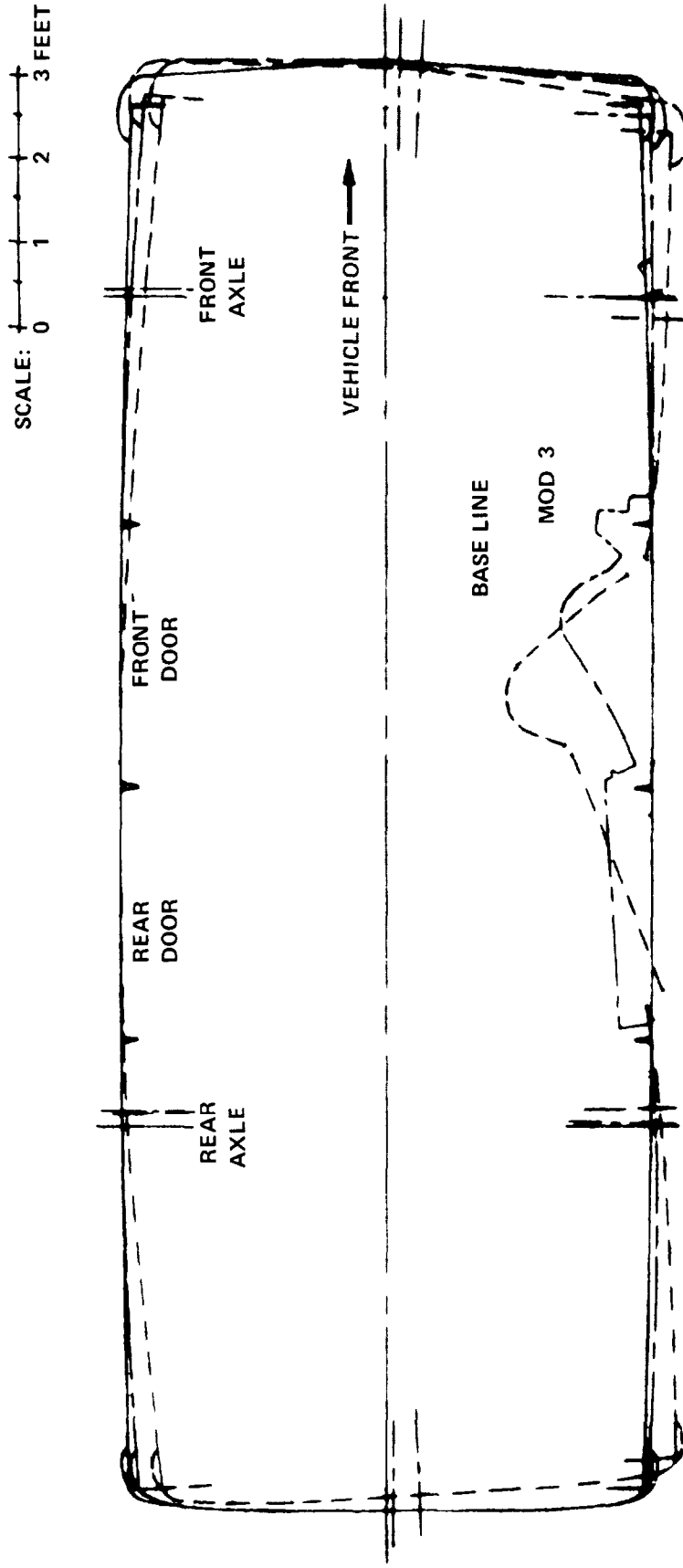
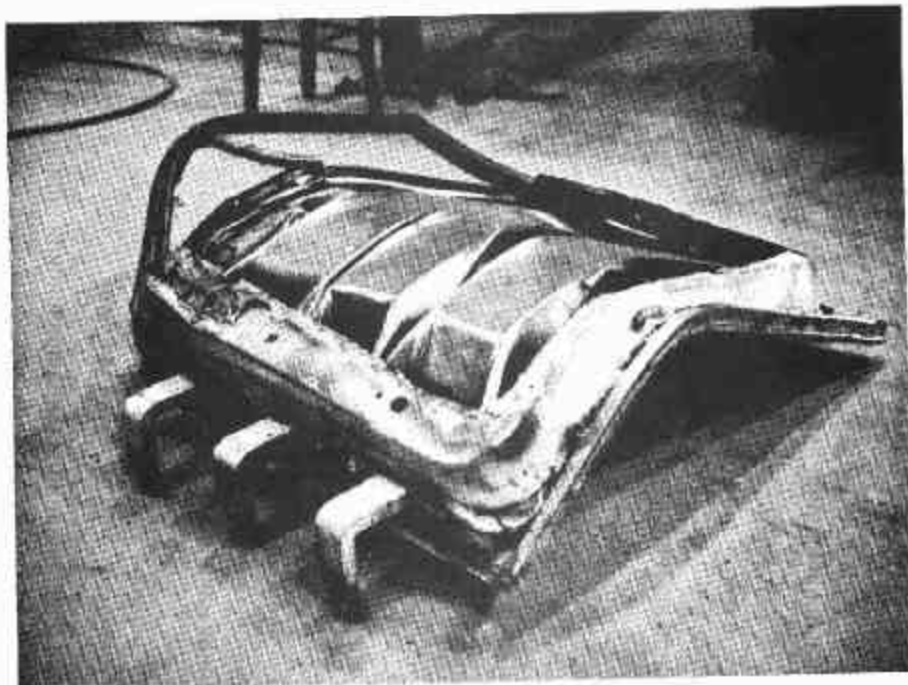


Figure 7-12 POST CRASH PROFILE OF SIDE IMPACT TESTS

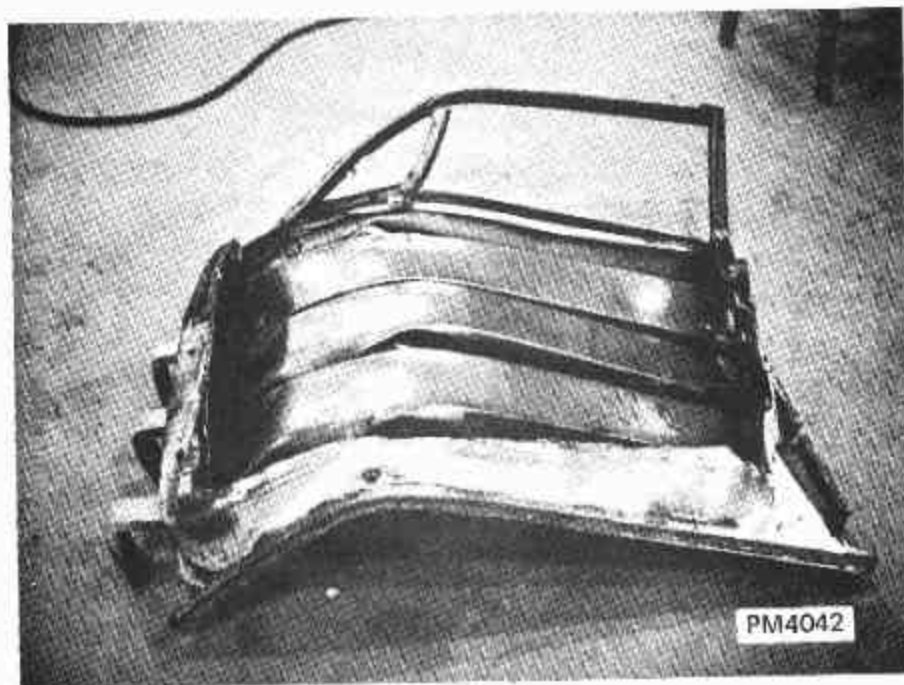
7.3 Evaluation of Performance

In evaluating overall structural performance, it is worthwhile to restate the two specific objectives of the modification: (1) to limit intrusion and (2) to spread the localized pole load by developing cable effects in the door beams. Figures 7-13(a) and 7-13(b) are photographs of the modified door which was removed for inspection. The pole impact point was at the third point of the beam toward the "A" post. This fact, coupled with an impact velocity under target, resulted in an undertest of the design concept. As a result, the "B" post door latches did not operate as anticipated. The loads were transferred through the tack welds that were added as a result of the component test failure (see Section 7.1) and by bearing, but not by the locking action hoped for. Also, the load carried by the transverse strut was somewhat less than 9000 lbs, whereas 15,000 lbs was expected. Accordingly, the design details were closely examined for evidence of cable action. The plates connecting the rods that simulated the action of a modified rear door (Figure 7-7) indicated that significant tensile loads were transmitted by each rod. The vertical seam added to provide the connection to the front fender was also subjected to high tensile loads. Based on examination of the above and other details, it can be conclusively stated that the desired tension action was achieved. The difference in crush between Mod. 3 and the base line vehicle (14 vs. 24 inches) is greater than that which could be attributed to the velocity difference (17.4 vs. 21.5 MPH).

Figure 7-14 is a comparison of the initial portions of the acceleration-time curves for the base line and Mod. 3. It is obvious that the modifications resulted in higher g's very early in the collision. There is no conclusive explanation for the low or negative decelerations apparent in both curves. This means, of course, that considerable deformation is not being used effectively. A tentative hypothesis is that the body is shifting relative to the frame. The fact that the strut load (Figure 7-10) increases monotonically to a peak without evidence of a dip supports this hypothesis. Also, the dips may be due to placement of the accelerometers on the floor which is subject to considerable distortion and probably not indicative of occupant loads.



(A)



(B)

Figure 7-13 MODIFIED DOOR AFTER IMPACT

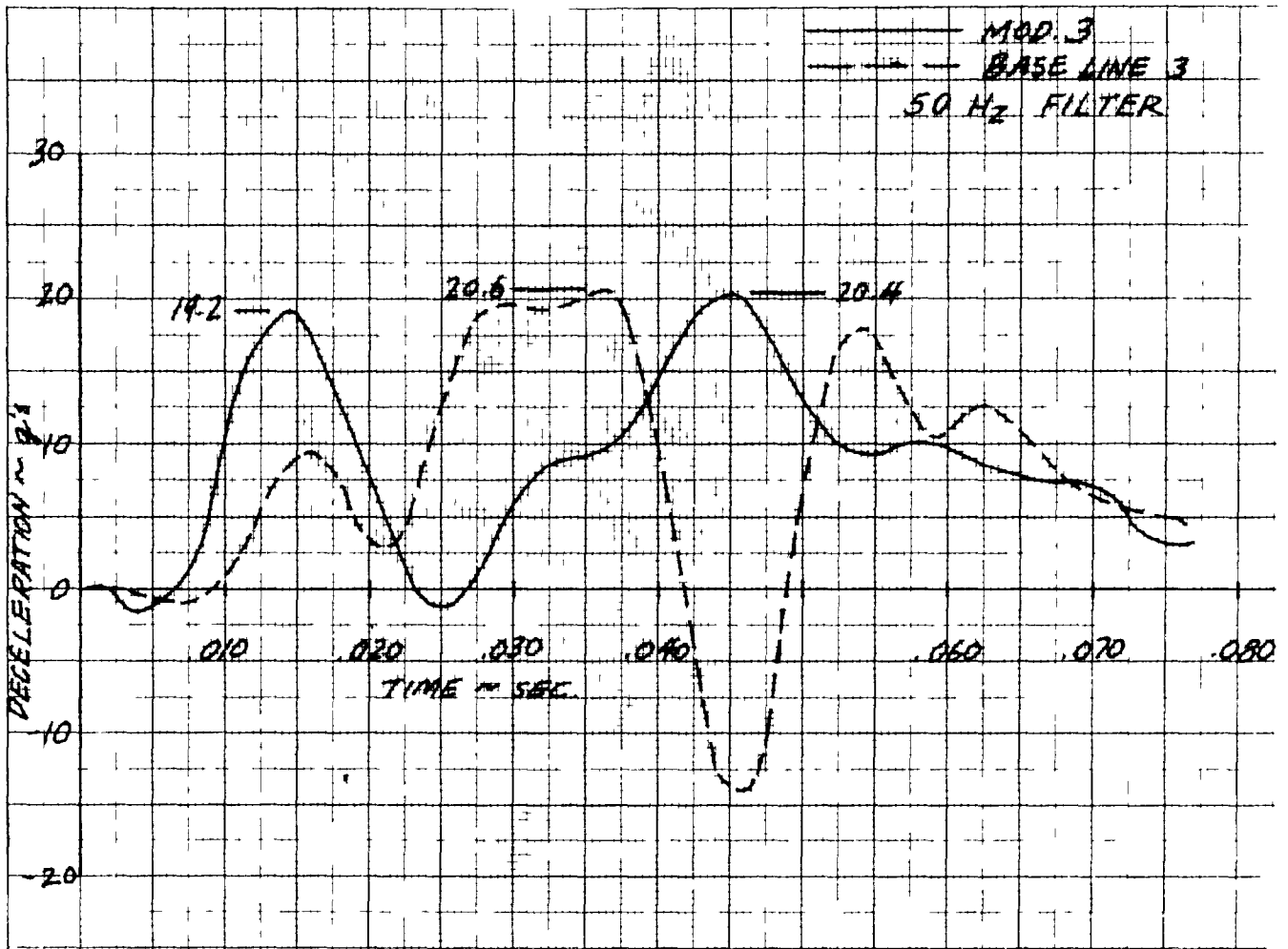


Figure 7-14 COMPARISON OF MOD. 3 AND BASE LINE 3 FILTERED DECELERATIONS

The two straps which were added to strengthen the bottom of the door followed the deformed contour. The clip angles at the "B" posts, Figure 7-4, showed no signs of overstress and could be reduced in size. The "A" post clip angle received substantial load and was certainly necessary. In examining the relative deformation of the three hat section door beams, Figure 7-13, it is apparent that the lower beam received less load than the upper two and could possibly be eliminated in a future test.

The low impact speed of Mod. 3 resulted in an undertest of the design concepts, yet examination of the details suggest that the desired loading paths were realized. For moderate weight increases (approximately 20 lbs per door), the intrusion resistance can be improved without significantly higher decelerations. Some other conclusions of the Mod. 3 test are: (1) in terms of time and effort, many detailed changes of the existing vehicle are as costly as a major modification, and (2) an investigation of the effect of accelerometer location on resulting data should be made.

8. D-2 DEVELOPMENTAL VEHICLE

8.1 Objectives

The objective of the development test, designated D-2, was to determine if the improved performance demonstrated by Mod. 3 could be achieved by the transverse strut and additional brackets only. A prime reason for considering such a modification was that it could be constructed and tested without extensive design and fabrication effort.

A secondary objective of the test was to use the full-scale crash test as an opportunity to improve and correlate techniques of data collection and interpretation by employing multiple data sensors. For this test, load cells were available to instrument the impacted pole. Thus, accelerometers mounted at different locations with each other and with accelerations computed from load cell data. The results of this comparison are given in Appendix B

8.2 Test Results

The D-2 vehicle was impacted into the CAL pole barrier at a speed of approximately 20.5 MPH¹ at a point about 4 inches forward of the right door center line. Test conditions and related data are given in Appendix C.

¹Based on trip switch data (±0.5 MPH estimated accuracy).

Acceleration data (unfiltered) from three different sensor locations in the vehicle are presented in Figure 8-1. Times of significant events are marked along the abscissa and referenced to the vehicle sketch. Accelerations from the sensor located under the driver's seat on the floorpan are shown at the top of the figure. Peak decelerations of approximately 30 g's were obtained from this sensor. The sensor at the bottom of the "B" pillar was mounted on a reinforcing plate, 11-1/2 inches aft of the intended impact center line. These data indicate a peak deceleration of approximately 20 g's. The curve at the bottom of Figure 8-1 was obtained from an accelerometer mounted directly on the left side frame side rail on line with the intended impact. Peak deceleration in this curve is approximately 28 g's.

Acceleration data from the remaining three on-board sensors were less significant in this test and are not presented. The location of these sensors were at the top of the left side "B" pillar, in the passenger compartment on the drive shaft tunnel and the fore-aft direction sensor under the driver's seat.

Filtered and unfiltered acceleration data (standard filter of 50 Hz cutoff and 100 Hz roll-off) from the driver's seat position are presented in Figure 8-2 along with associated velocity and displacement curves. The latter two curves were obtained by integration of the acceleration data. The maximum dynamic displacement was approximately 26 inches compared with the measured permanent deformation of 22 inches. The permanent deformation, obtained after the test, was measured from a line joining the outer edges of the front and rear fenders to the point of maximum penetration of the door. The filtered data indicates a maximum lateral acceleration of approximately 21 g's at .036 seconds.

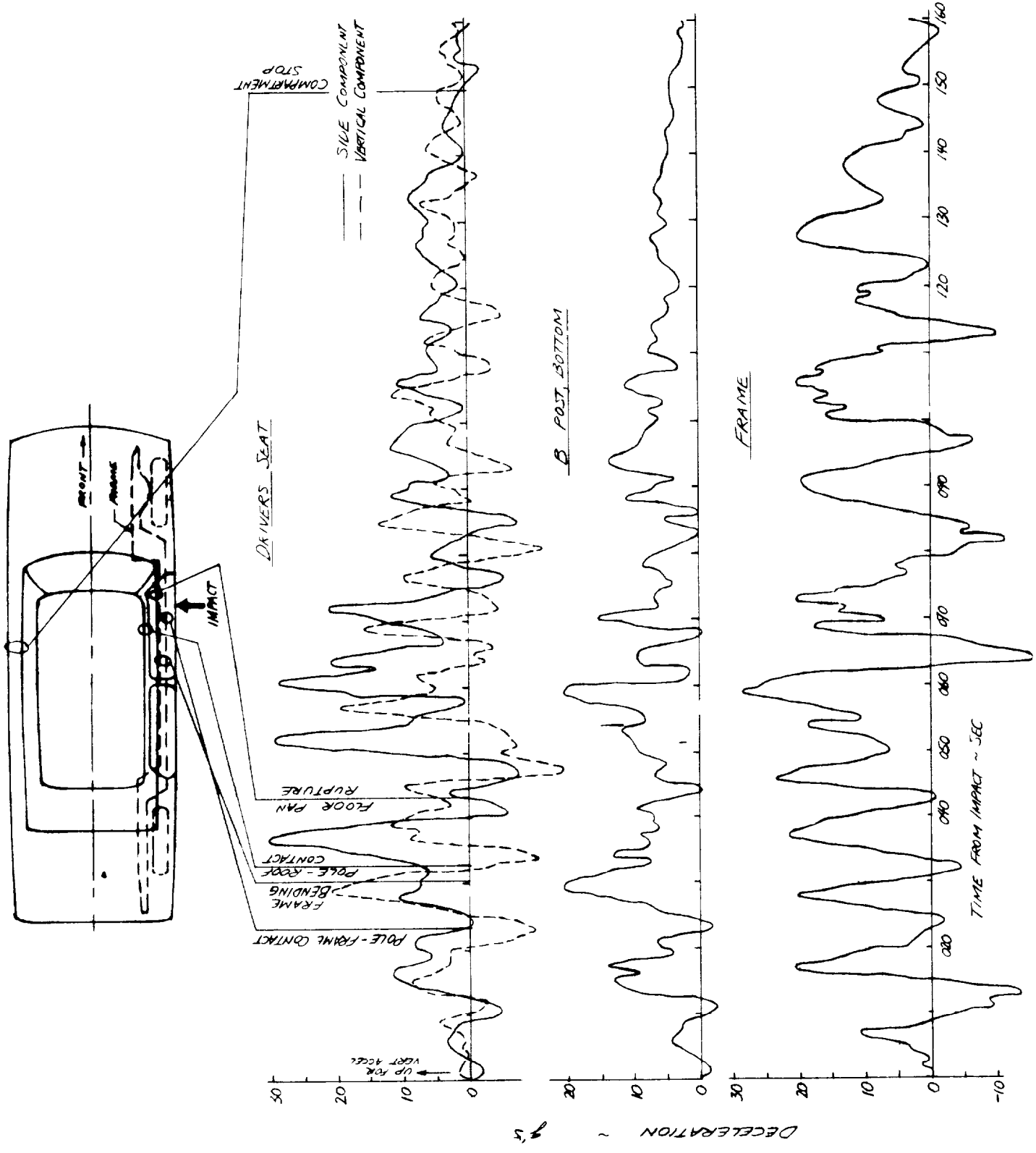


Figure 8-1 D-2 TEST: VEHICLE ACCELERATION DATA

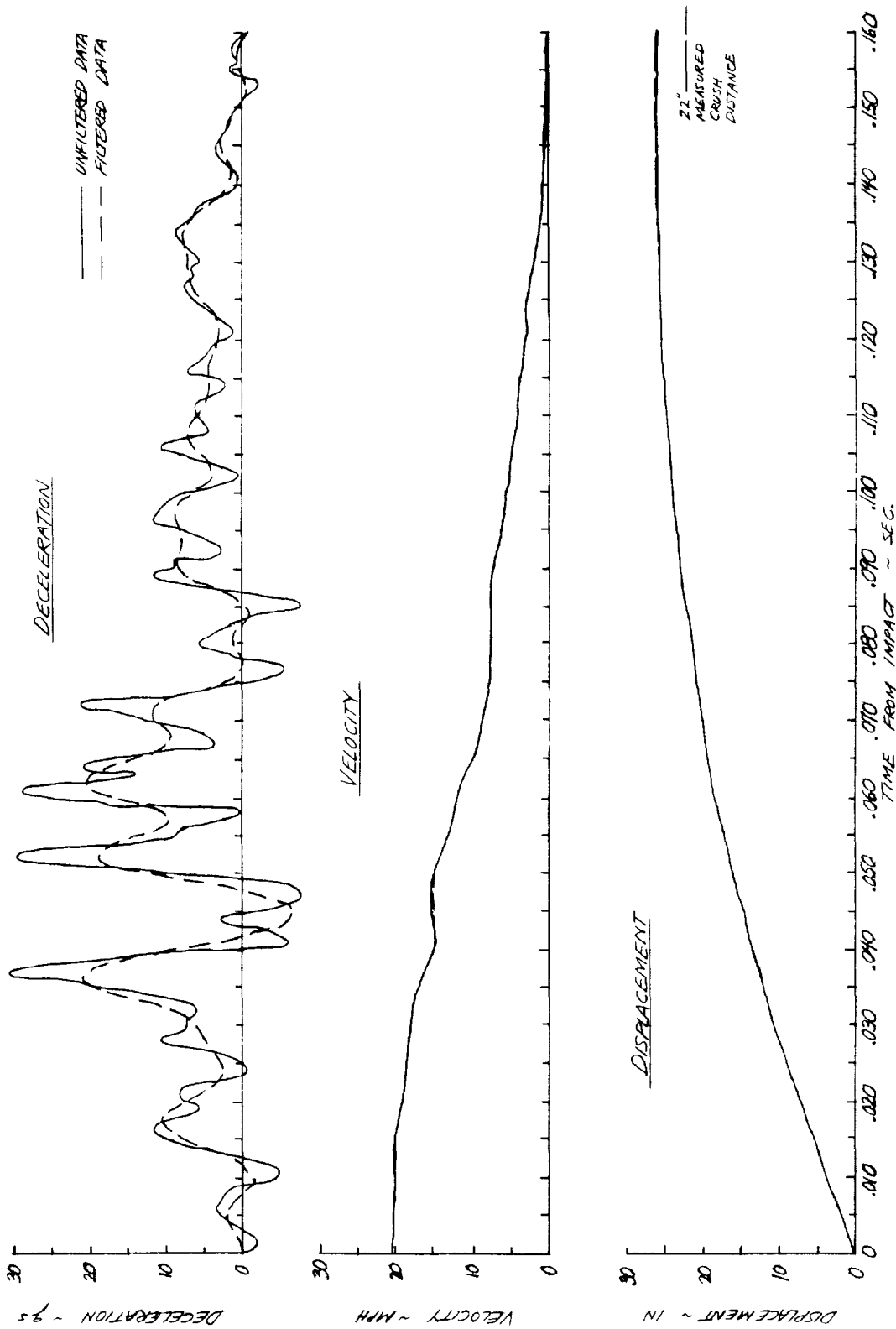


Figure 8-2 D-2 TEST: DRIVER'S SEAT, SIDEWARD ACCELEROMETER DATA

Figure 8-3 is a plot of filtered acceleration data versus computed displacement at the three different sensor locations. A maximum dynamic displacement of approximately 26 inches is indicated by integrating the driver's seat acceleration data; whereas, data from the "B" post and frame indicate about 24 inches of peak displacement. This difference can be attributed to structural deformation between sensors and measurement error.

Strain gauge measurements from the compartment internal brace mounted between the "B" pillars are presented in Figure 8-4. The axial strains in the pipe were converted to loads by assuming a Young's Modulus for steel of 30×10^6 psi. A peak axial load of 4800 pounds occurred at approximately .100 seconds.

Time histories of forces in the impacted pole from top and bottom mounted load cells are shown in Figure 8-5. Loads from the two cells which were in line with the impact were added and are presented as the solid curve. A maximum load of 38,000 pounds is indicated at approximately .052 seconds. The dashed curve is the sum of the two north side load cells which peaked at 11,500 pounds. Both south side cells produced comparatively small loads during the impact and are not presented.

For comparison purposes, a post-crash profile of the D-2 vehicle is presented in Figure 8-6 along with an undamaged car shape. A total permanent deformation of 22 inches can be noted from the scaled drawing, along with bending of the total vehicle.

Photographs of the D-2 test vehicle are shown in Figure 8-7. The interior pole brace between the "B" pillars can be seen in Figure 8-7(a) along with some of the on-board instrumentation. Figures 8-7(b) and 8-7(d) show the amount of damage sustained from the impact and the slight bowing of the left side "B" pillar is noticeable in Figure 8-7(c).

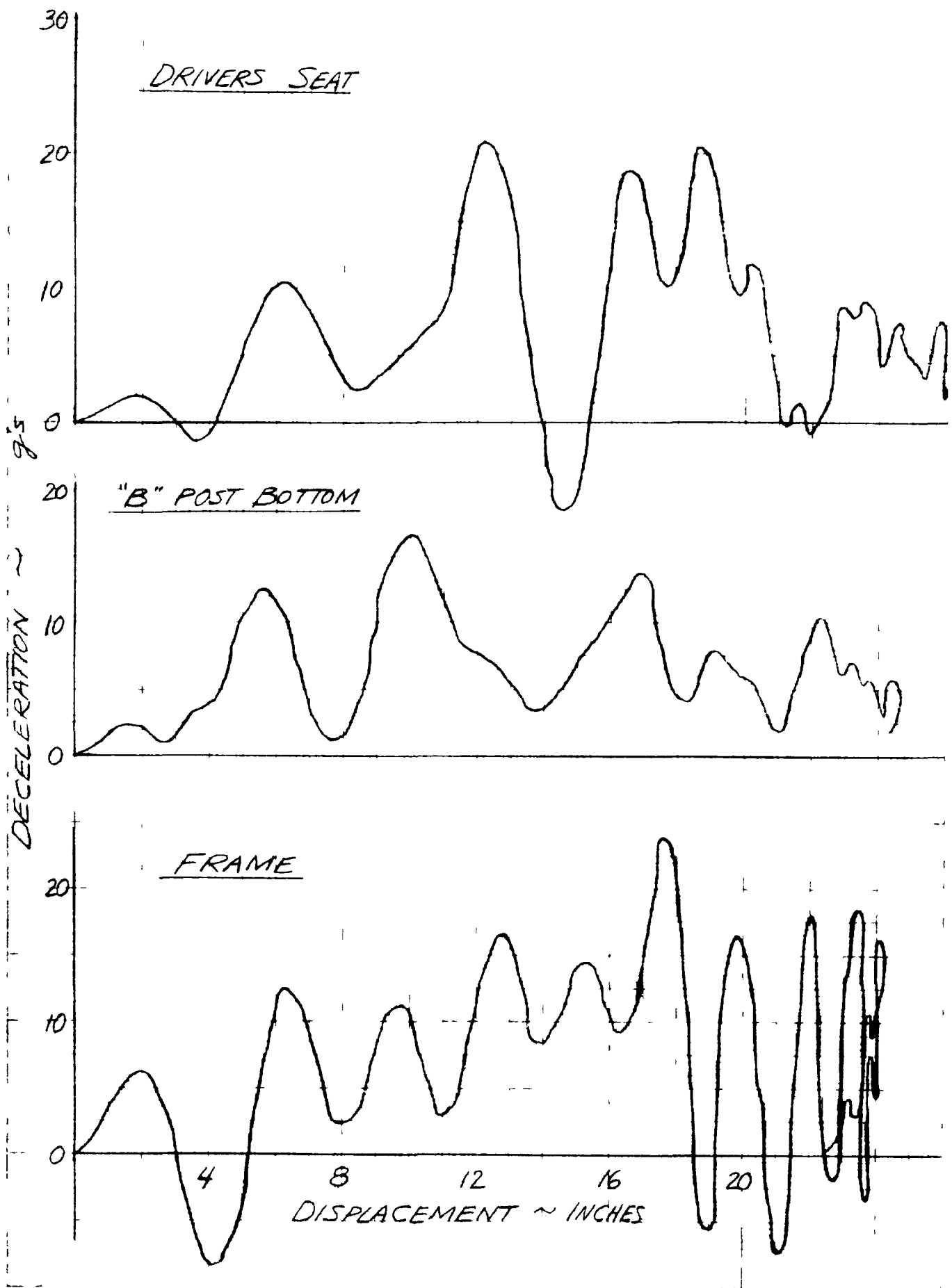


Figure 8-3 FILTERED (50 Hz) ACCELERATION DATA, D-2 TEST

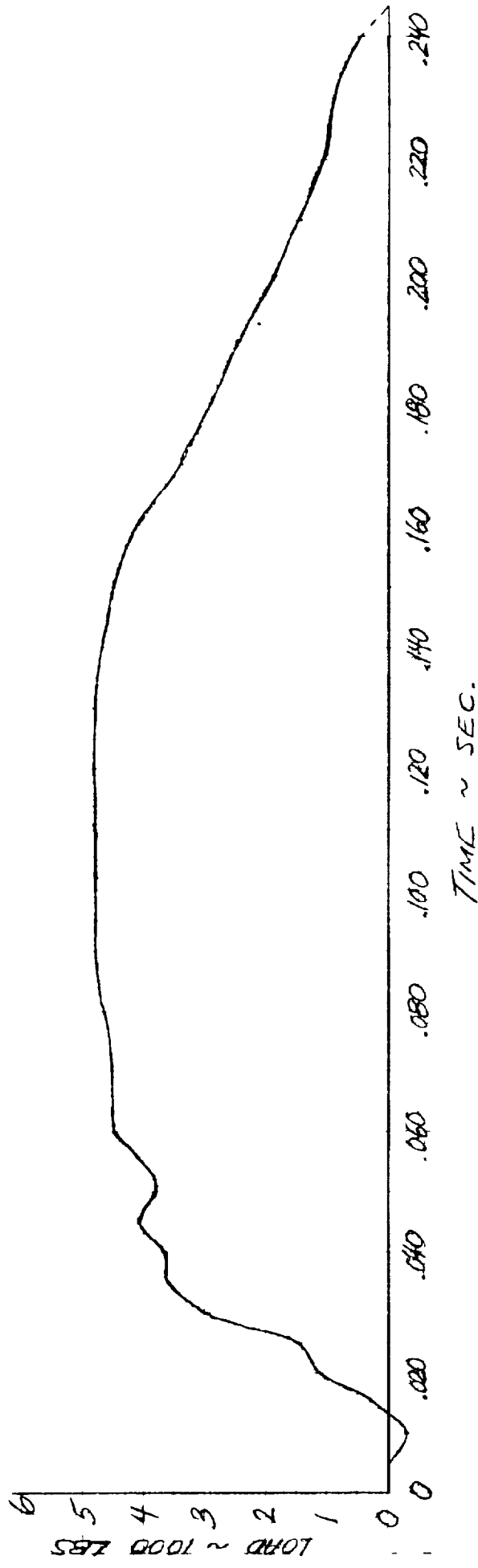
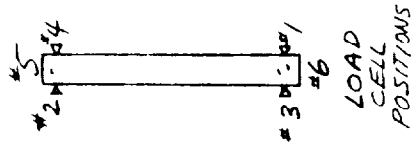


Figure 8-4 AXIAL LOAD IN STRUT BETWEEN "B" POSTS



TOTAL POLE LOADS

— ALIGNED WITH IMPACT, CELLS 5 PLUS 6
 - - - NORTH SIDE LOADS, CELLS 2 PLUS 3

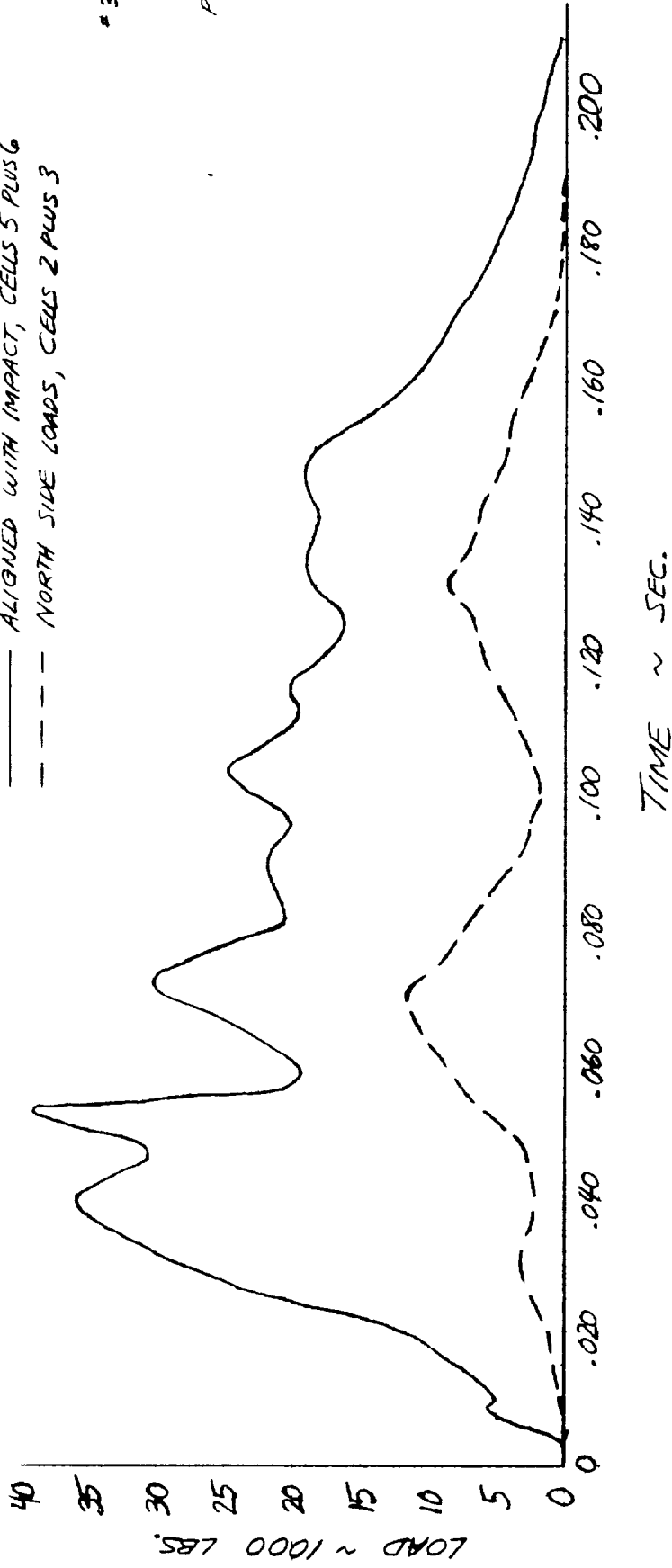


Figure 8-5 IMPACT POLE TOTAL LOADS

SCALE: 0 1 2 3 FT.

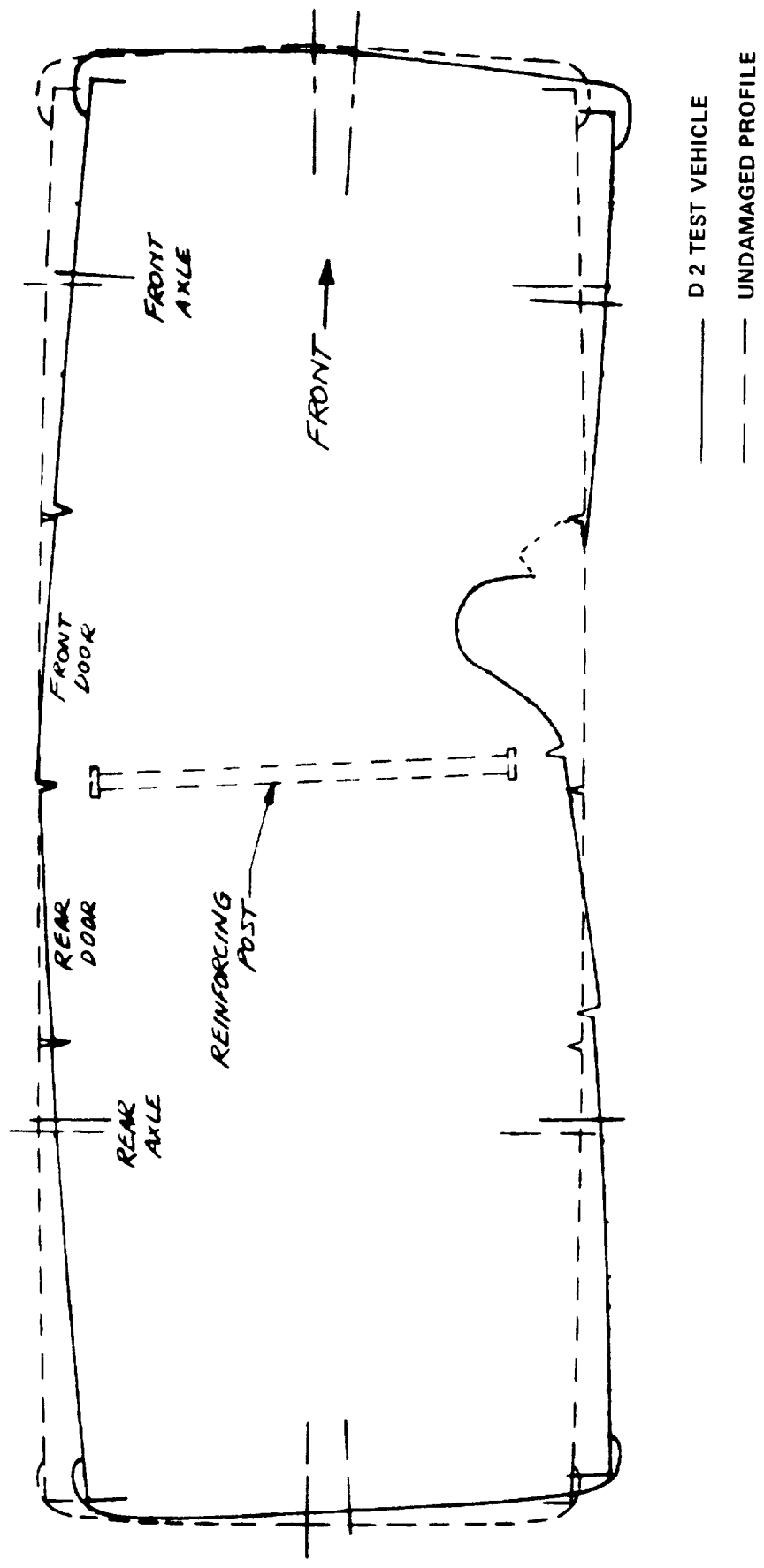
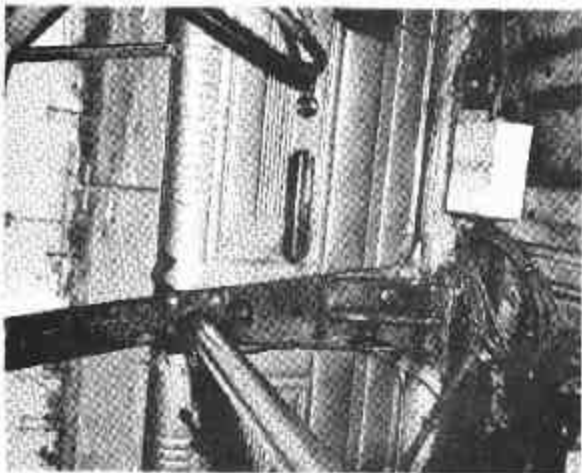


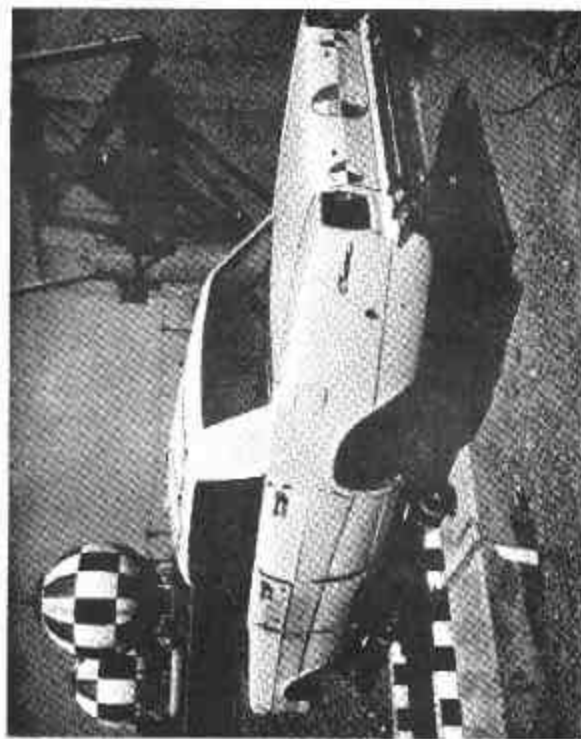
Figure 8-6 POST-CRASH PROFILE OF D-2



(a)



(b)



(c)



(d)

Figure 8-7 D-2 TEST, SIDE IMPACT WITH POLE

8.3 Evaluation of Performance

In evaluating overall performance in side collisions, both penetration and the magnitude of the compartment decelerations must be considered. Figure 8-8 shows the deformation caused by pole impact for all three side collisions that have been conducted. It is apparent that the deformation pattern of the D-2 is closer to that of the base line vehicle than to that of Mod. 3, which consisted of a modified door and supports in addition to the transverse strut. The observed deformation pattern correlates with displacements obtained by double integration of the various accelerometers and also with behavior of the frame as observed by a pit camera during the collision.

Comparison of the accelerometer data also supports the above noted general trends. Figure 8-9 compares, for three side tests, the time histories of accelerometers placed under the driver's seat (on the floorpan) in line with the impact. The peak at 14 msec for the Mod. 3 vehicle is attributable to the modified door; such a peak is not present for the D-2 vehicle. If a general characterization of the curves of Figure 8-9 is possible, D-2 is closer to the base line vehicle than to the Mod. 3, which had the modified door and supports. Measurements of the axial forces in the transverse strut between the B-posts also confirm the conclusions drawn from examination of the acceleration data and the deformation patterns. Figure 8-10 shows the time history of axial forces in the transverse struts of each modification. The difference in rise times can be seen and also the fact that the peak force of the Mod. 3 vehicle is approximately twice that of the strut of D-2. This occurs in spite of a difference in impact velocities which would tend to make the D-2 force larger (17.4 MPH vs. 20.5 MPH).

PLAN VIEW

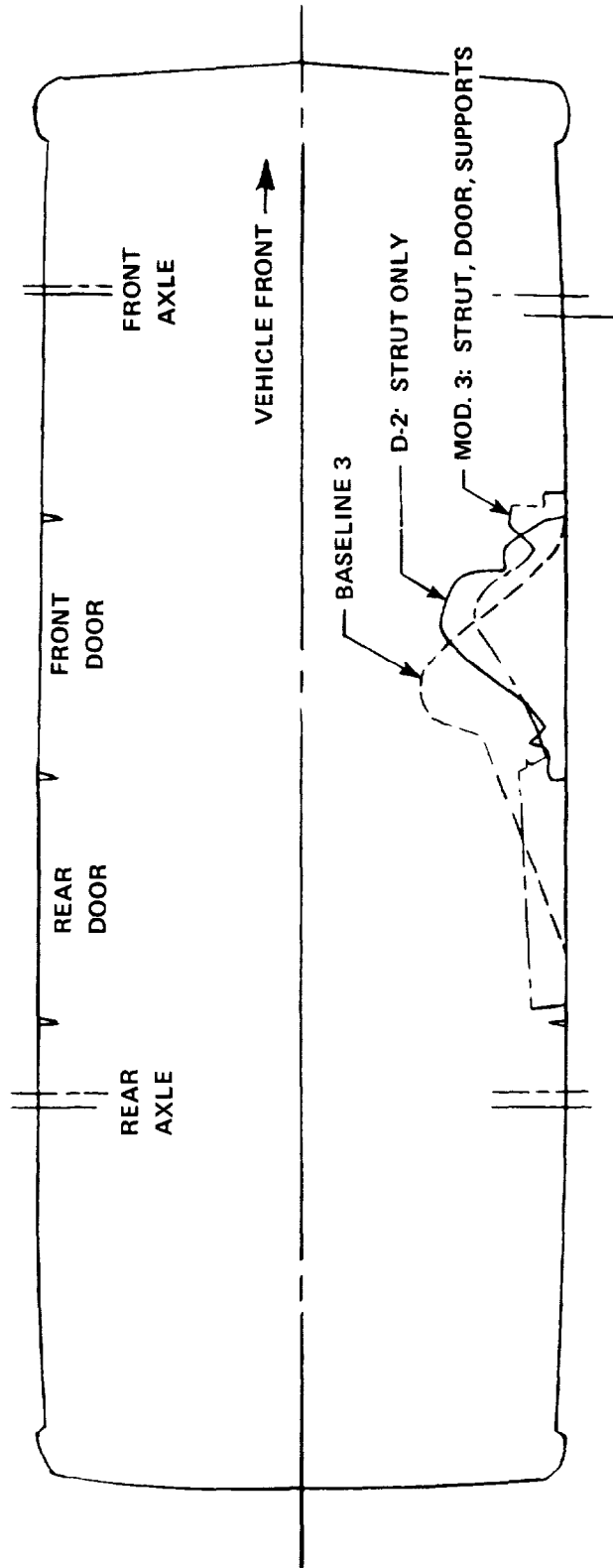


Figure 8-8 POST CRASH PROFILE OF SIDE IMPACT TESTS

FILTERED DATA
 50 HZ CUTOFF
 100 HZ ROLLOFF

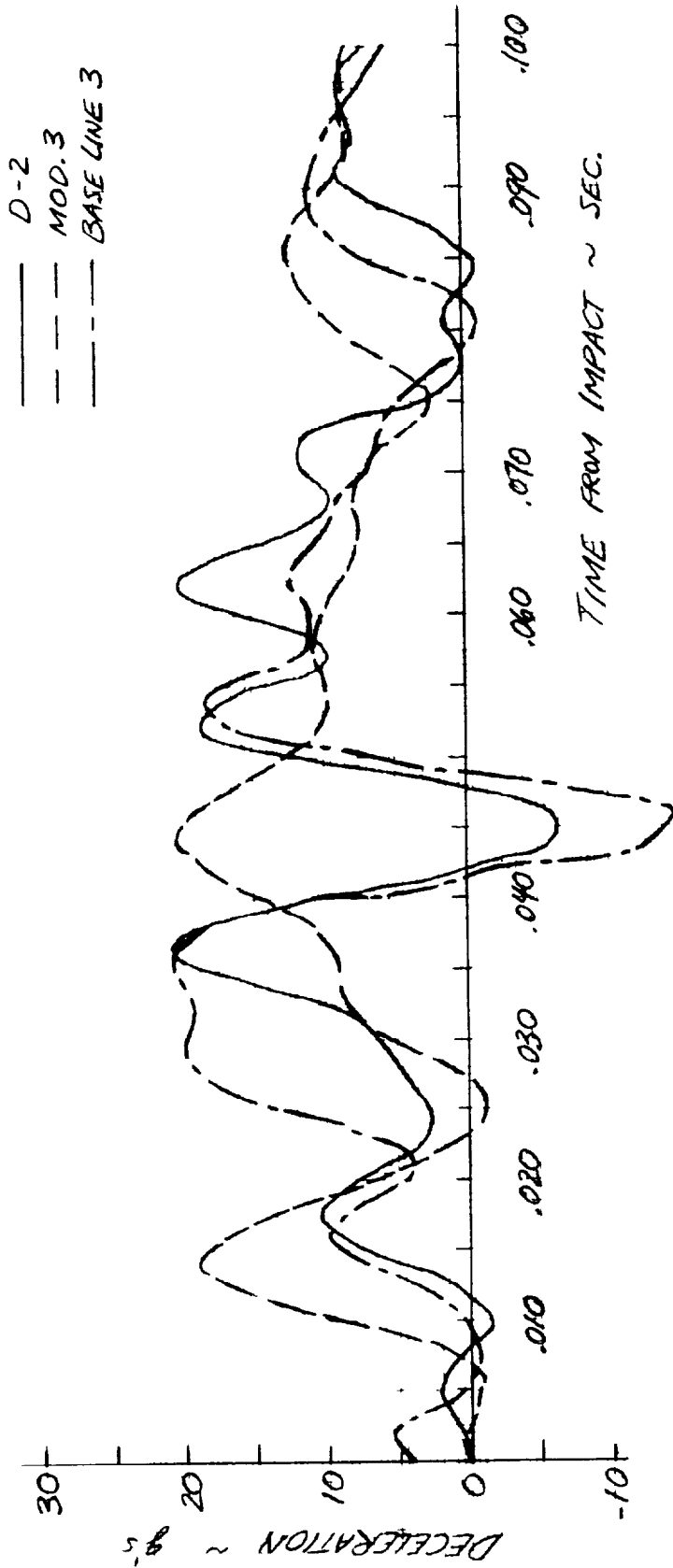


Figure 8-9 DRIVER'S SEAT, FILTERED SIDEWARD ACCELERATION DATA

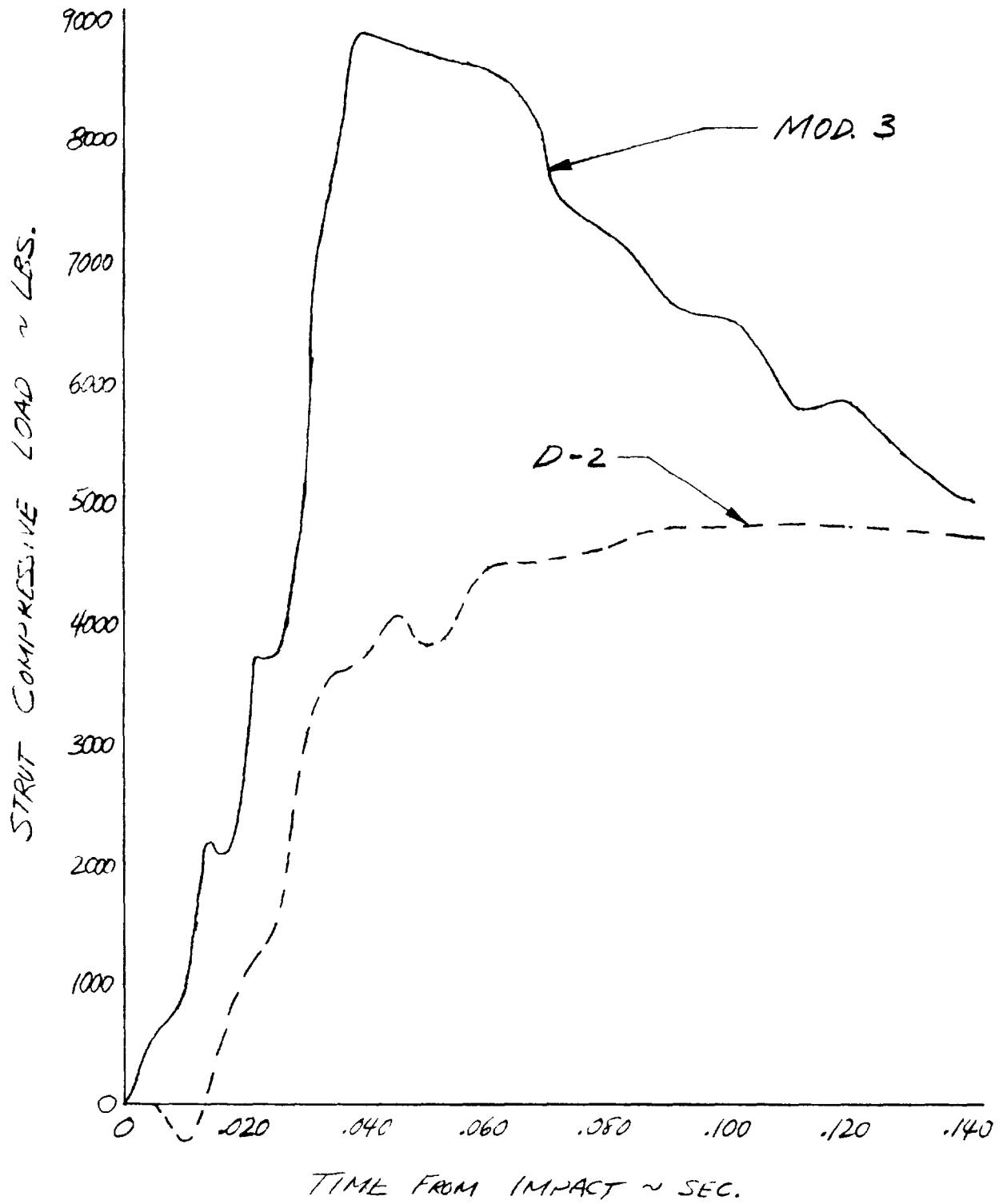


Figure 8-10 AXIAL FORCE IN TRANSVERSE STRUTS

Acceleration data, deformation patterns and force measurements all lead to the conclusion that D-2 behaves in a manner very similar to that of the base line vehicle. This conclusion implies that the improved structural performance demonstrated by the Mod. 3 cannot be achieved by the sole addition of a transverse strut between the "B" posts and reinforcement of the posts. Hence, the door beam structure included in the Mod. 3 design but omitted in the D-2 is indicated to be an integral part of the compartment reinforcing concept. Conclusions regarding correlation and interpretation of accelerometer data are contained in Appendix B.

9. MOD. 3A(1) VEHICLE

The Mod. 3A series consists of two vehicles designated as 3A(1) and 3A(2). Both vehicles were constructed essentially at the same time, but moderate changes were possible in the second vehicle (Mod. 3A(2)) depending on the test results of the first vehicle.

The primary objective of the Mod. 3A, as discussed in Section 6, is to improve load distribution and energy absorption capability in side impacts by modifying a perimeter frame structure. The general design philosophy is discussed in Section 6.2. Here design details are given, results of a 20 MPH side impact with a rigid pole are presented and the structural performance of the Mod. 3A(1) is evaluated.

9.1 Design Details

In the developmental side test (D-2), the impact pole was instrumented to obtain the time variation of the pole force on the vehicle. The maximum load was somewhat less than 45 kips. Since this was shown to generally agree with the accelerometer data, it was accepted as the peak load on the vehicle. As a preliminary step in determining the loading condition for the various frame members, the distribution of the total load along the vertical face of the vehicle shown in Figure 9-1 was assumed. It was further assumed that the division of the load between the impacted side and the nonimpacted side of the vehicle was in the ratio of 2 to 1. These assumptions enabled the apportionment of the total load to the various structural members. Conventional techniques were then used to select the member sizes and their connections.

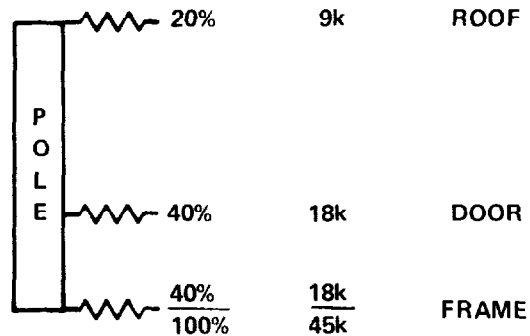


Figure 9-1 ASSUMED VERTICAL DISTRIBUTION OF POLE FORCE

Referring to Figure 6-5, which illustrates the structural concept and indicates cross-sectional sizes of the added components, the frame side rails and energy-absorbing knee-shaped cross members are shown to be fabricated from 3I5.7 (I-beam) structural steel. "B" posts were also reinforced using 3I5.7 beams. A 4 x 4 x 3/16 box beam was built into the impact side "A" post to carry load applied to the door into the main frame. The effect of including a practicable reinforced door was simulated by adding a beam between the stiffened "A" and "B" posts through the conventional door. Arcuated lateral struts fabricated from 1-5/8" O.D. pipe connect the stiffened "B" posts at roof level. These struts are intended to serve the dual purpose of absorbing energy in side impacts and providing additional rollover protection.

Photographs of the forward and rear knee-shaped struts between the frame side rails are shown in Figure 9-2. Figure 9-3 shows the redesigned torque box section and the frame connected "A" post reinforcing structure. The overall modified frame is shown in Figure 9-4.

This problem was addressed by the Mod. 3 design concept discussed in Section 6.1.

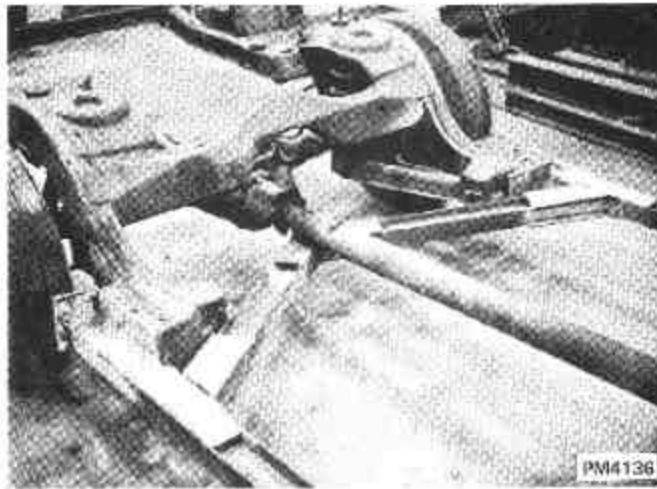
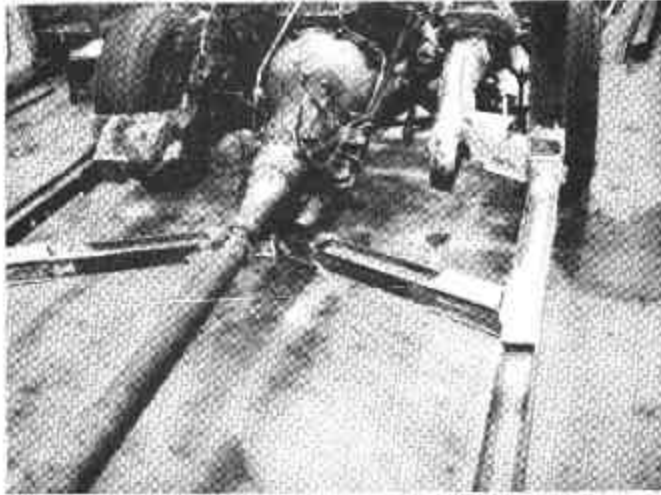


Figure 9-2 FORWARD AND REAR KNEES

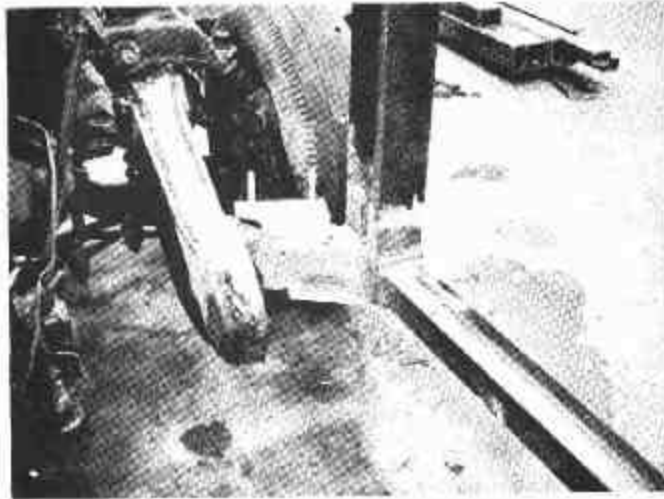


Figure 9-3 DETAIL AT "A" POST

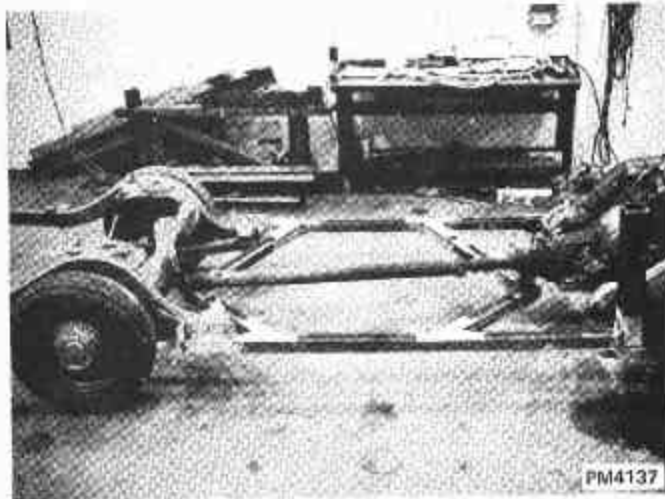


Figure 9-4 MODIFIED FRAME

A number of compromises were necessary in the design to expedite actual construction of the vehicle. Figure 6-5 shows that the outer periphery of the vehicle is 7-1/2 inches outboard of the vehicle frame. Ideally, it would be desirable to engage the heavier frame member at the earliest possible instant in the impact, i. e., the frame side rails should be at the outer periphery of the vehicle. Since the body has been designed to mate with the existing frame dimensions, a considerable effort would be required to rework the body structure if the frame width were increased, thus, it was decided to observe test results of the simpler modification before considering more extensive changes. Also, due to the interference of the drive shaft both the forward and rear knees between the side rails were sloped downward. Since this introduced weak axis bending and torsional moments in the knee, straps were added to tie the knees to the floorpan of the body.

9.2 Test Results

The Mod. 3A(1) vehicle was impacted laterally into the CAL pole barrier at a speed of approximately 21.7 MPH. Contact with the pole occurred at about 4 inches forward of the center of the right front door. Additional test data and related information are contained in Appendix C.

Acceleration data from three different sensor locations in the vehicle are presented in Figure 9-5. These data were taken directly from oscillograph traces which contained some filtering due to the frequency response characteristics of the galvanometers. The actual cutoff frequency corresponding to each trace is noted in the figure. Accelerations from the "standard" sensor located under the driver's seat on the floorpan are shown at the top of the figure.

Based on trip switch data (+0.5 MPH estimated accuracy).

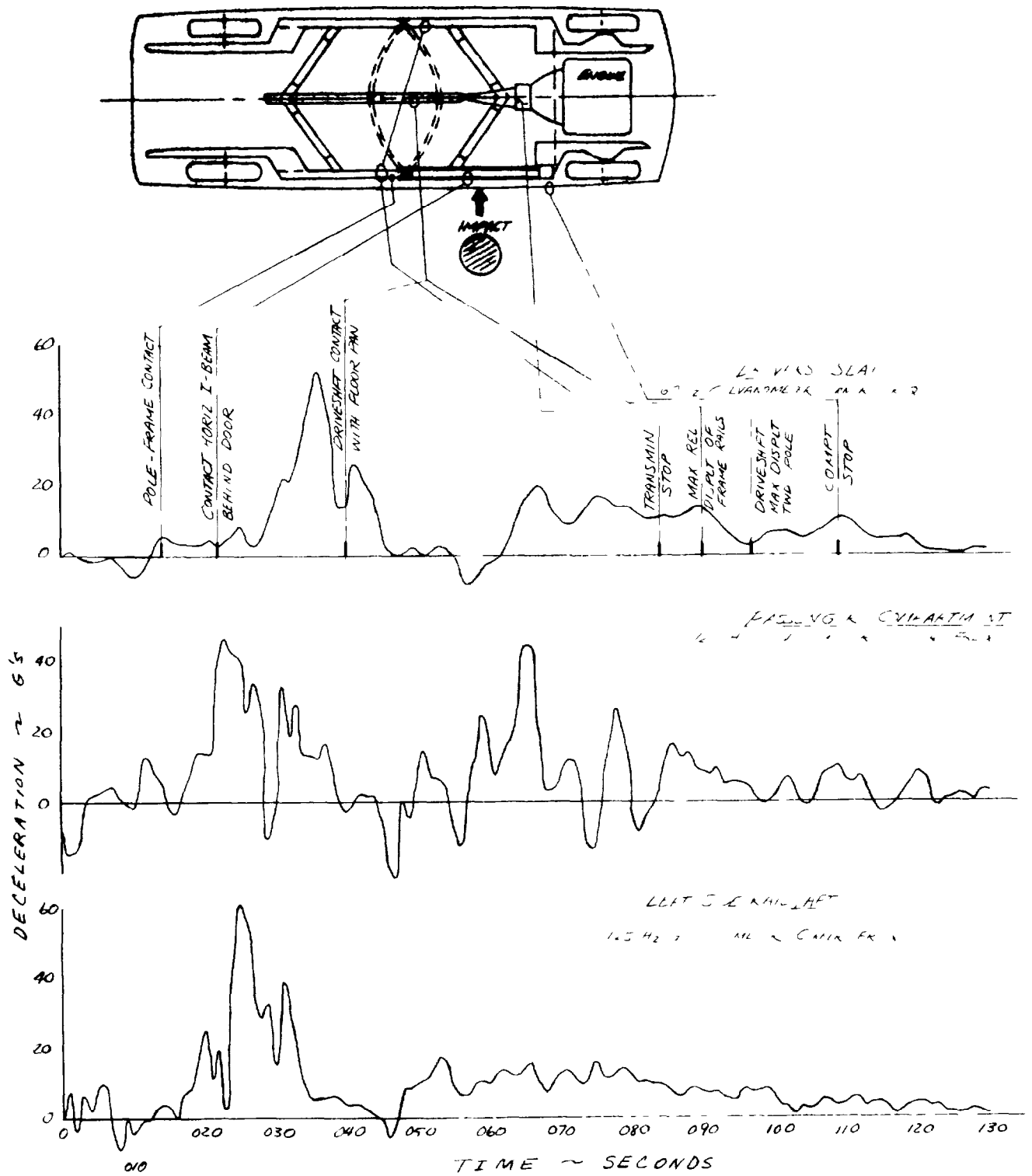


Figure 9-5 MOD. 3A(1) TEST: VEHICLE ACCELERATION DATA

Times of significant events obtained from film analysis are marked along the abscissa in Figure 9-5 and are related to various points on the vehicle through the sketch at the top. Passenger compartment motion toward the impact pole was noted to stop at approximately .109 second.

Acceleration data from the remaining four on-board sensors were less significant in this test and are not presented. The locations of these sensors were on top of the engine block, on the right side rail near the aft torque box, on the left side rail near the "B" post and on the rear frame.

Filtered and unfiltered acceleration data from the driver's seat position are presented in Figure 9-6 along with associated velocity and displacement curves. A 50 Hz cutoff and 100 roll-off frequency low pass filter was used. The velocity and displacement curves were obtained by integration of the acceleration trace. A maximum filtered deceleration of 42 g's was obtained at approximately .036 seconds. Also, the maximum dynamic displacement of the sensor under the driver's seat was computed to be approximately 23 inches compared to a measured permanent deformation of 19 inches. A graph of filtered acceleration of the driver's seat versus computed displacement is shown in Figure 9-7.

Time histories of forces in the impacted pole from top and bottom mounted load cells (in line with the impact) are presented in Figure 9-8. A peak total load of approximately 102,000 lbs occurred at .028 second. Lateral loads on the pole were small in comparison to the normal loads and are not presented. The peak lateral force was approximately 4800 lbs applied to the right side of the pole (south side of barrier) at .105 seconds.

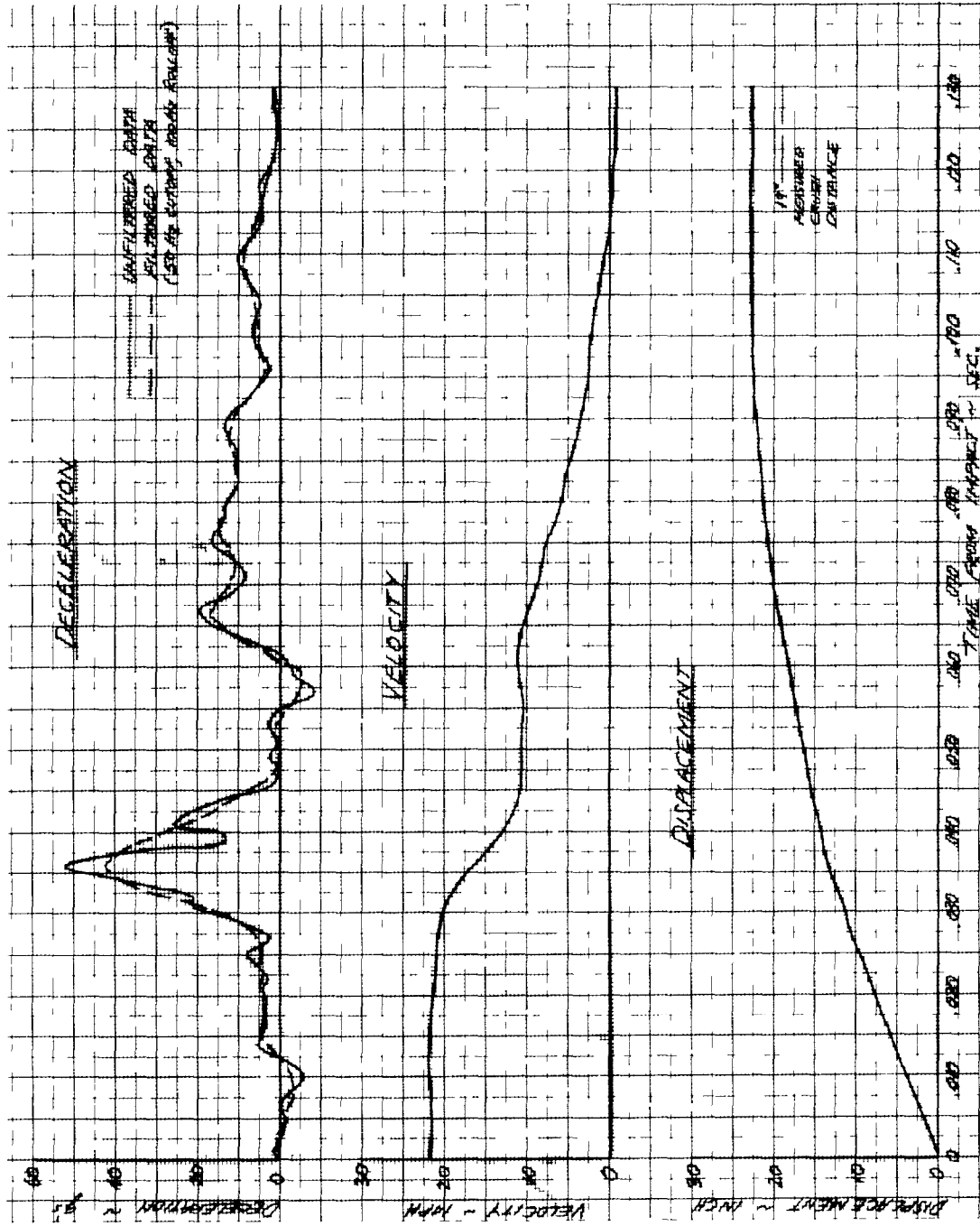


Figure 9-8 MOD. 3A(1) TEST: DRIVER'S SEAT ACCELEROMETER DATA

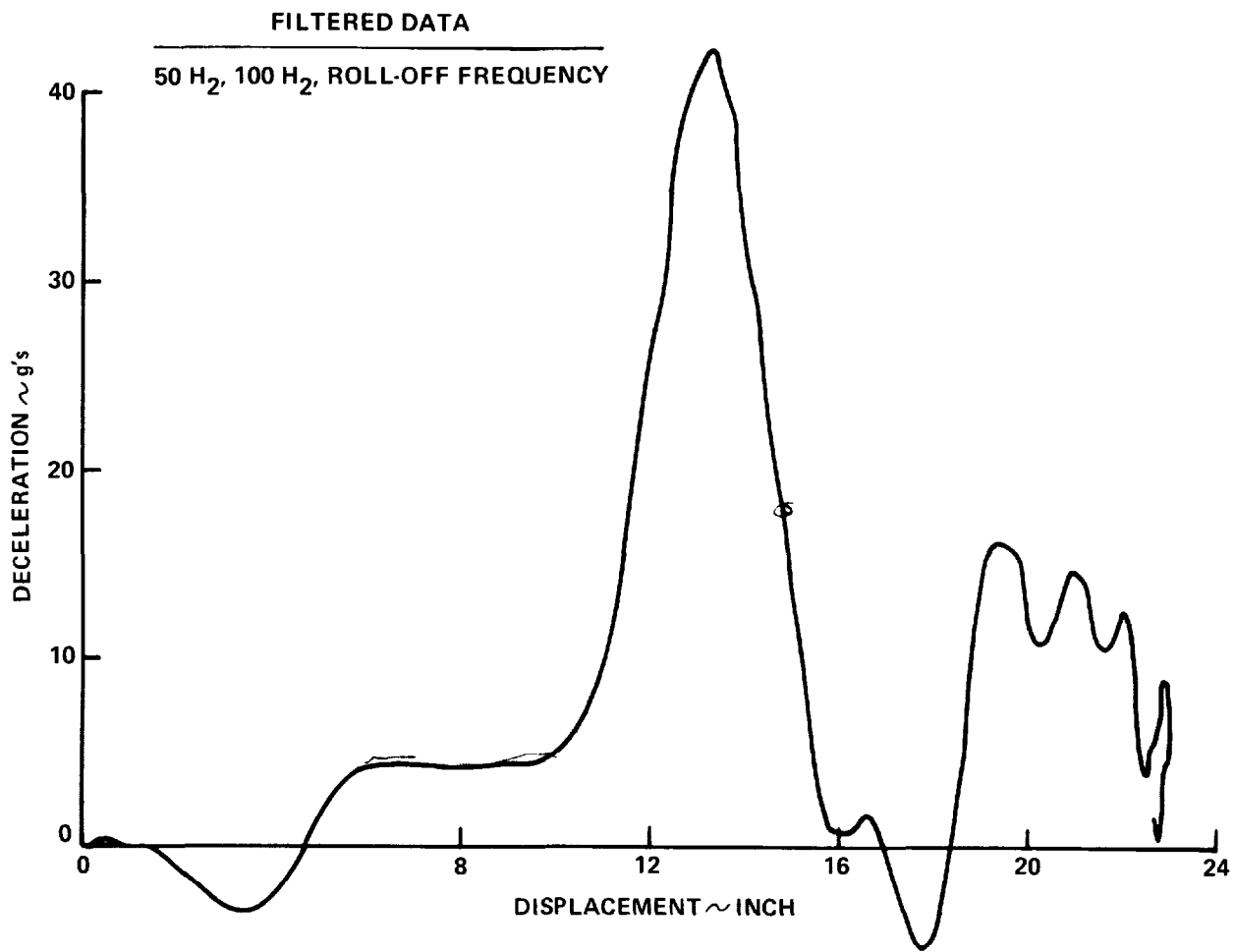


Figure 9-7 MOD. 3A(1): DRIVER'S SEAT ACCELERATION VS. DISPLACEMENT

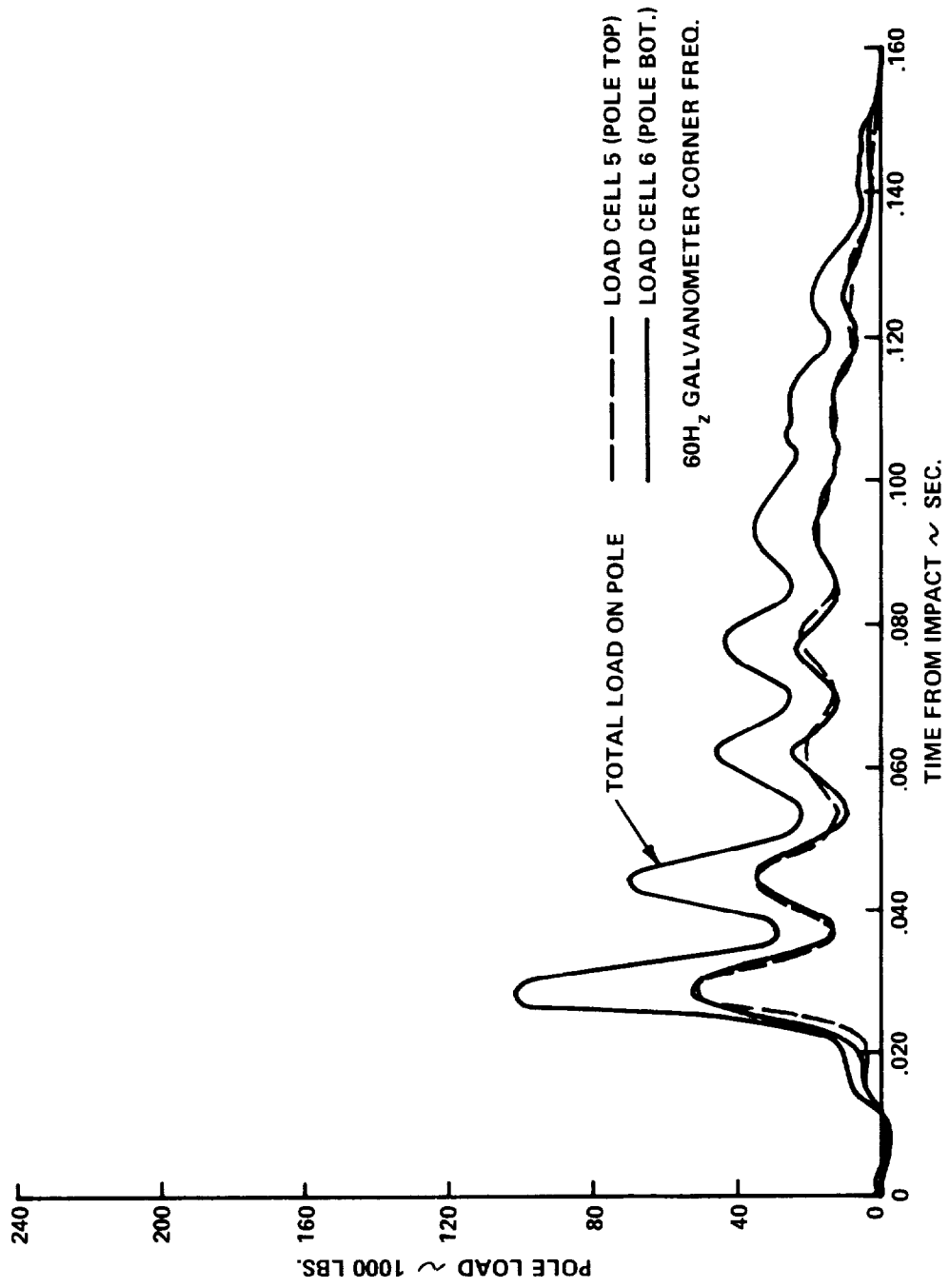


Figure 9-8 IMPACT POLE LOADS

The deformed profile of the impacted test vehicle is shown in Figure 9-9 along with a profile of an undeformed vehicle. The maximum permanent deformation of 19 inches was measured from a line connecting the front and rear fenders. Also evident is the slight bending of the total vehicle.

Photographs of the Mod. 3A(1) vehicle are presented in Figure 9-10. Figure 9-10(a) shows the car before the crash test and the remaining three photos indicate the degree of deformation obtained from the 22 MPH impact. An interior view of the impacted door and its reinforcing structure is shown in Figure 9-10(d).

9.3 Evaluation of Performance

Figure 9-11 presents a comparison of the Mod. 3A(1) and base line vehicle profiles. Permanent deformation, peak g's and impact velocity are compared with base line results below.

<u>Vehicle</u>	<u>Speed (MPH)</u>	<u>Permanent Deformation (in.)</u>	<u>Peak g's</u>
Base Line 3	21.5	24	20
Mod. 3A(1)	21.7	19	42

At driver's position (50 Hz cutoff filter).

Since the impact velocities for the Mod. 3A(1) and base line tests are very close, a straightforward comparison of performance can be made. The structural modification reduced deformation by about 5 inches; however, the twofold increase in peak g's diminishes the attractiveness of the reduced intrusion. It is apparent that deformation is not being utilized effectively, i.e., in a uniform manner. Figure 9-8 shows that no significant loads were developed during the first 20 msecs of the collision, which corresponds to about 8 inches of deformation. This fact is supported by the low level of

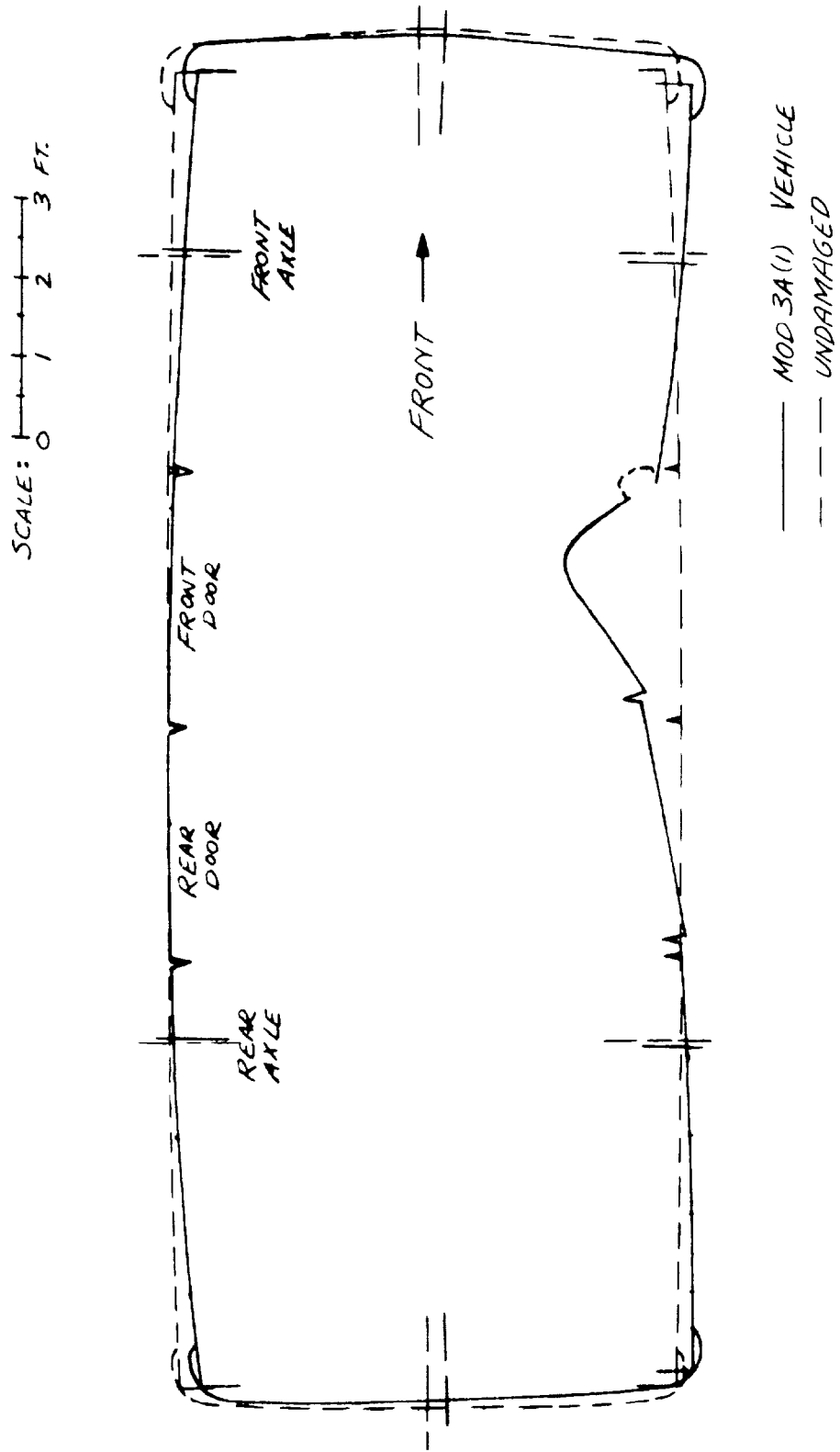
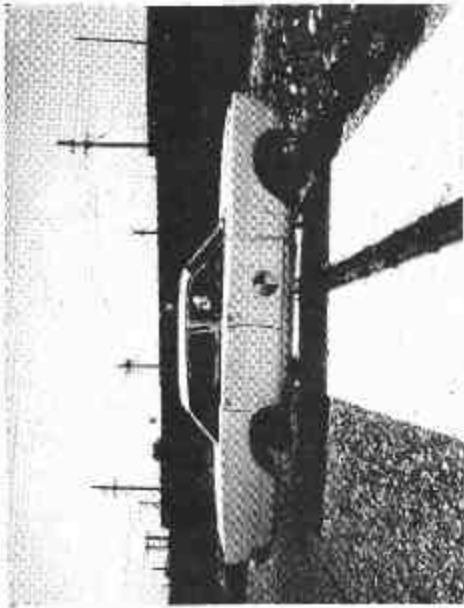


Figure 9-9 POST CRASH PROFILE OF MOD. 3A(1)



(a)



(b)



(c)



(d)

Figure 9-10 MOD. 3A(1): SIDE IMPACT WITH POLE

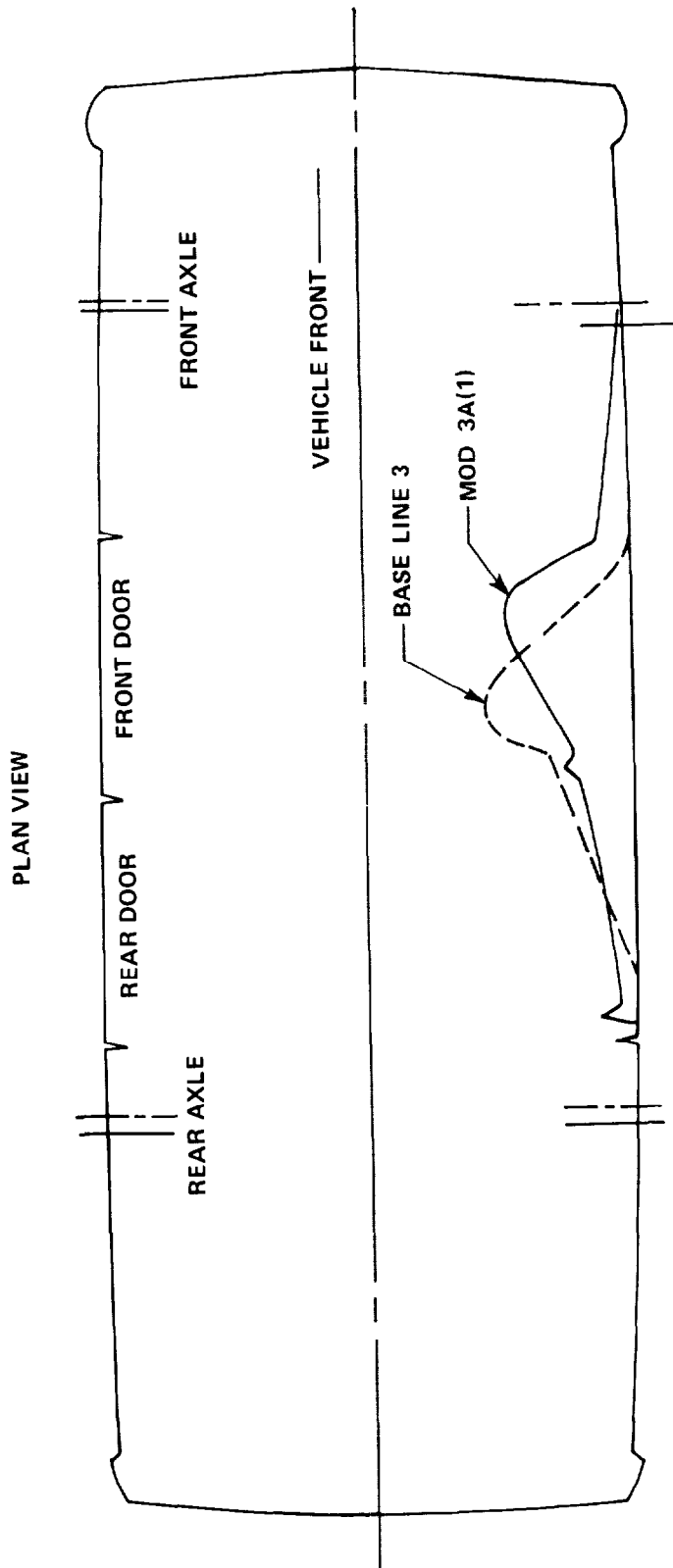
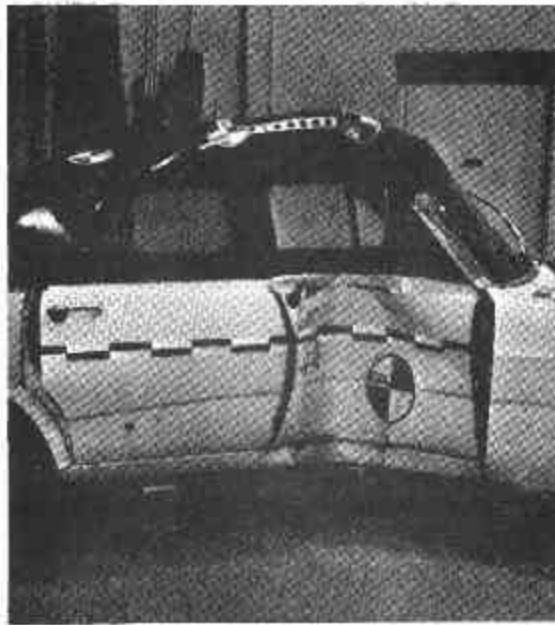


Figure 9-11 POST CRASH PROFILE OF SIDE IMPACT TESTS

deceleration at the driver's position during the first 10 inches of deformation as indicated in Figure 9-7. This behavior is largely a result of the protrusion of the body shell outside the frame perimeter, as was noted in the design discussion of Section 9.1. The abrupt bottoming against the stiffened frame side rails of the Mod. 3A(1) accounts for the high level of compartment deceleration, as compared with the response of the base line vehicle. Compartment damage for the modified and unmodified vehicles is compared in Figure 9-12.

The structural changes in the D-2 developmental vehicle were of such a minor nature that the response was very similar to that of the base line vehicle. It is convenient to compare results of the present modification with D-2 as a base line because it contained more instrumentation and pole loads were measured. Figure 9-13 is a comparison of the pole loads for the present modification and D-2 (designated as the base line vehicle). As previously indicated, the initial 20 msec of data reflects contact with the weak outer door panel and is the same for both vehicles. The large spike in the pole load for the modified structure coincides approximately with contact of the pole with the 4 inch I-beam through the door and the 3 inch I-beam side rail. Such contact, however, does not adequately explain the cause of the very large forces since the combined theoretical collapse load of these members is 45 kips, based on static loads and previous test data. The period from 50 msec to approximately 90 msec shows an oscillation about a constant load of 36 kips. From the underside camera, this period is when collapse of the knee struts joining the side rails occurs. Comparison of 25 Hz filtered data from accelerometers placed on the frame away from the impact side, Figure 9-14, indicates the same relative behavior. The modification behaves initially as the base line vehicle, following a large spike at 25 msec there is a constant deceleration thereafter.



(a) BASE LINE 3



(b) MOD,3A(1)

Figure 9-12 COMPARISON OF COMPARTMENT DAMAGE

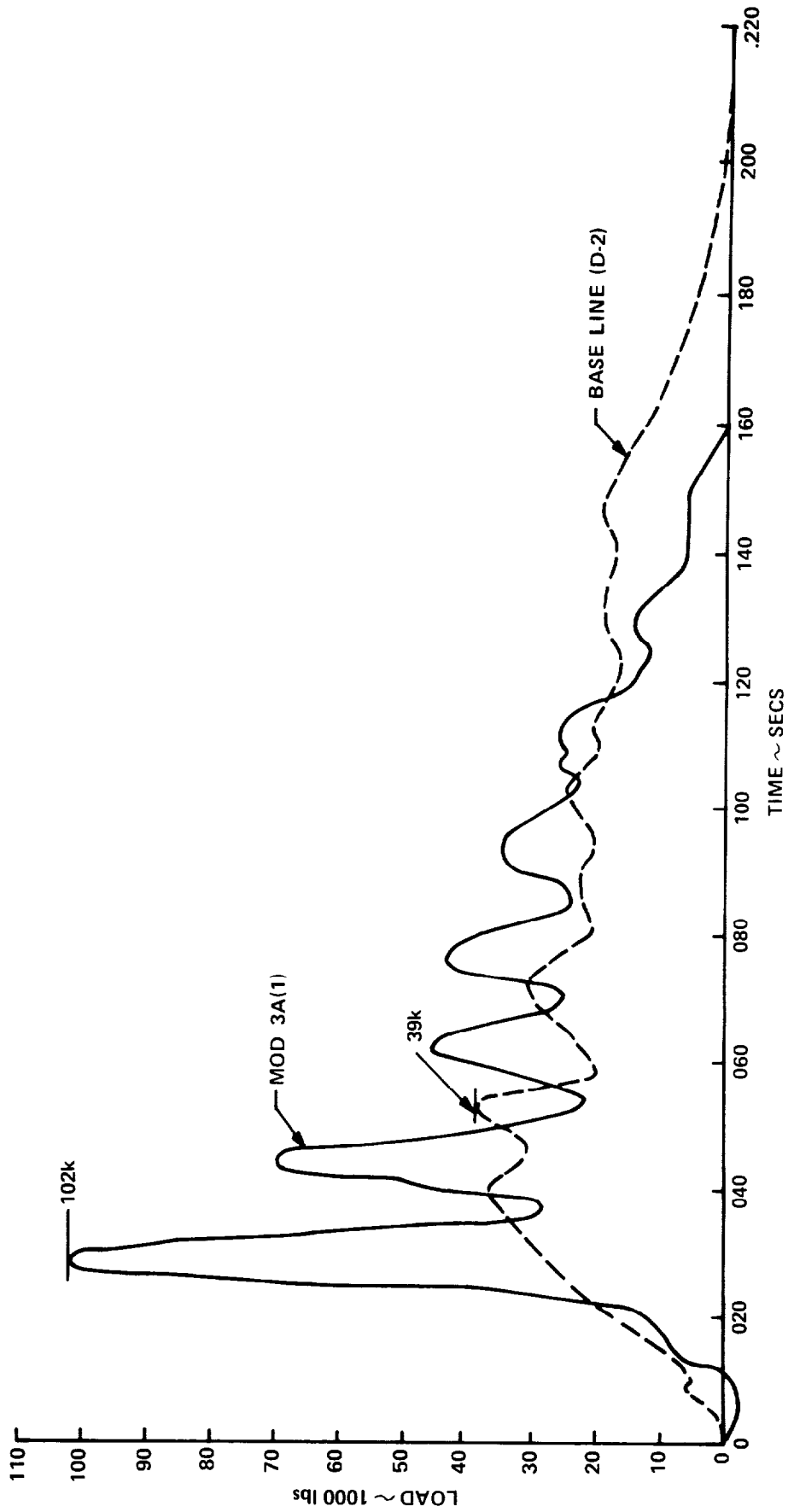


Figure 9 13 SIDE IMPACTS COMPARISON OF POLE FORCES

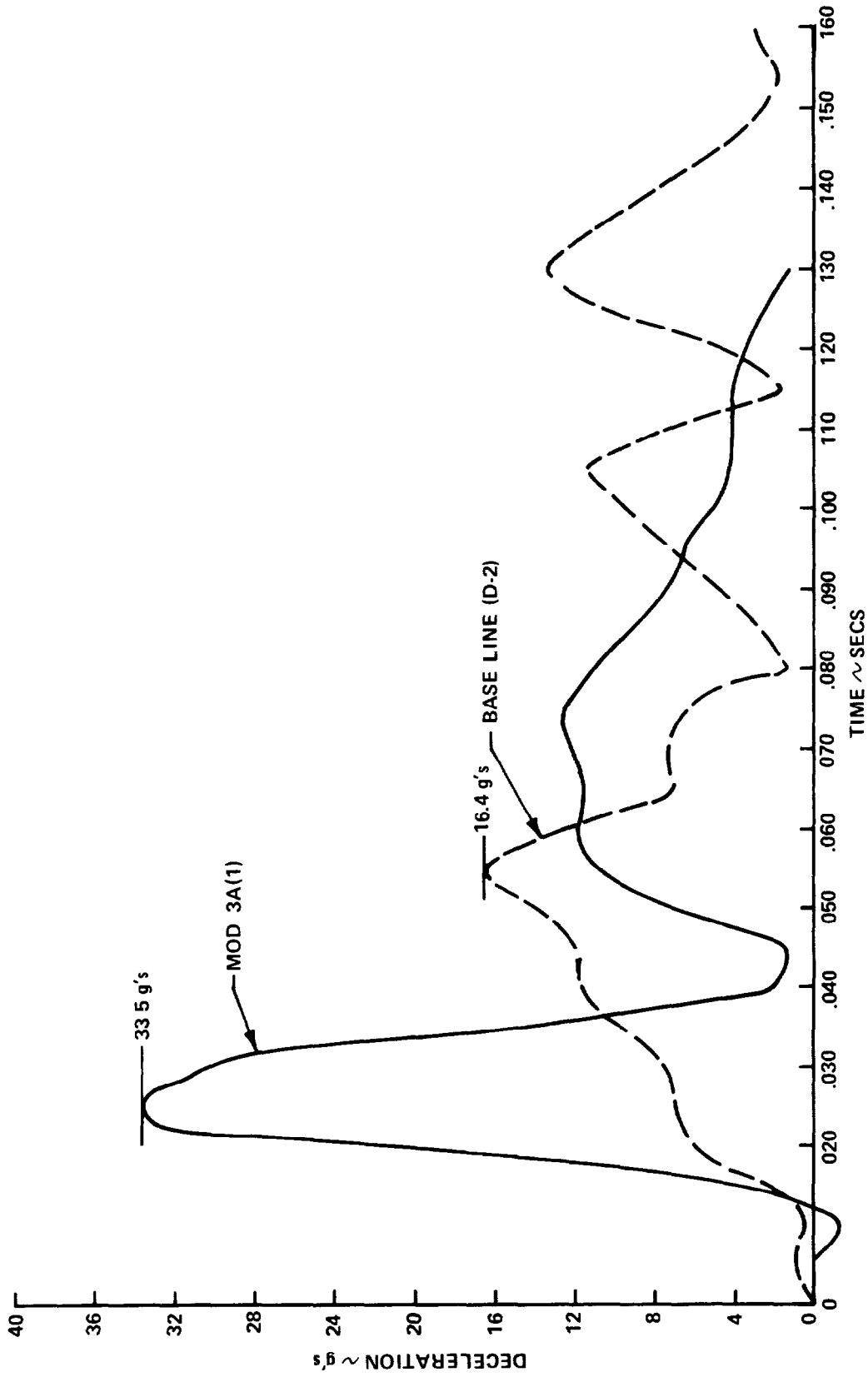


Figure 9-14 COMPARISON OF FRAME ACCELERATION (NONIMPACT SIDE) 25 Hz FILTER

Post-crash examination and high speed camera data were studied to determine to what extent the design objectives were realized. Figure 9-15 is a photo showing the forward and rear knee struts joining the side rails. It is evident from the photograph and also from the underside movie that both struts behaved generally as intended. The rear knee participated in absorbing energy although it is removed from the impact point. Deformation of the rear knee can be seen in the photo. Figures 9-17(a) and 9-17(b) are close-in photographs of the impact and nonimpact side of the forward strut. Figure 9-17(a) shows the plastic hinge formed in the side rail at the impact point and also the twisting effect in the strut caused by the necessity to dip under the drive shaft. Figure 9-17(b) is a photograph of the portion of the strut away from the impact showing the broken straps which tied the strut to the floorpan. The deformation of the side rail away from the impact is also visible. Comparison of the deformation pattern of the knees with that observed in the static test (Figure 9-16) tends to indicate that the desired constant load response of the knee struts occurred.

Figure 9-18 is a post-crash photo of the split roll bar, which failed to yield or to absorb energy during the impact. This behavior is attributed to excessive twisting of the I-beam used for the "B" post (see Figure 9-10 (d)). This implies that either the I-beam is too weak in torsion or the roll bar structure is too stiff. Although the roll bar did not operate as planned, it was only a proportionally small feature of the whole, the frame modification being the salient feature.

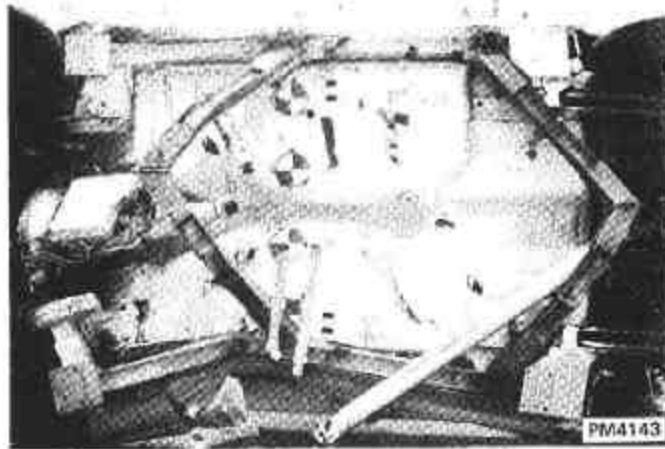


Figure 9-15 FRAME DAMAGE - OVERALL

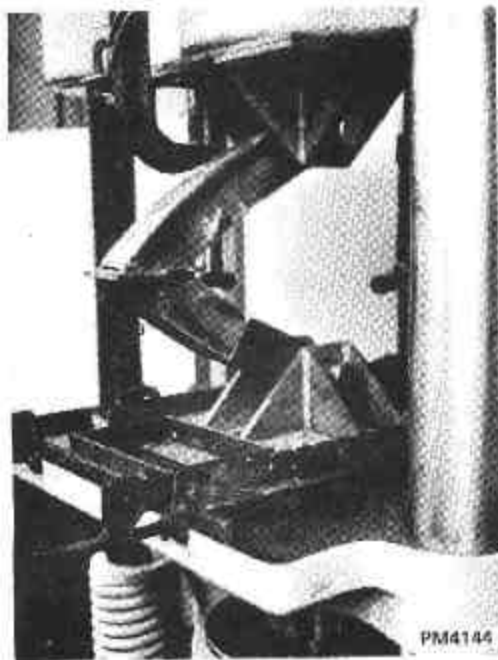
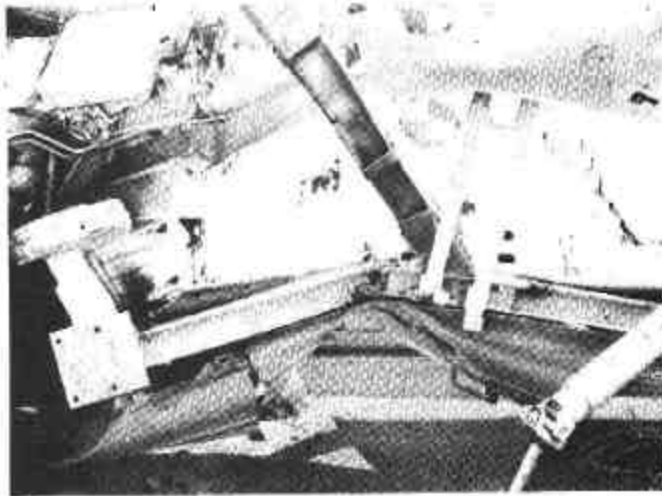
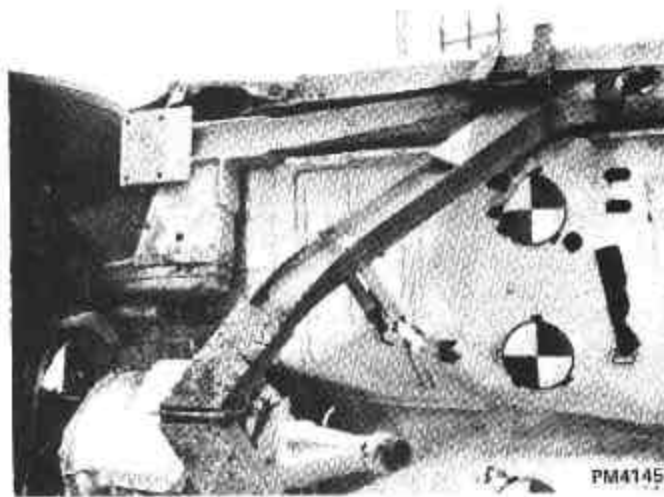


Figure 9-16 DEFORMED SHAPE OF I-BEAM KNEE
STIFFENED WITH WEB PLATES



(a) FORWARD KNEE IMPACT SIDE



(b) FORWARD KNEE NON-IMPACT SIDE

Figure 9-17 FRAME DAMAGE

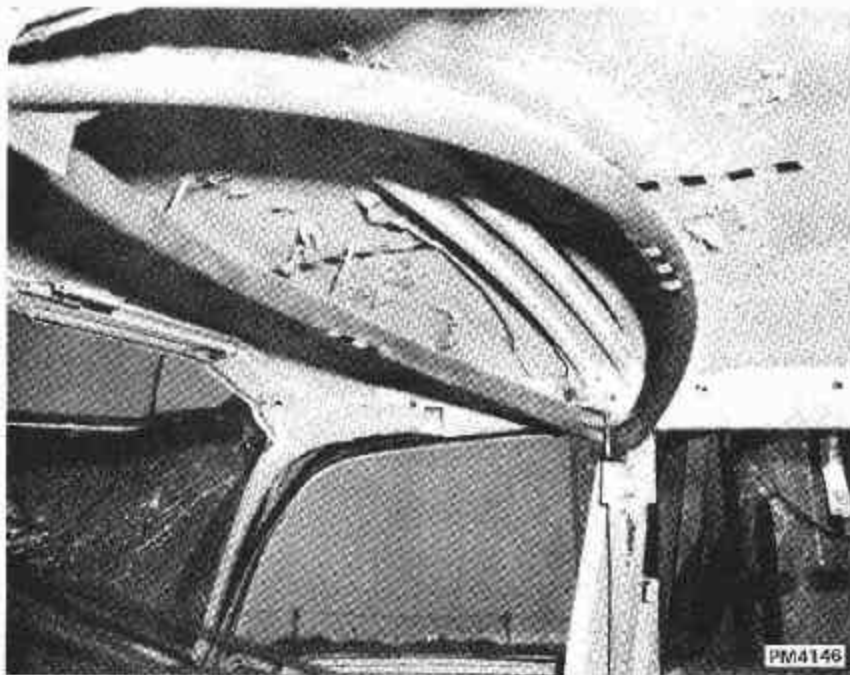


Figure 9-18 ROLL BAR AFTER IMPACT

In the very limited space available in side impacts with fixed objects, failure to develop significant crush resistance as early as possible is concluded to be a serious design defect. Possible solutions would be to extend the width of the frame side rails to the outer periphery of the vehicle or to substantially reinforce the body shell, particularly the outer door sheet metal. The first approach (extending the frame side rails) is believed to be the more reasonable of the two. The design of the Mod. 3A sister vehicle, Mod. 3A(2), will incorporate changes based on these results in an attempt to improve structural performance, particularly deceleration uniformity. For example, the design will be changed to prevent twisting of the "B" post. Major changes cannot be made, however, since the Mod. 3A(2) vehicle was partially fabricated along with the Mod. 3A(1).

10. MOD. 3A(2) VEHICLE

In this section, detailed changes in the Mod. 3A structural concept which are incorporated into the design of the Mod. 3A(2) are described, test results are presented and the structural performance of the Mod. 3A(2) is discussed. The general design philosophy for the Mod. 3A frame modification concept is presented in Section 6. In particular, it may be helpful to refer to Figure 6-5, which illustrates the structural modifications.

10.1 Design Changes Based on Mod. 3A(1) Results

As previously stated, Mod. 3A(1) and 3A(2) are substantially the same structural concept. Completion of the latter vehicle was purposely delayed to permit minor changes based on the results of the Mod. 3A(1) test. Since the design objectives, loads and most of the features are the same for both vehicles, the present description will concentrate on the differences between the vehicles.

- The 315.7 "B" post which was obviously weak in torsion has been replaced by a 3 x 3 x 3/16 tube.
- In order to develop high forces early in the collision, wood blocking (Figure 10-1) was fitted between the I-beam and the outer door panel at the point of impact. This configuration is not intended to represent a realistic door design, but only to demonstrate the effect of stiffening the outer periphery of the vehicle.

Extending the frame side rails outward to increase effective deformation would have required a substantial amount of redesign and fabrication effort.

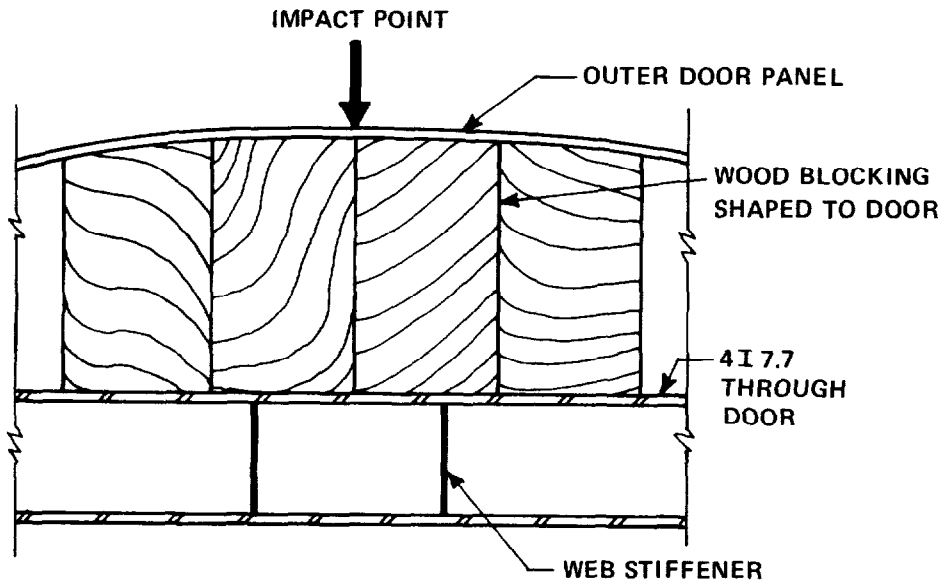


Figure 10-1 HORIZONTAL SECTION THROUGH DOOR

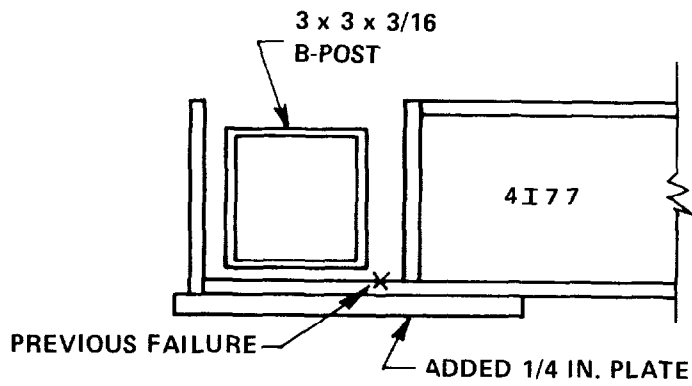


Figure 10-2 B-POST/DOOR BEAM DETAIL

- The connection between the I-beam through the door and the "B" post was strengthened by adding a plate (see Figure 10-2). In the previous test, excessive rotation occurred at the point indicated in the figure. The free connection is intended to simulate a positive latching mechanism for transmitting high loads.
- Light clip angles were added to the connection where the split roll bar joins the top of the "B" post to reduce sideways of the roll bar that was observed in the Mod. 3A(1) test from an on-board high speed camera.

10.2 Test Results

The Mod. 3A(2) vehicle was impacted laterally into the CAL pole barrier at a speed of approximately 20.5 MPH. Contact with the pole occurred very close to the center of the right front door. Pertinent test data and related information are contained in Appendix C.

Acceleration data from three different sensor locations in the vehicle are presented in Figure 10-3. These data were taken directly from oscillograph recordings which contained some filtering due to the frequency response characteristics of the galvanometers. The actual cut-off frequency associated with each trace is noted in the figure. Accelerations from the sensor position under the driver's seat on the floorpan are shown at the top of the figure. Times of significant events as determined through film analysis are marked along the abscissa in Figure 10-3 and are related to various points on the vehicle through the sketch at the top. Passenger compartment motion toward the impact pole was noted to stop at approximately .097 seconds. Acceleration data from the remaining three on-board sensors were less significant in this test and are not presented.

Based on trip switch data (+0.5 MPH estimated accuracy).

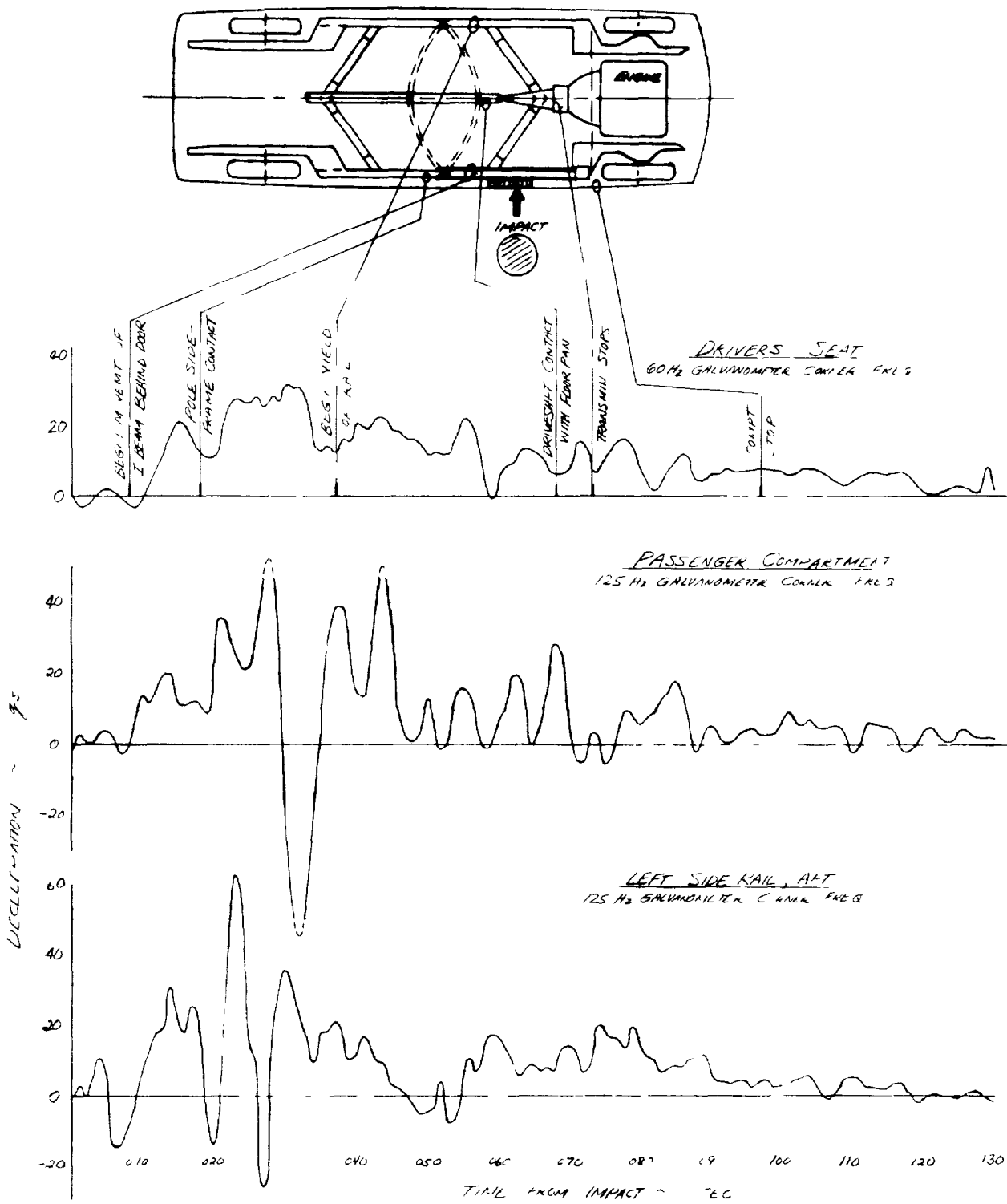


Figure 10-3 MOD. 3A(2) TEST: VEHICLE ACCELERATION DATA

Filtered and unfiltered acceleration data from the driver's seat position are presented in Figure 10-4 along with associated velocity and displacement curves. A 50 Hz cutoff and 100 Hz roll-off frequency digital filter was used to process the data. The velocity and displacement curves were obtained by integration of the acceleration trace. A maximum filtered deceleration of 29.5 g's is indicated at approximately .028 seconds.

The calibration factor used in the conversion of the raw oscillograph data to the acceleration data (driver's seat sensor) possibly contained some error. This is indicated by the resulting vehicle velocity obtained by integrating the acceleration data over the collision time interval. The calculated residual vehicle velocity or rebound velocity, in this case, was 9.9 MPH, which is high compared to the rebound velocity of 3.0 MPH measured from the photographic data. Also, the calculated vehicle stopping time of .063 seconds appears early compared to previous tests and the photographic time of .097 seconds. For these reasons, the unfiltered acceleration curve (Figure 10-4) should be shifted downward about 2 or 3 g's to show agreement with the photo data. A graph of filtered acceleration of the driver's seat versus computed displacement is shown in Figure 10-5. This plot exhibits low values of displacement which further indicates that the deceleration shown may be somewhat high.

Time histories of forces in the impacted pole from top and bottom mounted load cells (in line with the impact) are presented in Figure 10-6. A peak total load of approximately 82,000 lbs occurred at .031 seconds. Lateral loads on the pole were small in comparison to the normal loads and are not presented.

The deformed profile of the impacted test vehicle is shown in Figure 10-7 along with a profile of an undamaged vehicle. The total permanent deformation of 15 inches can be noted in the door when measured from a line connecting the front and rear fenders. Also evident is the slight bending of the total vehicle.

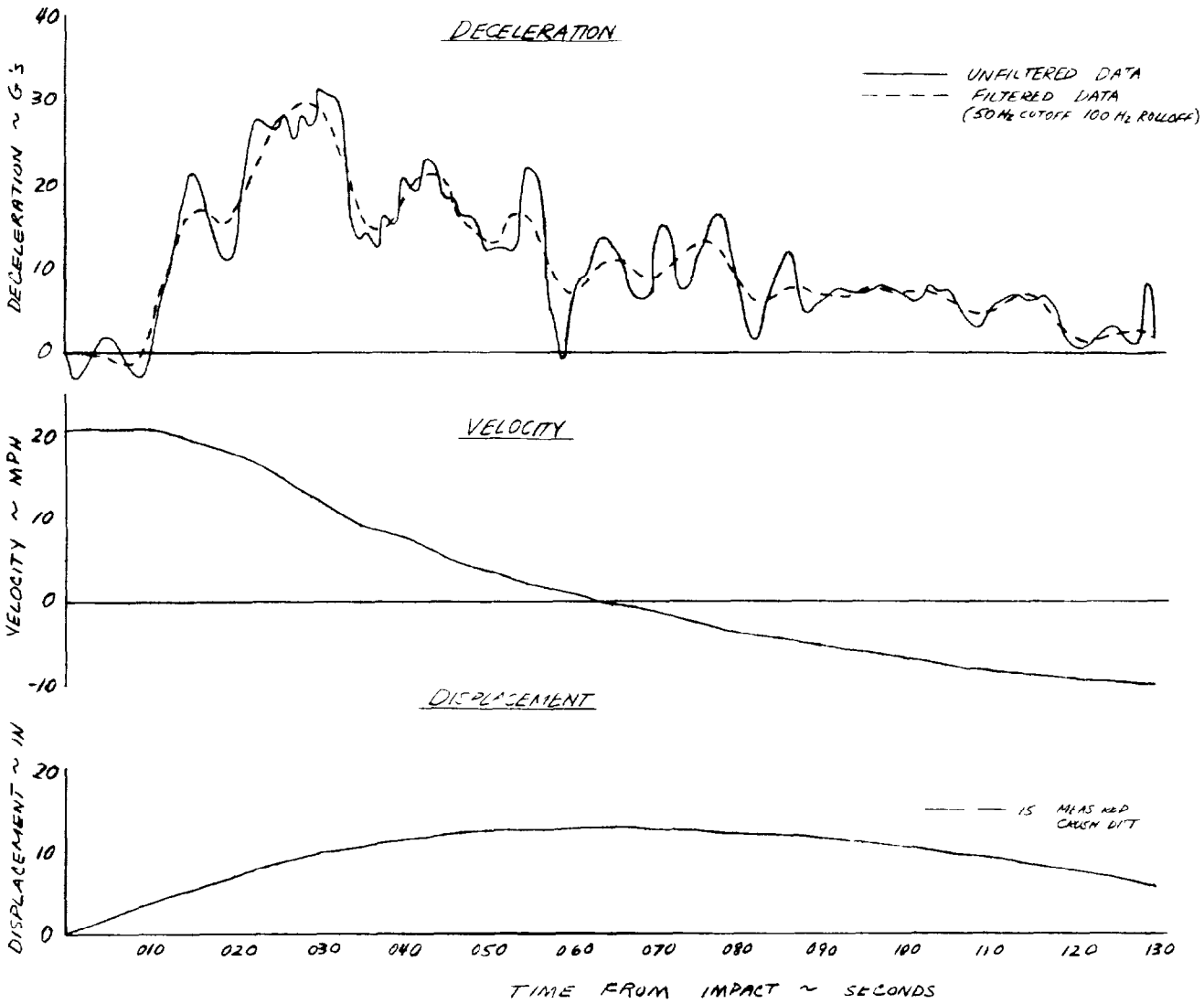


Figure 10-4 MOD. 3A(2) TEST: DRIVER'S SEAT ACCELEROMETER DATA

FILTERED DATA
5 Hz CUT OFF, 100 Hz ROLLOFF FREQ.

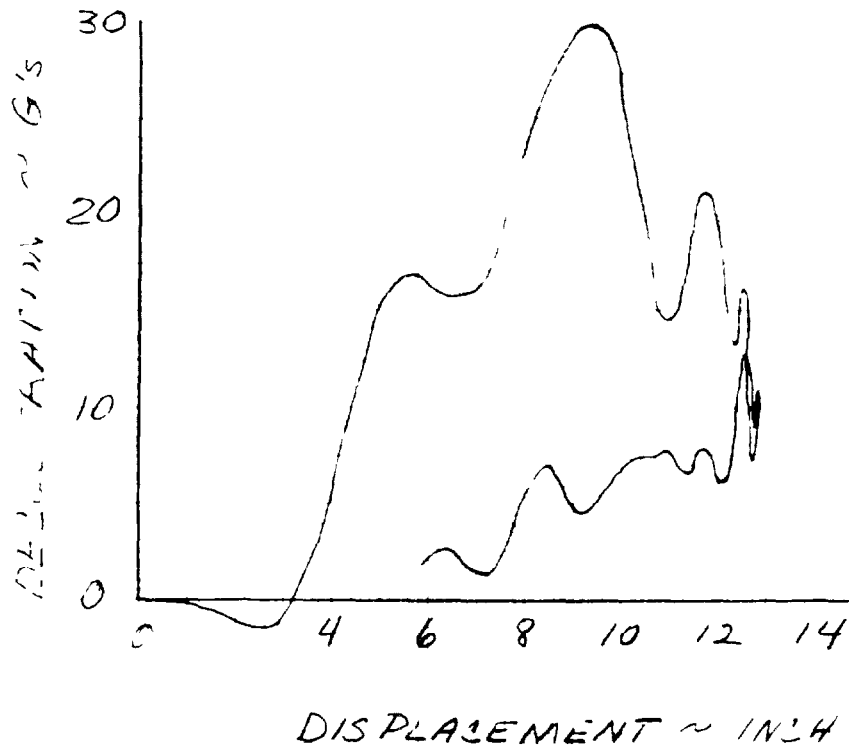


Figure 10-5 MOD. 3A(2): DRIVER'S SEAT ACCELERATION VS DISPLACEMENT

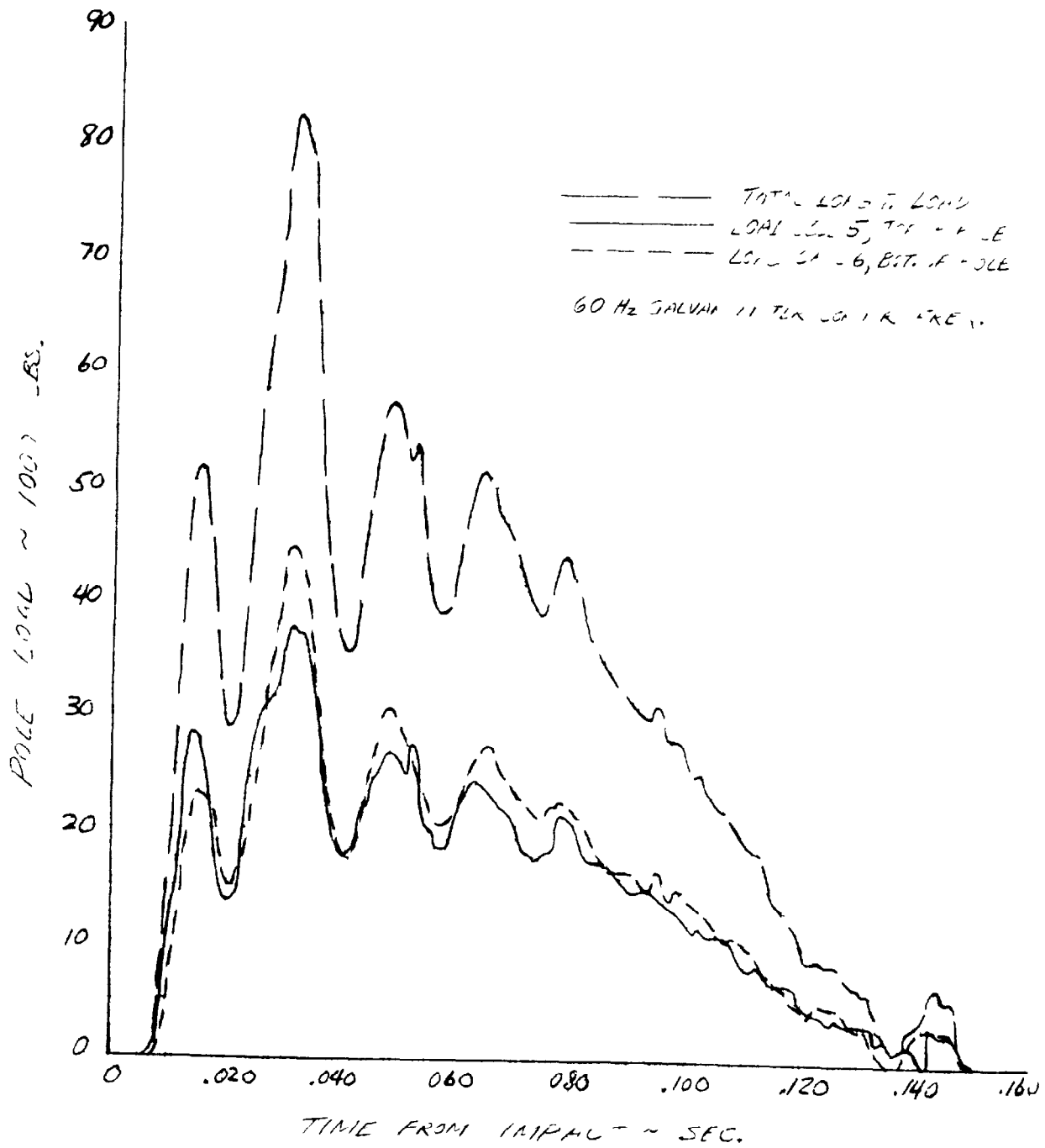
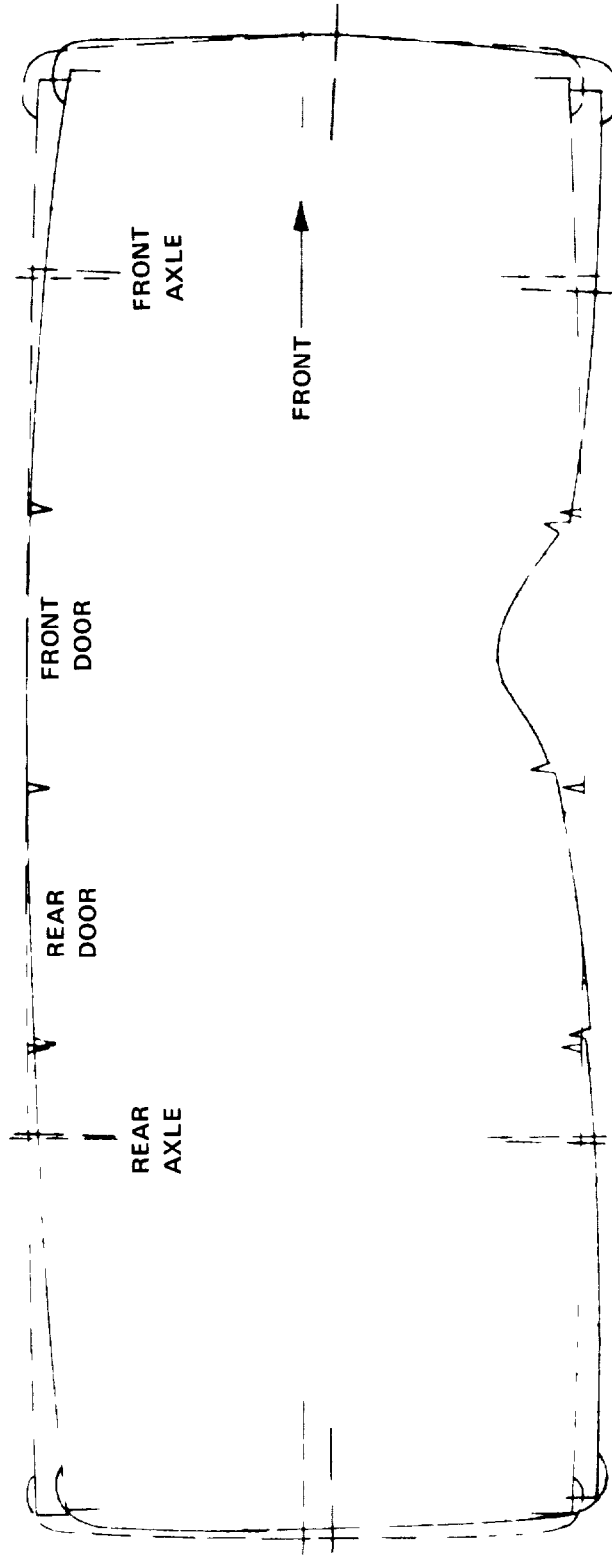


Figure 10-6 IMPACT POLE LOADS

SCALE 0 1 2 3 FT.



MOD 3A(2) VEHICLE
UNDAMAGED

Figure 10-7 TOP PROFILE COMPARISON OF MOD. 3A(2) AND STANDARD VEHICLE

Photographs of the Mod. 3A(2) vehicle are presented in Figure 10-8. Figure 10-8(a) shows the car before the test and the remaining three photos indicate the degree of deformation resulting from the impact. Note in Figure 10-8(c) that the pole penetrated inward only as far as the roof line.

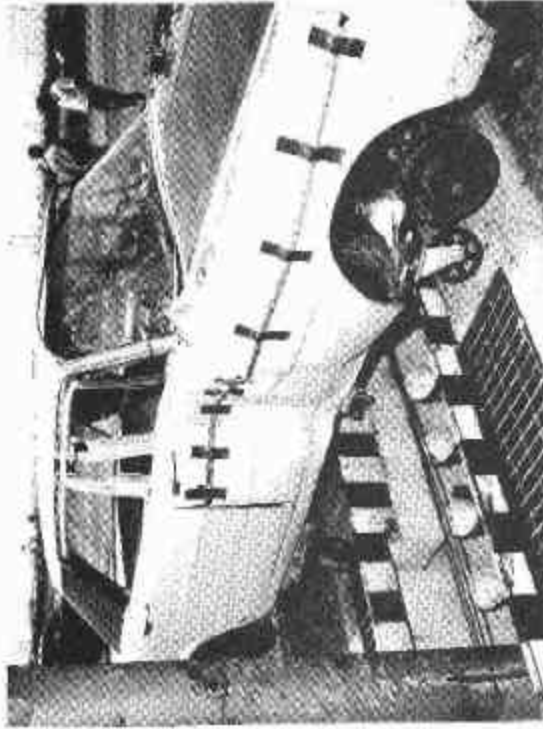
10.3 Evaluation of Performance

Figure 10-9 compares the localized deformation profile of the Mod. 3A(2) with the base line and Mod. 3A(1) profiles. It is apparent that compartment intrusion has been reduced by the Mod. 3A(2). Permanent deformation, peak g's and impact velocity for these three vehicles are compared below.

<u>Vehicle</u>	<u>Speed (MPH)</u>	<u>Permanent Deformation (in.)</u>	<u>Peak g's</u>
Base Line 3	21.5	24	20
Mod. 3A(1)	21.7	19	42
Mod. 3A(2)	20.5	15	30

At driver's position (50 Hz cutoff filter).

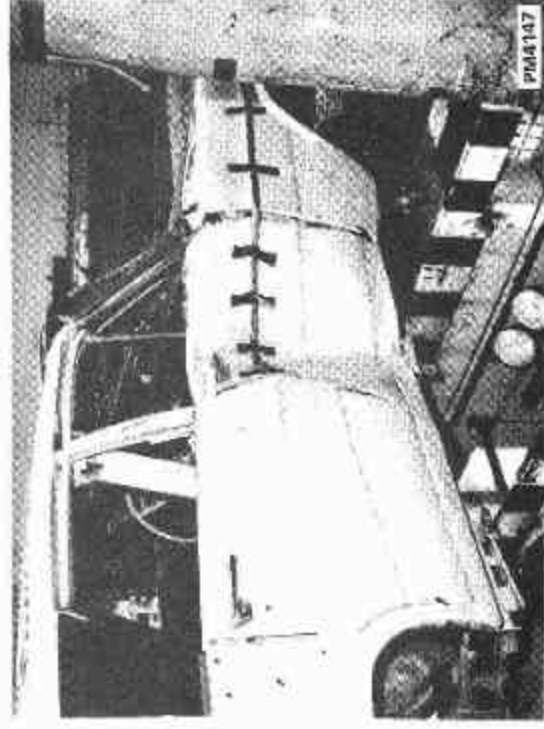
Since both deformation and peak g's of Mod. 3A(2) have been reduced from the Mod. 3A(1) performance, an improvement in structural design has been achieved; the small velocity difference is not likely to have affected gross performance significantly. A substantial reduction in compartment intrusion has been demonstrated when compared with the base line vehicle collapse; however, peak g's are still higher, but not to the drastic extent of the Mod. 3A(1). An improvement in passenger compartment deceleration uniformity has certainly been made, as Figure 10-4 shows. The nominal 20 g response between 10 and 55 milliseconds is particularly impressive.



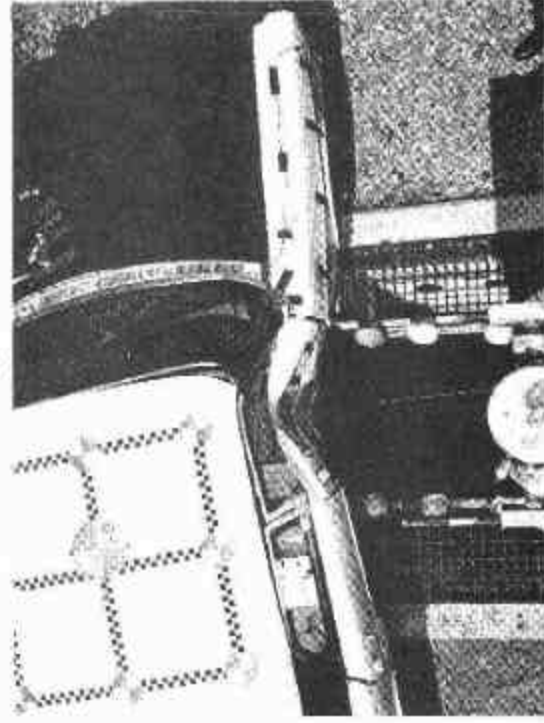
(a)



(b)



(c)



(d)

Figure 10-8 MOD. 3A(2); SIDE IMPACT WITH POLE

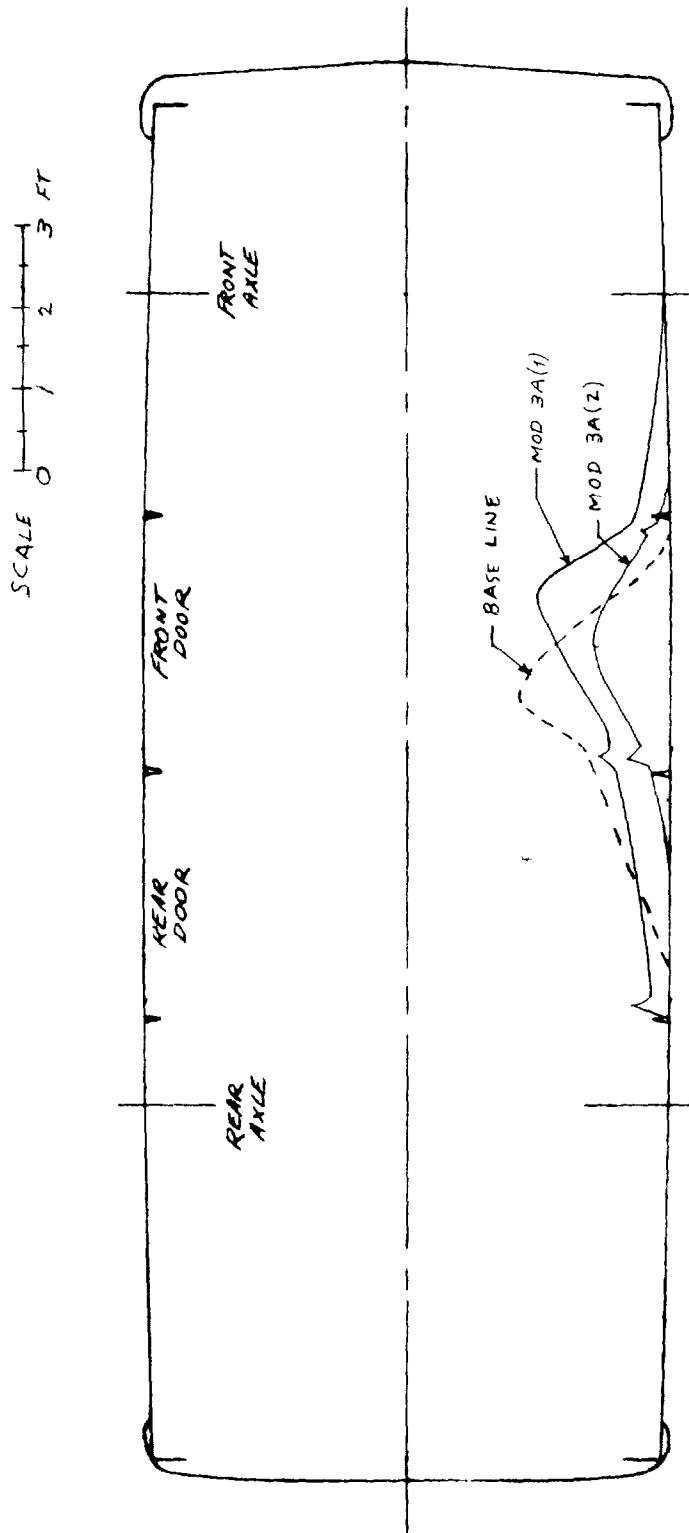


Figure 10-9 POST CRASH PROFILE OF SIDE IMPACT TESTS

The initial period of small resistance and deceleration which characterized the 3A(1) performance and which contributed to increased penetration has been significantly reduced. All three acceleration histories of Figure 10-3 show initial rise times in the vicinity of .015 second as compared to rise times from .020 to .035 second for the Mod. 3A(1). The event times of Figure 10-3 suggest that the first deceleration peak is due to the action of the upper door structure which has been brought into play early in the collision by the addition of the wood blocking, the second peak, from .020 to .035 second, occurs during action of the main frame. The load cell data, Figure 10-6, also exhibit the dual peak phenomenon. To achieve a more constant deceleration response, the above results indicate that the frame structure should be weaker and should also be contacted earlier.

Figure 10-10 is a comparison of measured pole forces where, as in the previous test, the developmental test (D-2) is treated as a base line. The effect of the increased stiffness of the Mod. 3A(2) is seen in the shorter rise time and increased load. Comparison of filtered passenger compartment acceleration data, Figure 10-11, indicates the same relative behavior.

As for Mod. 3A(1), the photographs of the deformed frame, Figure 10-12, present evidence of effective distribution of the loads to the non-impact side of the frame and substantial energy absorption by the knee-shaped frame cross members. Figure 10-13 shows the hinge formed at the center of the square tube serving as the "B" post. The interior photo, Figure 10-13(B), also shows the arcuated roll bar which again failed to yield or absorb energy. However, post-collision examination of the roll bar structure and analysis of high speed movies from an on-board camera (which showed 1 inch maximum separation at center) reveal that yielding was incipient. The roll bar is, therefore, too strong for effective energy

Pole forces were not measured for Base Line 3.

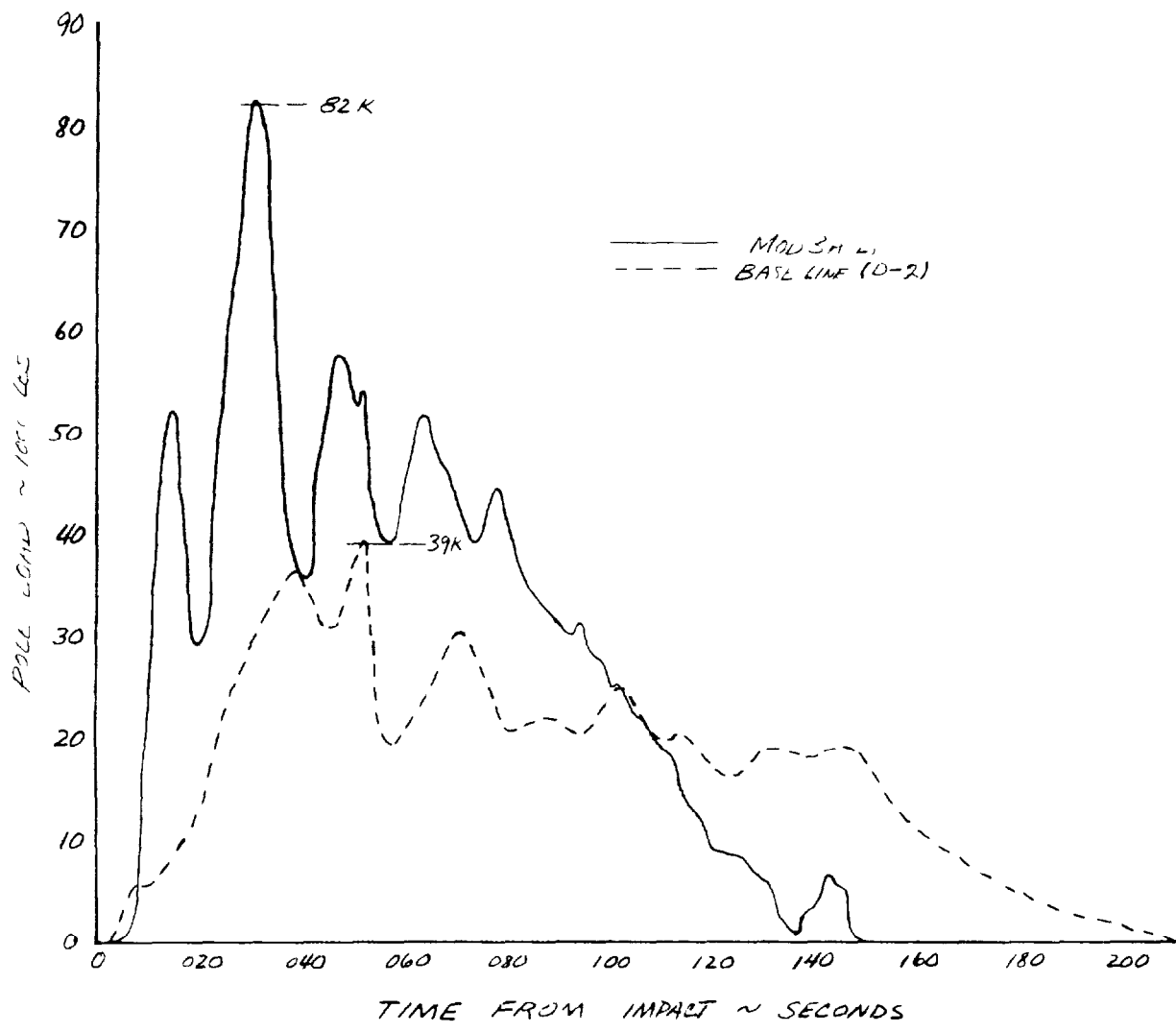


Figure 10-10 SIDE IMPACT: COMPARISON OF POLE FORCES

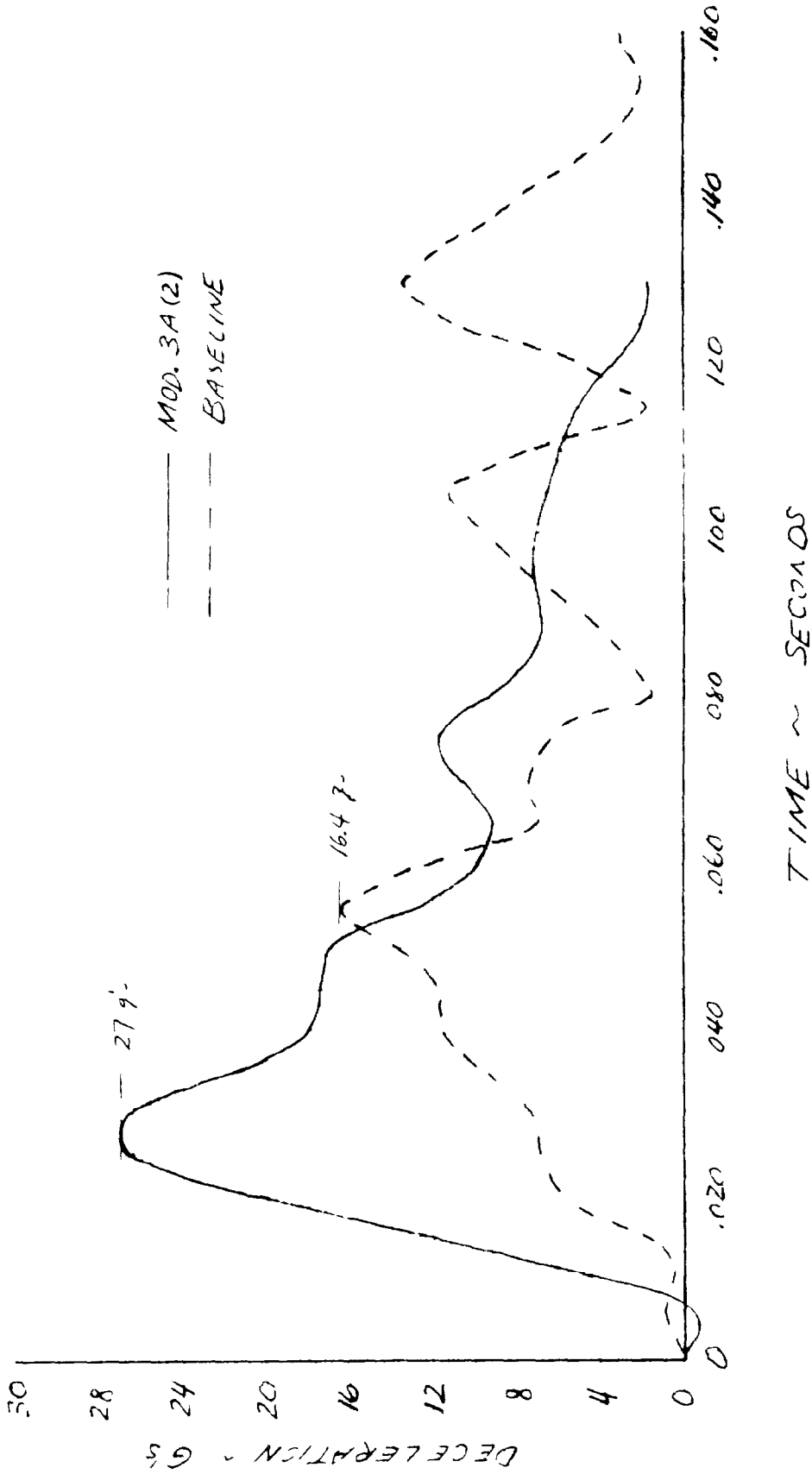
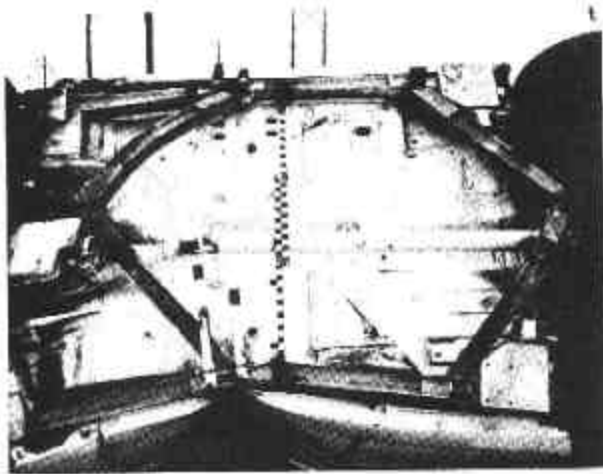
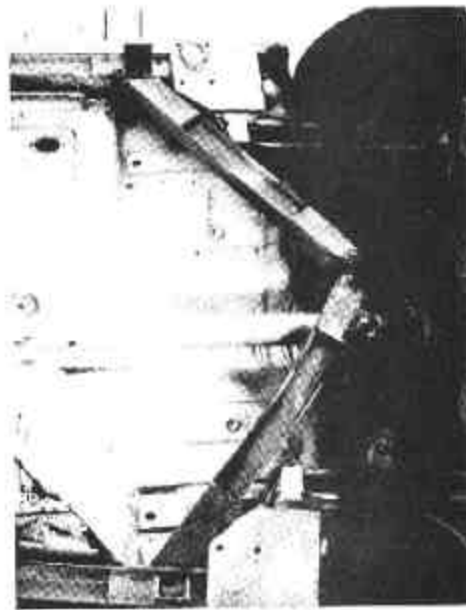


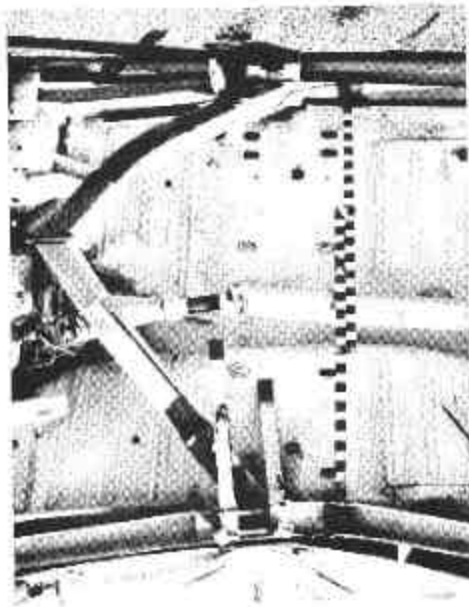
Figure 10-11 COMPARISON OF PASSENGER COMPARTMENT ACCELERATIONS, 25 Hz FILTER



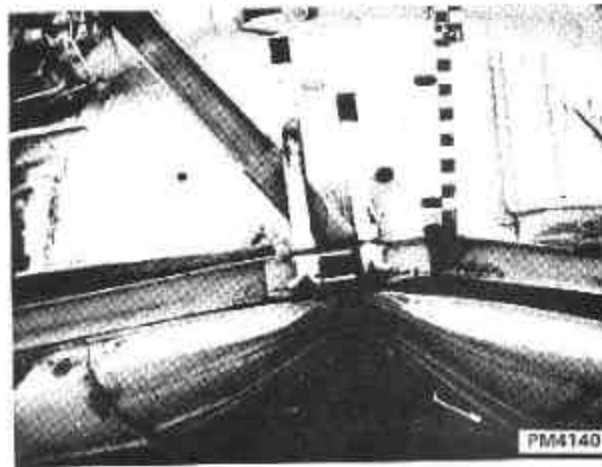
(a) OVERALL



(b) REAR KNEE

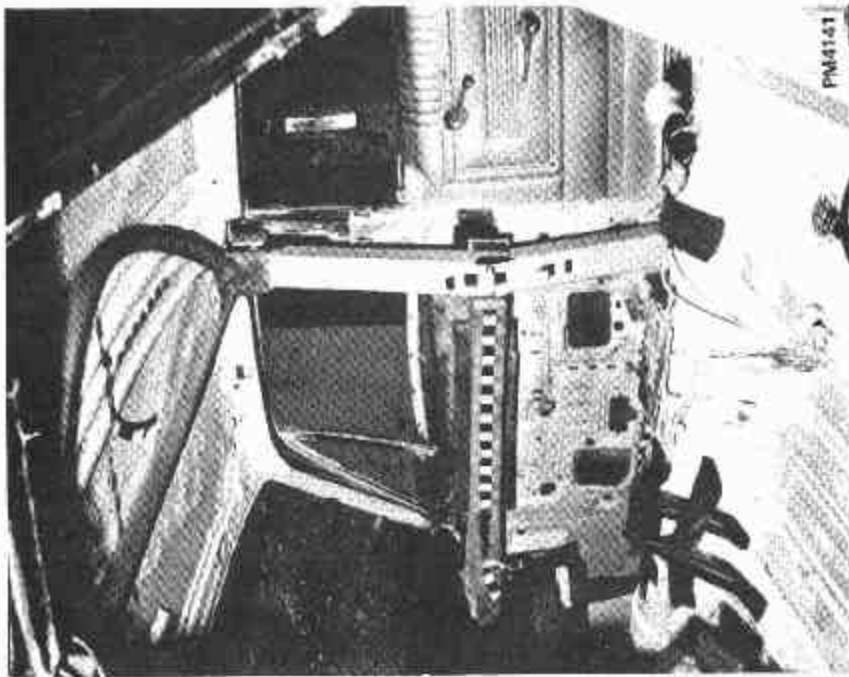


(c) FORWARD KNEE

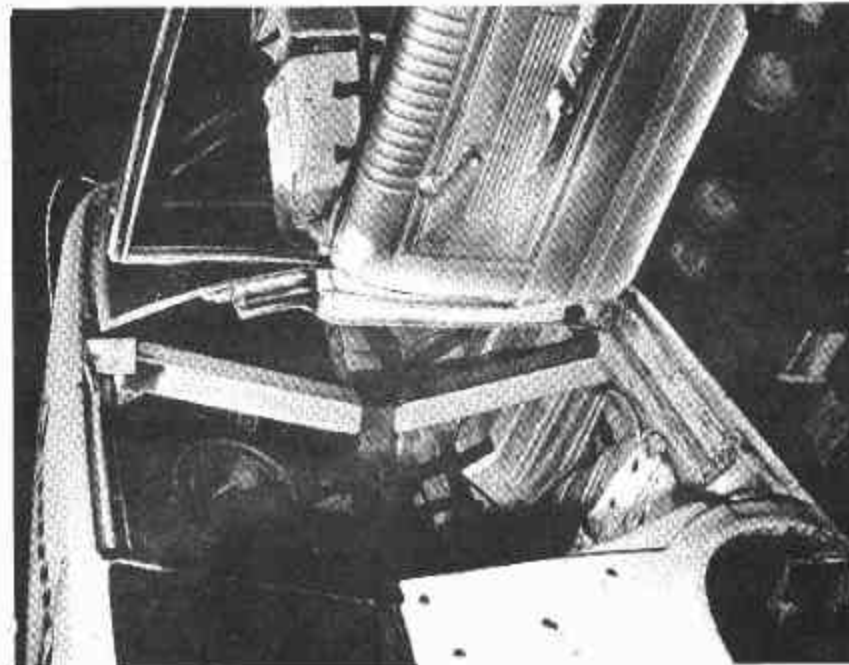


(d) POINT OF IMPACT

Figure 10-12 MOD. 3A(2): FRAME DAMAGE



(B)



(A)

Figure 10-13 MOD. 3A(2): INTERIOR DAMAGE

absorption in 20 MPH side impacts. Weakening could be accomplished either by a reduced cross section or a sharper center line curvature. In its present configuration, the roll bar may be more effective in higher velocity side impacts where the roof structure is directly contacted by the impacted obstacle.

In conclusion, the changes that were made to the Mod. 3A(2) vehicle are improvements over Mod. 3A(1) since both peak deceleration and pole penetration were simultaneously reduced from those of Mod. 3A(1). To achieve the desired 20 g constant deceleration behavior in 20 MPH side impacts, further changes in the same direction are needed. Specifically, the roll bar and the main frame structure should be weakened. Also, the frame design should promote involvement earlier in the collision.

Observation of the impact response of the various structural assemblies that make up Mod. 3A(2) strongly suggests that the 20 MPH pole impact is an undertest of the concept. By "undertest" is meant that the modified vehicle would demonstrate a clearer improvement over the base line vehicle in comparative tests at higher impact velocities.

11. DISCUSSION OF RESULTS

The side impact study focused on two general structural configurations -- (1) a door reinforcement and supporting structure modification (Mod. 3) and (2) a frame modification concept (Mod. 3A). Results from tests of these structural concepts are summarized in Table 11-1, along with corresponding results from the base line (unmodified vehicle) test and the developmental vehicle (D-2) test. The latter vehicle incorporated only minor structural changes which were intended to aid in evaluating the performance of the Mod. 3 and, as is apparent from a comparison of the data, behaved in a manner very similar to that of the base line vehicle.

Since some scatter in the impact velocity is present, maximum permanent deformation is predicted for exact 20 MPH side impacts based on the assumption that deformation is directly proportional to initial kinetic energy, or in terms of a ratio:

$$\frac{d_p}{d_A} = \left(\frac{V_p}{V_A} \right)^2$$

where

d_A = actual deformation (in.)

d_p = predicted deformation (in.)

V_A = actual impact velocity (MPH)

V_p = 20 MPH.

This relationship is believed to be reasonable for the small velocity differences involved here. Predicted deformations for equivalent 20 MPH impacts

Mod. 3A included a simulated reinforced door and integrated roll bar structure.

Table 11-1
SUMMARY OF SIDE IMPACT TEST RESULTS

VEHICLE	DESCRIPTION	TEST WEIGHT (LB)	IMPACT VELOCITY (MPH)*	PEAK G'S (50 Hz FILTER)	ACTUAL PERMANENT DEFORMATION (IN.)	PREDICTED DEFORMATION AT 20 MPH)	REMARKS
BASE LINE 3	1966 FORD SEDAN	3600	21.5	20	24	20.8	PERFORMANCE BASE
MOD. 3	DOOR REINFORCEMENT	3594	17.4	20	14	18.5	REDUCED DEFORMATION
D-2	STRUT BETWEEN B-POSTS ONLY	3524	20.5	21	22	21.0	DEVELOPMENTAL TEST - ADDITIONAL INSTRUMENTATION
MOD. 3A(1)	FRAME MODIFICATION	3692	21.7	42	19	16.2	HIGH PEAK G-LEVEL
MOD. 3A(2)	IMPROVED FRAME MODIFICATION	3876	20.5	27	15	14.3	REDUCED DEFORMATION

*TRIP SWITCH MEASURE (± 0.5 MPH ESTIMATED ACCURACY)

are included in Table 11-1 and serve to facilitate correlation of data. Some variation in the point of impact also occurred, however, all impacts were within six inches of the door center.

Along with reducing compartment intrusion (interior deformation resulting from exterior collapse), an additional objective is to limit peak g's. Since a uniform ("square") deceleration waveform automatically minimizes displacement (deformation) for a given g-limit, it is thought to be a desirable design goal -- at least from a structural performance standpoint. Twenty g's is within the limit of human tolerance but corresponds to only eight inches of deceleration distance for a velocity change from 20 MPH to a stop, hence, a 20 g uniform deceleration response was used as a design goal. Comparative evaluation of structural performance can then be made on the basis of relative deviation from an ideal 20 g square wave. Figure 11-1 compares the Mod. 3, Mod. 3A(2) and base line compartment deceleration responses (of the floorpan below the driver's position) with the idealized waveform. Data from Mod. 3A(1) is not shown here since it exhibited inferior performance (see Figure 9-4), Mod. 3A(2) is considered to be more representative of the performance that can be expected from a frame modification concept.

Comparing the performance of the Mod. 3 with the base line (refer to Table 11-1 and Figure 11-1), it is seen that the door beam structure and related modifications (including a transverse strut between the "B" posts) reduced pole penetration by approximately two inches, based on predicted deformations at 20 MPH. The lack of substantial improvement in effective deceleration magnitude and uniformity, except for the higher initial response, further illustrates the relatively minor improvement in gross structural performance that was achieved by the Mod. 3 configuration for a 20 MPH impact. The close similarity in behavior of the developmental vehicle (D-2), which contained only a transverse strut between the "B" posts, and the base line vehicle demonstrates that the door beam was an integral part of the Mod. 3 structural design.

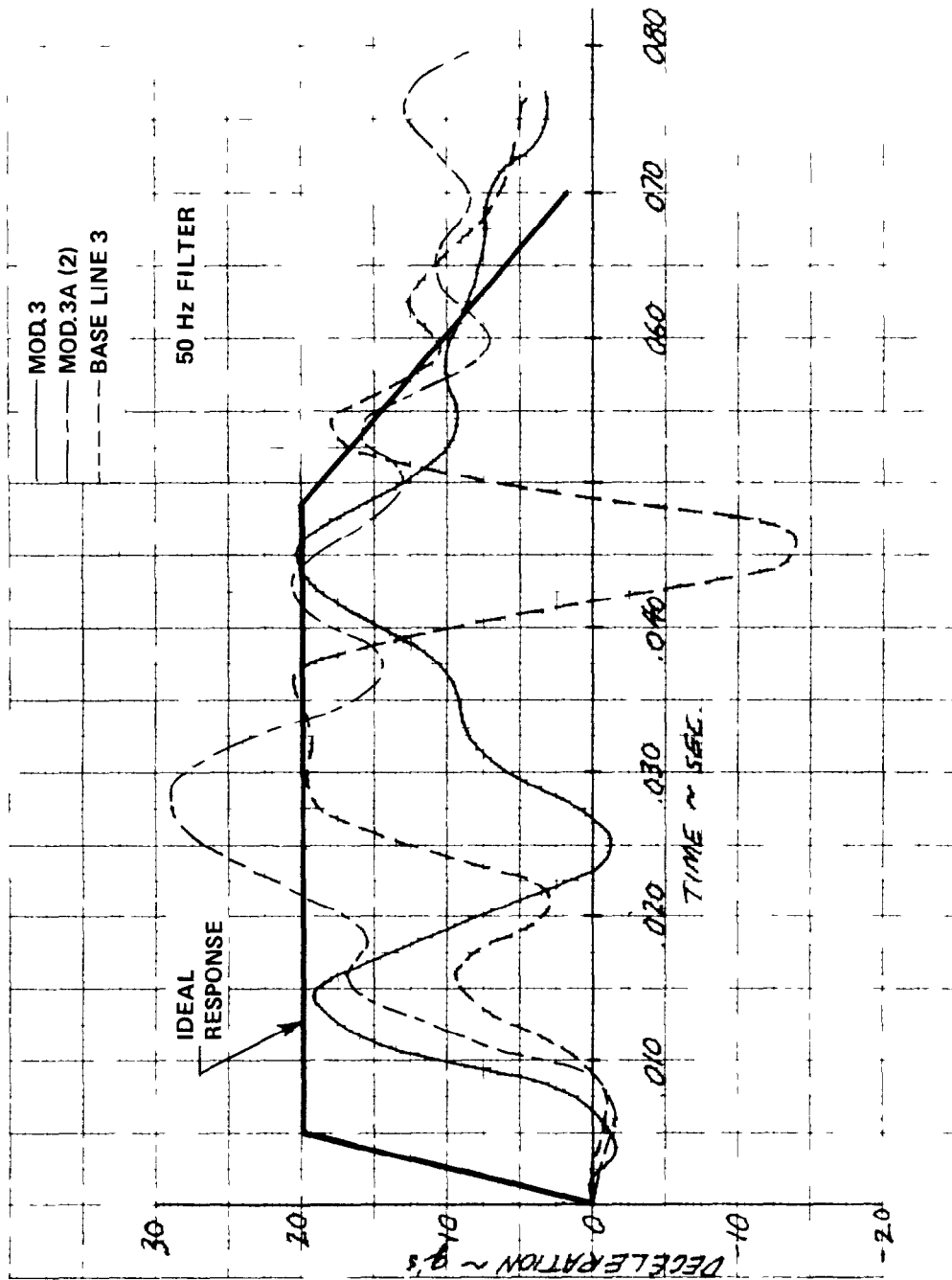


Figure 11-1 COMPARISON OF DECELERATION RESPONSES WITH IDEALIZED WAVEFORM

It is thus concluded that more substantial modifications (e.g., frame alterations) are essential to produce more significant improvement in structural performance. However, a reinforced door has been shown to be important for increasing initial deceleration effectiveness in side impacts that occur at a door location.

The Mod. 3A structural design provided for extensive frame modifications and the effect of a reinforced door. In assessing the performance of this concept, as characterized by the Mod. 3A(2) vehicle, it is instructive to compare deformation with that of the base line (see Table 11-1). Note that maximum deformation has been reduced by approximately 6-1/2 inches, or about 30%, based on 20 MPH predictions. The reduction to about 14.3 inches is more impressive when considering that 8 inches of deformation is required even under "ideal" conditions (20 g square wave). Comparing the deceleration response with the idealized waveform and with the base line response in Figure 11-1, it is apparent that a significant improvement in deceleration uniformity has been achieved; the Mod. 3A(2) response is much closer to the idealized design response than the base line. The increased deceleration effectiveness is, of course, consistent with the substantial reduction in deformation.

It is thus clear that the structural performance of the Mod. 3A(2) configuration represents a marked improvement over the base line performance since deformation has been substantially reduced and the deceleration waveform is much more uniform and closer to a 20 g mean value. Furthermore, for higher velocity impacts, the present configuration would likely show more dramatic improvement over an unmodified vehicle. However, additional improvement is believed to be possible through further frame modification, in particular, engagement with the main frame side rail should take place earlier and the peak g-level should be diminished somewhat by reducing the stiffness of the modified frame structure. A more effective roll bar design would also be helpful. A more practicable reinforced door, e.g., the Mod. 3 type design, should also be integrated into a further improved frame modification concept.

This study amply demonstrates that improvement in structural crashworthiness in side collisions with fixed objects is feasible. The inherent lack of occupant protection in this kind of collision is well known, and has been further substantiated by a 20 MPH test with an unmodified vehicle. However, based on the results presented herein, it has become increasingly clear that a significant increase in side impact protection will require extensive structural modification of present automobiles.

12. REFERENCES

1. Mayor, R. P., Theiss, C. M. and Schuring, D. J., "Basic Research in Automobile Crashworthiness - Analytical Studies", CAL Report No. YB-2684-V-5, November, 1969.
2. States, J. D. and States, D. J., "The Pathology and Pathogenesis of Injuries Caused by Lateral Impact Accidents", Proceedings of the 12th Stapp Car Crash Conference, Published by SAE, 1968.
3. Hedeem, C. E. and Campbell, D. D., "Side Impact Structures", SAE Paper No. 690003, January 1969.
4. Haythornthwaite, R. M., "Beams with Full End Fixity", Engineering, 25 January 1957, page 110.

APPENDIX A: LATCH MECHANISM TEST

A-1 General

The limited space available in side collisions must be used as effectively as possible. One method of doing this is developing resistance of a beam by cable action after exhausting the capacity of the beam in bending. As outlined in the design objectives for Mod. 3, cable type action depends on the longitudinal restraint of the supports. Since the door must open, it is not possible to build in the longitudinal restraint beforehand. The following describes two exploratory drop tests to develop a latch mechanism that would come into play in a collision and provide the desired lateral restraint.

Chronologically, the first drop test, which failed, preceded the full-scale test of the Mod. 3 vehicle. To avoid delaying the Mod. 3 test, the latch device was tack welded in the locked position on the test vehicle. This permitted an evaluation of the test results under the assumption that the latching mechanism could be made to work. Following the full-scale test the second drop test was successfully conducted. However, the latching mechanism has not been tested in a vehicle impact.

A-2 Theory

Experimental and theoretical studies, Reference 4, of small [1" x 1/2"] beams indicate that when deformations are approximately equal to the beam depth, a substantial increase in capacity can be obtained by restraining the supports against longitudinal motion. If the supports are prevented from moving longitudinally, axial tension forces develop in the beam which acts as a cable as the deflection becomes large. The slope, or the effective spring rate, k_e , of the beam after it has yielded in tension is (Reference 4):

$$k_e = \frac{4 T \Delta}{L}$$

where T is the tensile yield and Δ and L are the center deflection and span, respectively. For the properties of one of the hat sections and assuming a tensile yield of 45 ksi,

$$k_e = 3.3 \text{ K/in.}$$

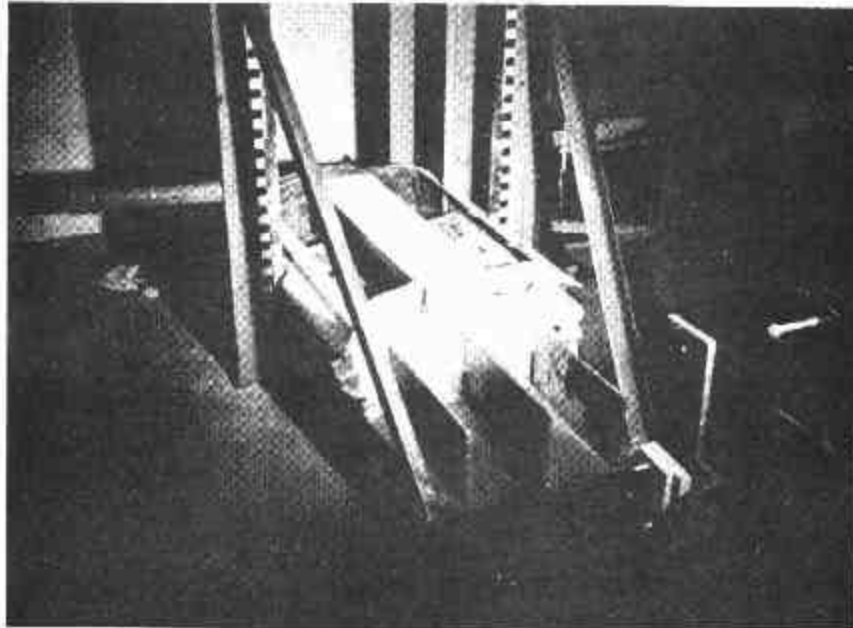
Using the above spring rate, a one foot deflection for each of the three hat beams is sufficient to absorb the kinetic energy of a 4000 pound vehicle at 22 MPH. In reality, however, the spring rate will be lower, because complete longitudinal rigidity of the beam supports (i.e., the "A" and "B" posts) is not possible.

A-3 Door Impact Tests

A-3.1 Test No. 1

The objective of the door drop test was to observe the latching mechanism under impact conditions. Figure A-1(a) shows the door in the guillotine drop mechanism. Figure A-1(b) shows the door after the test. The latching mechanism, which failed to engage, is shown in the foreground of Figure A-1(b). Figure A-1(c) shows another view. To better approximate actual conditions, the latching mechanism was mounted on an actual "B" post taken from a previously tested vehicle.

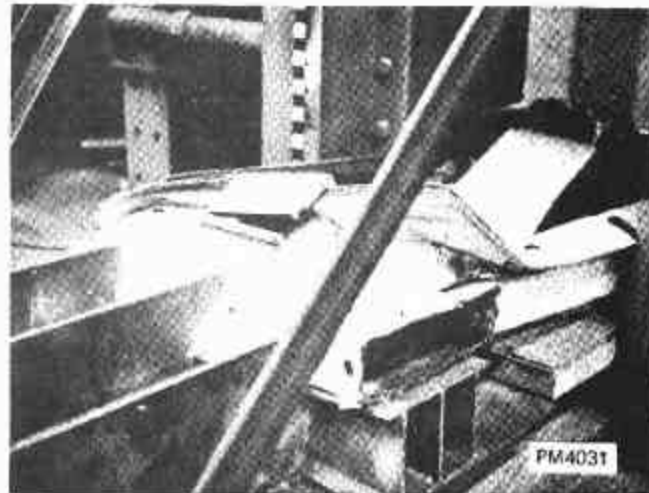
The test consisted of dropping a 450 lb weight from a height of 17 ft, furnishing an impact velocity of 22.5 MPH. The weight had a semicircular end to approximate the conditions of a full-scale pole impact. Based on a calculated stiffness of 3.3 K/in. for the hat section (if latching occurs), the drop weight was selected to deflect the hat section approximately 7.5 inches. This deflection provides an adequate test of the mechanism for collisions.



(A)



(B)



(C)

Figure A-1 DOOR DROP TEST No. 1

Figure A-2 is a simplified sketch of the tested impact actuated locking mechanism. Note that the device does not interfere with normal door operation. The translation and rotation of the door mounted portion of the mechanism were anticipated; however, uncertainty about the relative magnitude and particularly the sequence of the motions suggested the need for the test. Examination of the high speed motion pictures of the test showed that the rotation occurred first and was large enough to prevent locking by translation.

A-3.2 Test No. 2

As shown in Figure A-3, the latch was modified by the addition of a backing plate to prevent initial rotation and by enlarging the dovetail engaging slots; otherwise, the test conditions were the same as Test No. 1. Figure A-4(a) shows the door mounted in the drop test facility, the backing plate can be seen in the foreground.

The condition of the door following impact can be seen in Figure A-4(b). The latch engaged successfully, as revealed by high speed film of the impact and obvious deformation of the "A" and "B" post supports which was caused by the cabling effect of the beam. The cabling effect was somewhat diminished, however, by a hinge formed at the connection between the hat section and latch which caused the latch to rotate while engaged. The magnitude of the rotation is apparent in Figure A-4(b). As a result of the reduced cabling effect, the deflection of the hat section was larger than anticipated and was crushed against the foundation of the supporting fixtures.

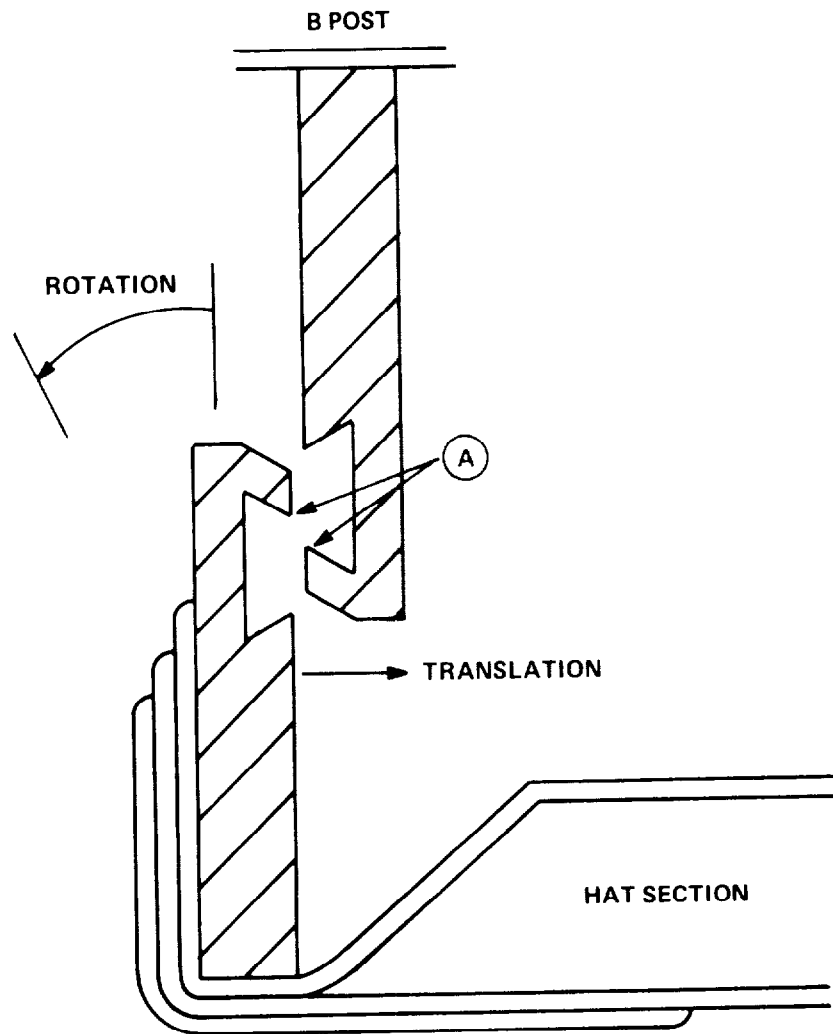


Figure A-2 LATCHING DEVICE TEST NO. 1

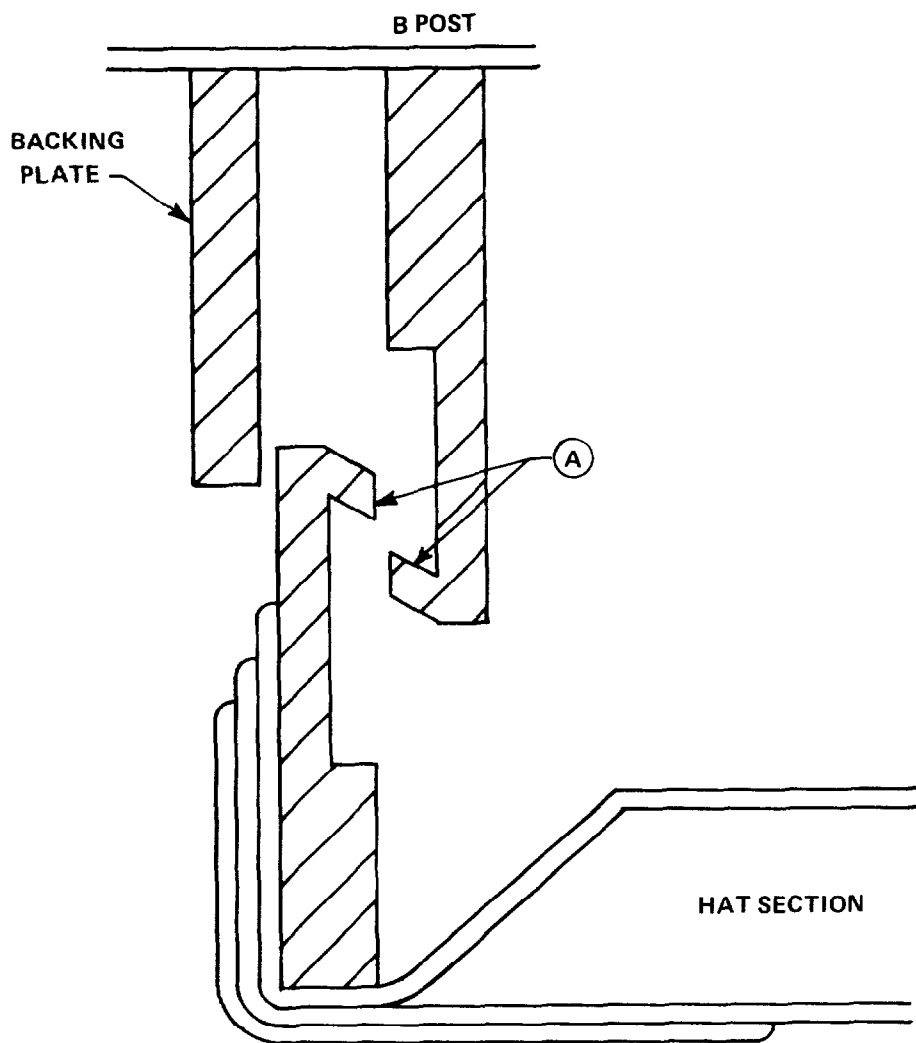
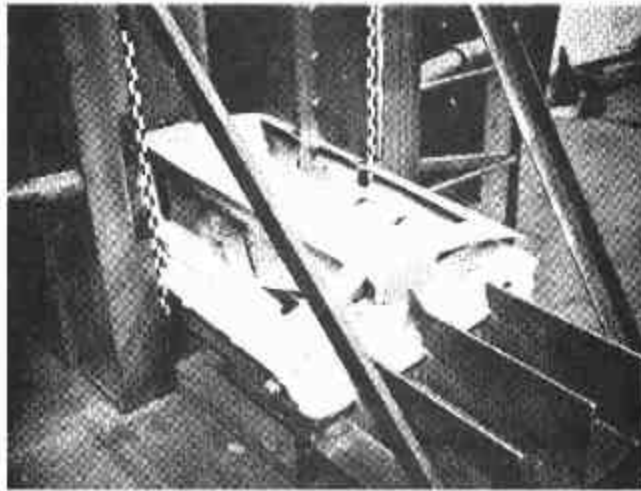


Figure A-3 LATCHING DEVICE TEST NO. 2



(a)



(b)

Figure A-4 MODIFIED DOOR IMPACT TEST

The dynamic load-deflection characteristic of the door, as developed from acceleration data from the impact head, is contained in Figure A-5. The curve reflects the "two-stage" behavior of the hat section beam, the first portion of the curve resulting from beam bending only (before latch engagement) and the second portion due to cabling action. The dashed line on the curve shows the calculated spring rate (for cable effects) of 3.3 K/in. Although the theoretical value was not realized, it is apparent that cable action due to lateral restraint did occur. The events noted in the figure were determined from high speed film analysis.

A-4 Concluding Remarks

Both theory and the results of the second drop test show that the "second effort" cable effect does contribute to energy absorption and reduced penetration. The latching mechanism tested represents one method for achieving the cabling action; other conceptual devices should also be considered since acceptable deformation will continue to be at a premium in side collisions.

Sliding doors, overhead doors and rear entry have often been proposed for safety cars as well as futuristic "idea" cars. For such radical departures from existing practice, it should be relatively simple to build in the potential cable behavior.

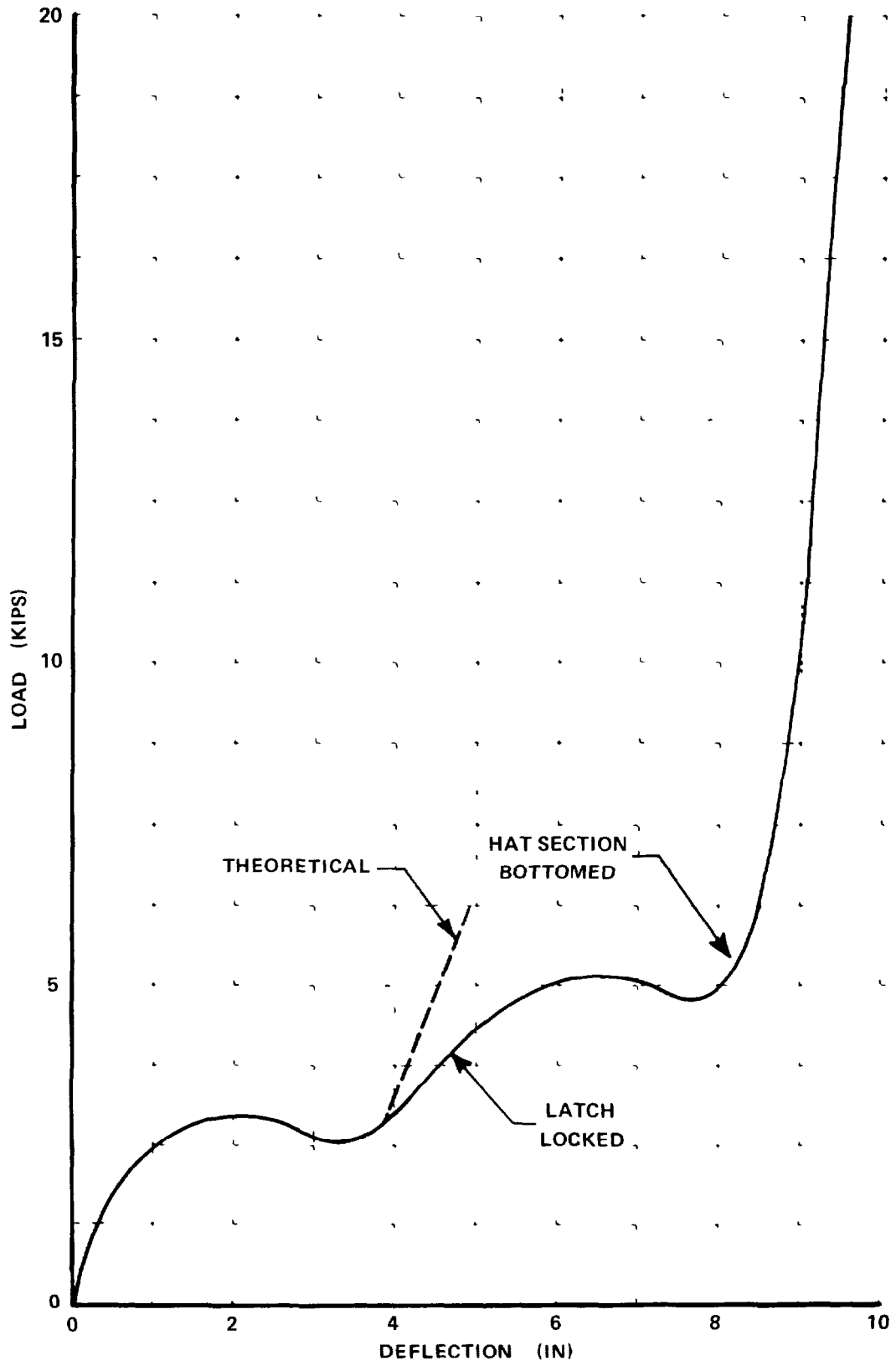


Figure A 5 DYNAMIC LOAD-DEFLECTION BEHAVIOR OF TEST NO. 2 DOOR

APPENDIX B: EVALUATION OF MULTIPLE DATA SENSORS

B-1 General

As previously indicated in the test objectives, a secondary objective of the D-2 test was to improve and correlate methods of data collection and interpretation. In addition to pole load cells, six accelerometers at various vehicle locations were mounted to record data in the direction of impact. From preliminary examination of all six channels, three were selected for further processing. These were:

- floorpan -- under driver's seat,
- frame -- on the side opposite impact,
- bottom of B-post -- opposite impact.

These accelerometers are Nos. 2, 5 and 3, respectively, as shown on the sketch of the D-2 test data summary contained in Appendix C. It is doubtful that including all six accelerometers in the comparative study would have affected the conclusions.

B-2 Comparisons

B-2.1 Load Cells

A check on the total load can be obtained by comparing the impulse (the area under the force-time curve) to the change in momentum of the vehicle during the collision. By planimeter, the impulse was determined to be 3555 lbs-sec. Equating the impulse to the momentum change and using the measured weight of the test vehicle (3524 lbs), the calculated

velocity change is 22.1 MPH. This value compares favorably to the sum of the impact and rebound velocity of 22.8 MPH as determined by the trip switch and high speed camera data. The discrepancy, which is less than 4 percent, is an index of the reliability of the load cell forces. In contrast to the human tolerance area where acceleration is of primary interest, force data are of most utility in the detailed design of a structural modification and acceleration data are primarily a means of inferring magnitudes of the expected loads. Direct measurement of forces by means of load cells is normally the best method of measuring loads.

B-2.2 Effect of Filtering

In all previous tests acceleration data has been filtered using a 50 Hz cutoff. Although the selection of 50 Hz cutoff is arbitrary, such a cutoff frequency does aid in data interpretation by removing the sharp spikes in the acceleration trace which do not affect human response and, consequently, should not be used in assessing the performance of a vehicle modification. It was also noted that the total velocity change and the displacement were not influenced significantly by filtering the data. This is a strong indication that the high frequency content of an acceleration trace is due to the motion of the localized point where the accelerometer is attached, rather than the gross motion of the vehicle.

Since the accelerations derived by dividing the force measured by the load cells by the vehicle weight should be indicative of the gross vehicle, it is of interest to compare these inferred accelerations to those directly measured and filtered with various cutoffs. Figure B-1 presents this comparison for the output of the accelerometer mounted on the floor pan which has been processed through 25 and 10 Hz cutoff filters. Figures B-2 and B-3 present corresponding results for accelerometers attached to the frame and to the B-post. Close examination of the three figures leads to the following observations. The 10 Hz data is filtered too heavily to reproduce the excursions sensed by the load cell; alternatively, the 25 Hz filter appears to be

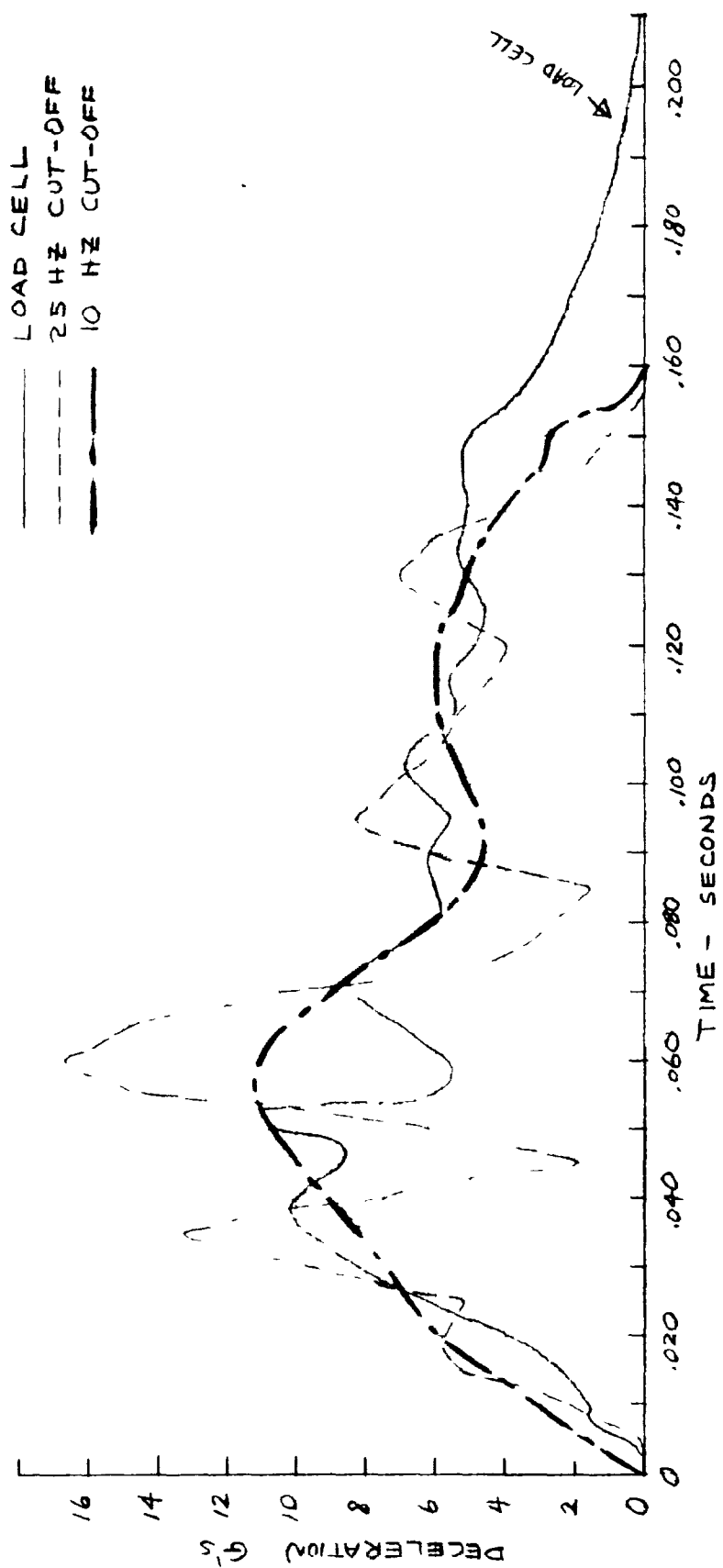


Figure B-1 COMPARISON OF ACCELERATION DERIVED FROM LOAD CELL (FORCE) DATA WITH FLOOR PAN ACCELEROMETER FOR VARIOUS FILTERS

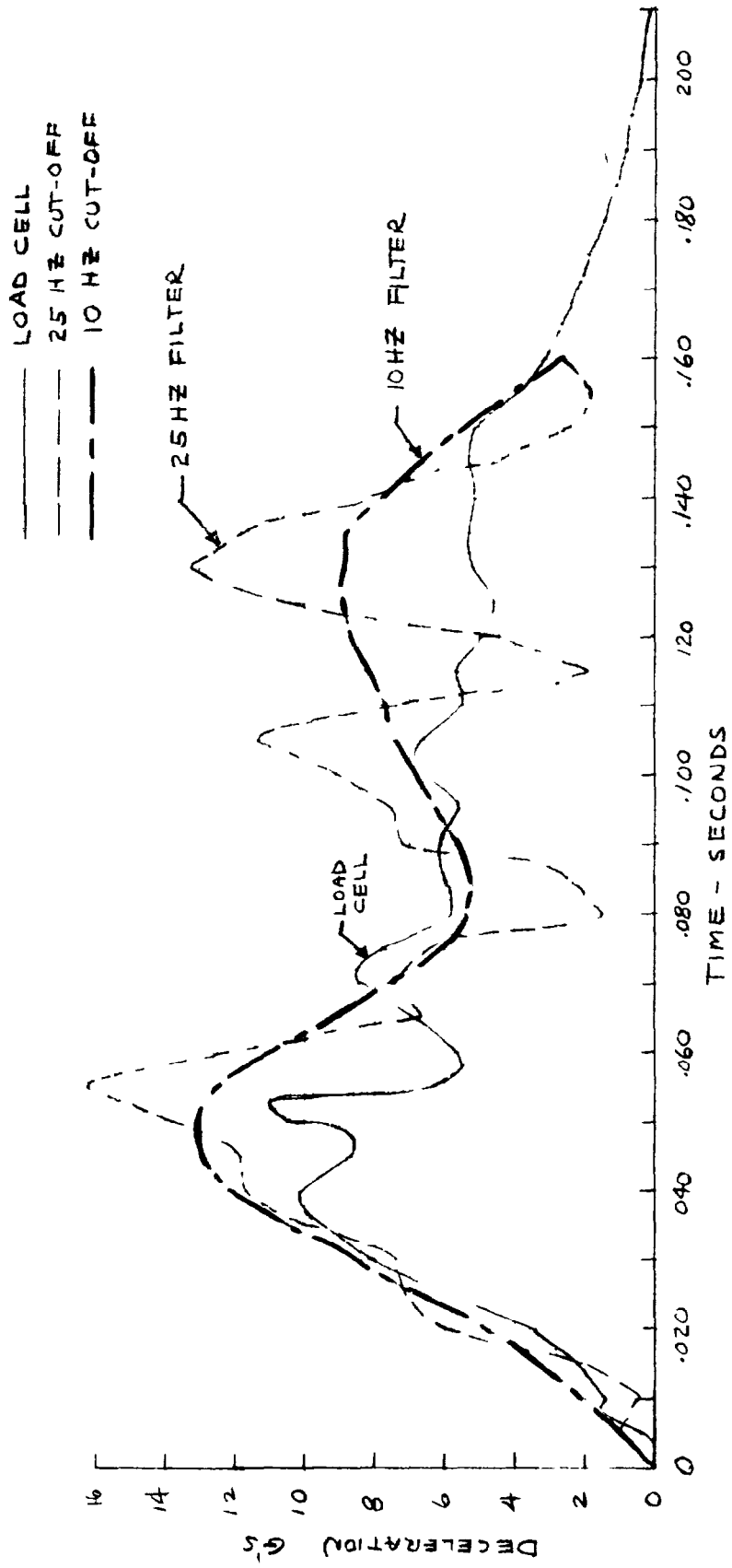


Figure B-2 COMPARISON OF ACCELERATION DERIVED FROM LOAD CELL (FORCE) DATA WITH FRAME ACCELEROMETER FOR VARIOUS FILTERS

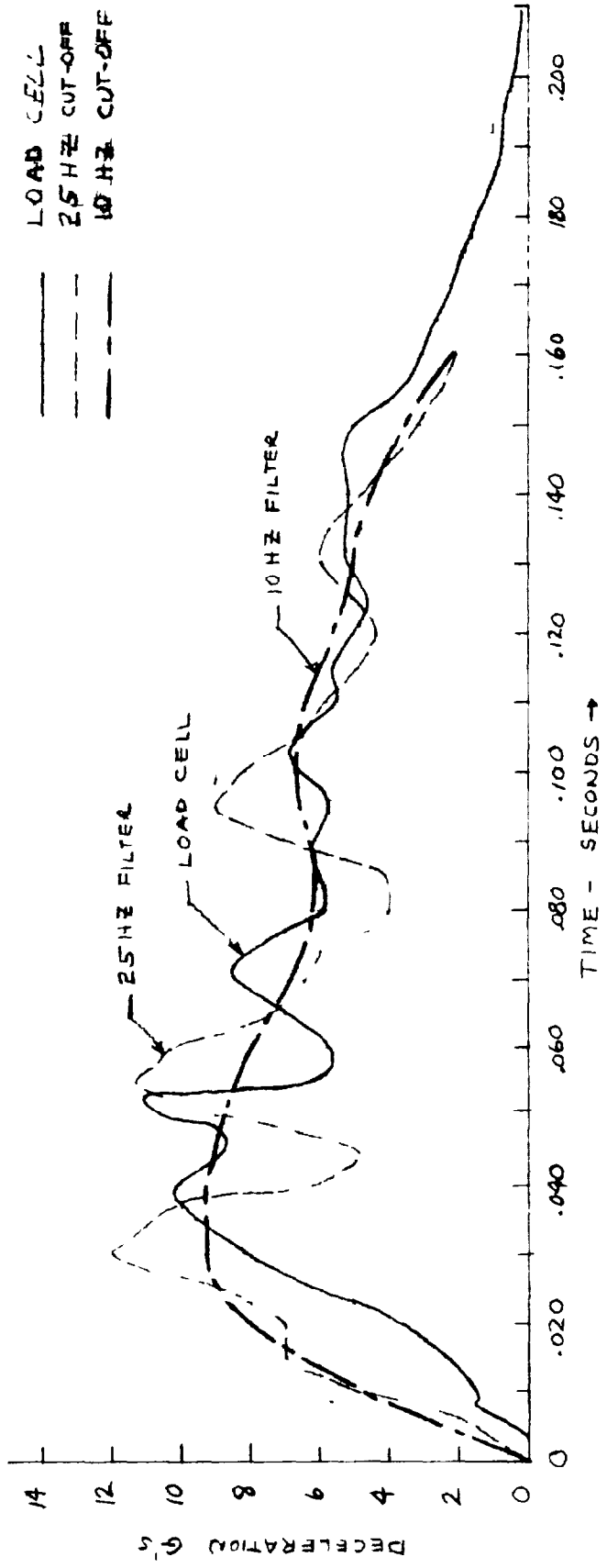


Figure B-3 COMPARISON OF ACCELERATION DERIVED FROM LOAD CELL (FORCE) DATA WITH B-POST ACCELEROMETER FOR VARIOUS FILTERS

too light. Consequently, the accelerations derived from the load cell appear as if they have been equivalently filtered at approximately 20 Hz. Physically, this may simply mean that the substantial mass of the pole prevents it from responding with significant amplitudes at higher frequencies. Also, the relation between peaks in the region of maximum acceleration (40 to 60 milliseconds) is noteworthy. For example, multiplying the load cell accelerations by approximately 1.3 would provide a fairly good approximation for the peak frame acceleration (Figure B-2), particularly if 20 Hz filtered data were plotted. The same is true for the B-post accelerometer (Figure B-3) with a slight time shift and a smaller amplification factor, and for the floor accelerometer (Figure B-1) with a greater amplification. In any case it is apparent that all curves are basically measuring the same phenomenon.

Peak g is often presented as a simple index of the severity of a collision, and it is informative to compare peak acceleration for various filters and accelerometer location to that inferred by the load cell data (11.0 g's). Table B-1 summarizes the various comparisons. A reasonable conclusion of the tabular comparison is that calculating load from unfiltered data, or even from data that has not been filtered through a low enough cut-off frequency, results in a sizable overestimate of peak load.

B-2.3 Effect of Accelerometer Location

An added reason for the redundant measurements was to see what conclusion could be made concerning accelerometer location. Figure B-4 is a plot of the calculated load cell accelerations and data from all three locations which have been processed through a 25 Hz cutoff filter. It can be seen that the rise times are similar -- the first peak for all four curves occurs at approximately 30 milliseconds. It can also be observed that subsequent peaks show good agreement in their time of occurrence. A further observation is that the "noise" of the individual curves increases as the flexibility of the attachment point. The floor is the most flexible

Table B-1
COMPARISON OF PEAK g's
LOAD CELL DATA VS. ACCELEROMETERS
AT VARIOUS LOCATIONS WITH VARIOUS FILTERS

FILTER CUTOFF (Hz)	FRAME	B-POST	FLOOR-PAN	AVERAGE
10	13.1	9.3	11.2	11.2
25	16.2	11.9	16.7	14.9
50	24.2	17.0	20.8	20.1
NONE	25.9	19.8	24.6	23.4

PEAK g FROM LOAD CELL = 11.0 g's

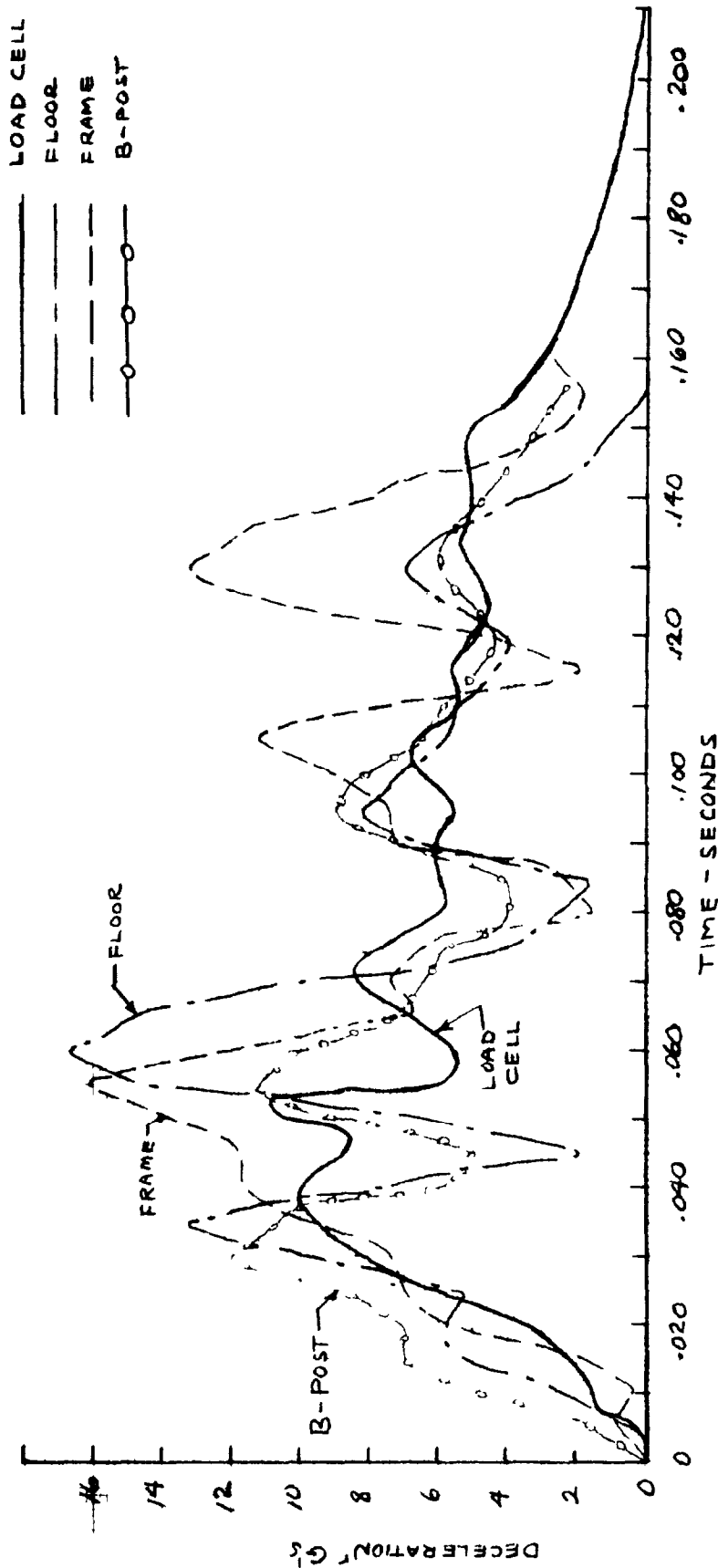


Figure B-4 COMPARISON OF ACCELERATION DERIVED FROM LOAD CELL (FORCE) DATA WITH ACCELEROMETERS FILTERED AT 25 Hz CUTOFF

location, and the B-post is the stiffest location -- the accelerometer is, in fact, attached to a heavy gusset added to the base of the post. One possible conclusion is that the stiffer the accelerometer location, the better the agreement with the load cell data. It was originally thought that filtering with a very low cutoff would tend to remove localized effects and all curves, including the accelerations derived from the load cells, would converge to the "true" deceleration curve for the vehicle. Figure B-5 depicts the same data as in the previous figure, but the cutoff frequency is now 10 Hz. While much of the differences between the curves have been filtered out, substantial percentage differences still exist. For example, the peak amplitude of the accelerometer on the frame is 13.1 g's compared to 9.3 for the B-post. Also, the variations between accelerometers are greater than the variation between an accelerometer and the load cell data. Whenever two points undergo different accelerations, then it follows that the relative displacement between the points must be varying. Figure B-6 plots the relative displacement between the frame and the B-post as a function of time. The curve was obtained by a double integration of both accelerometer outputs. The low magnitude of the relative displacement, especially at times when differences in acceleration levels between the points are pronounced, is particularly significant. Displacements of this magnitude could easily escape detection by camera coverage or post-collision examination. Due to the small times involved, only small relative displacements result when sizable differences in accelerations exist between points on the same vehicle. Because of this fact, the original hypothesis that filtering with a very low cutoff would result in all curves converging to the "true" curve must be abandoned.

LOAD CELL
 FLOOR
 FRAME
 B-POST

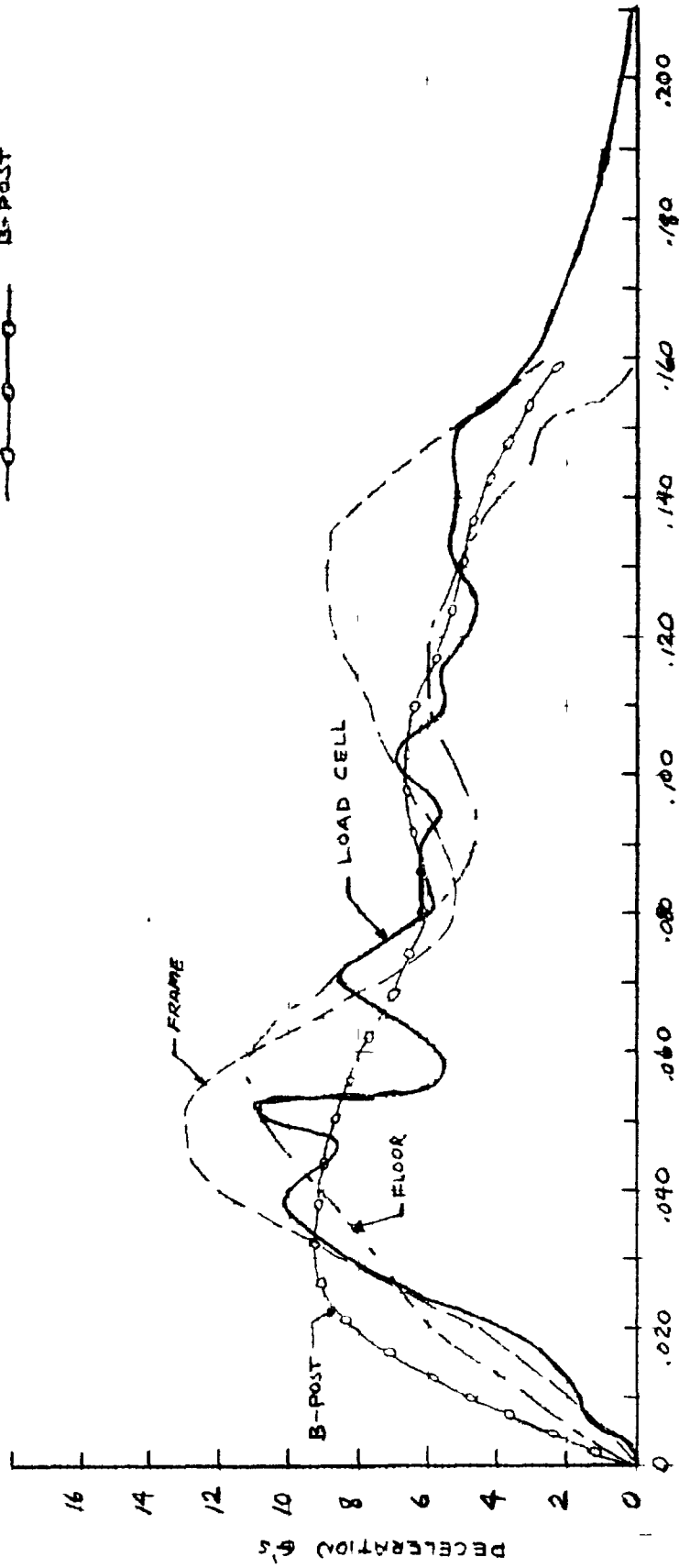


Figure B-5 COMPARISON OF ACCELERATION DERIVED FROM LOAD CELL (FORCE) DATA WITH ACCELEROMETERS FILTERED AT 10 Hz CUTOFF

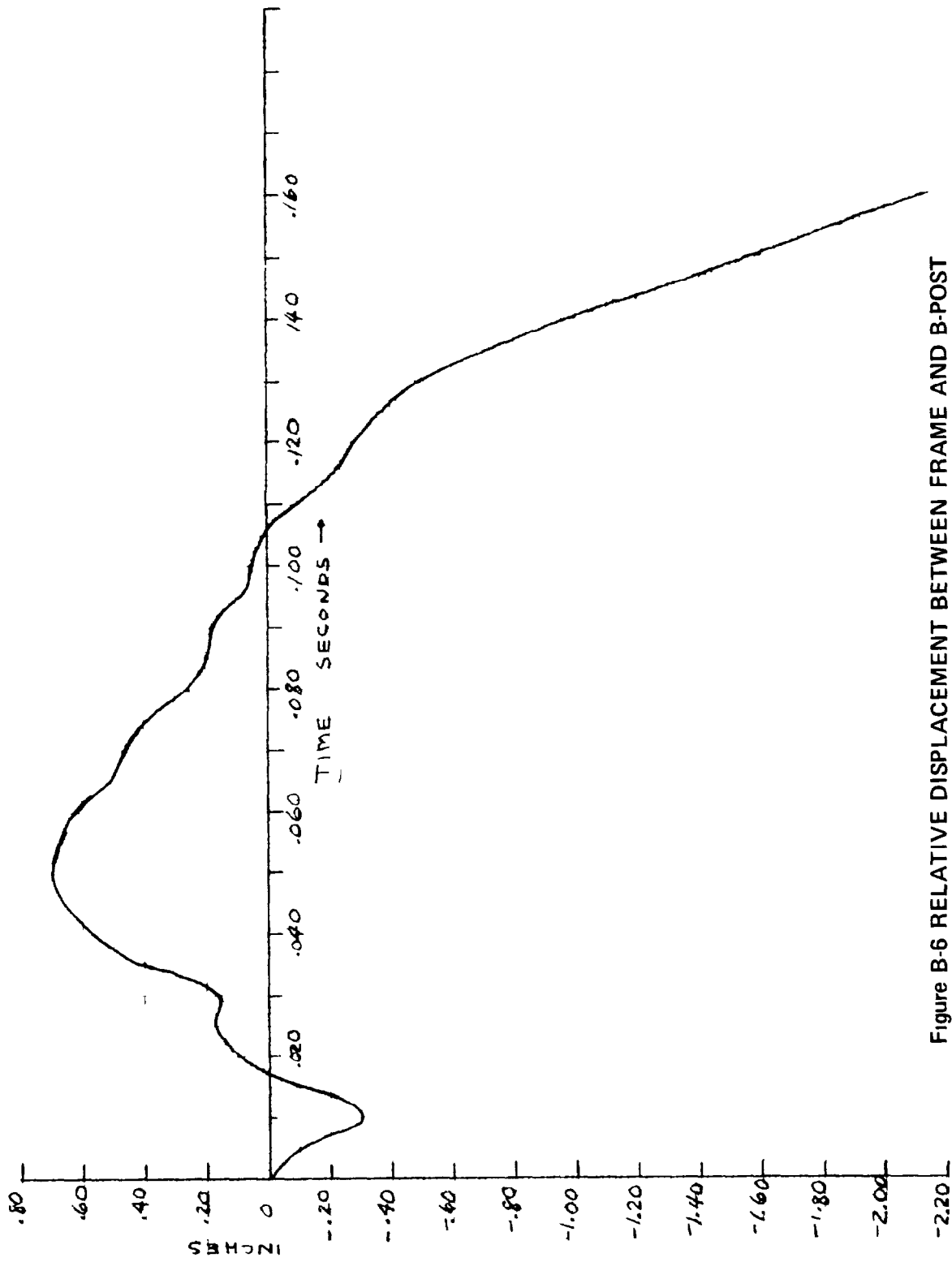


Figure B-6 RELATIVE DISPLACEMENT BETWEEN FRAME AND B-POST FROM ACCELEROMETER DATA

B-3 Conclusions of Study

The 50 Hz cutoff filter, which has been used as standard for previous tests, is apparently too light for inferring structural loads, on the other hand, a 10 Hz cutoff is too heavy. A 20 Hz low pass filter is a reasonable compromise for estimating forces from accelerometer data. While a location near the seat belt attachment point is seemingly a desirable location to measure input accelerations for occupant response, the flexibility of the floorpan can cause difficulties when interpreting acceleration data for evaluation of structural performance.

Dynamic loads can be inferred from acceleration data by filtering with a 20 Hz cutoff and using an amplification factor of 1.3 if the accelerometer is at a flexible location (e.g., floorpan), or 1.1 if the location is in a stiff region (e.g., frame). Peak g's, or loads, derived from data containing high frequency content can be considerably in error.

Complete characterization of vehicle motion by a single acceleration time history is not possible; small and easily undetectable relative displacements can lead to large percentage differences in instantaneous acceleration for different structural locations.

APPENDIX C: SUMMARIES OF TEST DATA
AND RELATED INFORMATION

VEHICLE IMPACT TEST ~ DATA SUMMARY

VEHICLE TESTED Base Line 3, 1966 Ford Sedan, DATE 1-31-69
NOMINAL TEST CONDITIONS 20 mph, 90° Side Pole Impact
VEHICLE WEIGHT 3600 LBS. CAL TEST NO 5

MEASURED VEHICLE IMPACT VELOCITY (MPH):

ROAD TRIP SWITCHES 21.5 ± 0.5 *
FILM DATA 20, REBOUND N. A.
COMPARTMENT ACCELEROMETERS 22 **

MEASURED VEHICLE IMPACT ANGLE N. A. DEGREE
IMPACT POINT ON VEHICLE Right Front Door, 6 Inches Aft of Door Center
TOW ROAD CONDITIONS N. A.
AMBIENT TEMPERATURE N. A. °F
CHANNELS RECORDED ON FM TAPE None

POST TEST VISUAL INSPECTION

FINAL REBOUND DISTANCE 17 INCHES
FINAL CRUSH DISTANCE 24 INCHES

REMARKS

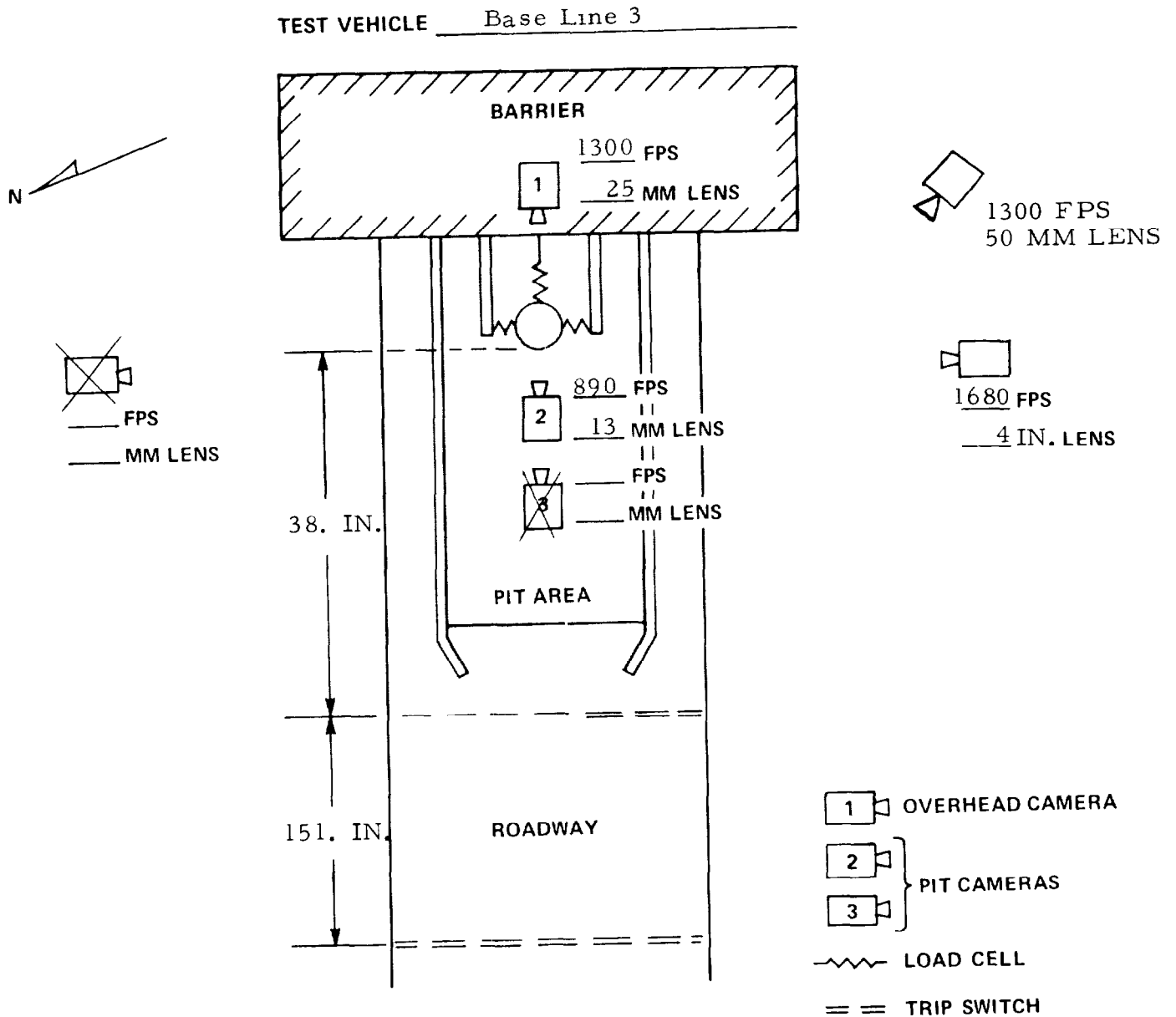
1. Pole penetrated well into roof of vehicle.
2. Front windshield was cracked over the total area.
3. Front bench seat was buckled up at its center along with the floorpan.

* MOST ACCURATE MEASURE OF VEHICLE VELOCITY

** INCLUDES REBOUND VELOCITY

N. A. = Not Available

TEST SITE LOCATION OF SENSORS AND CAMERAS

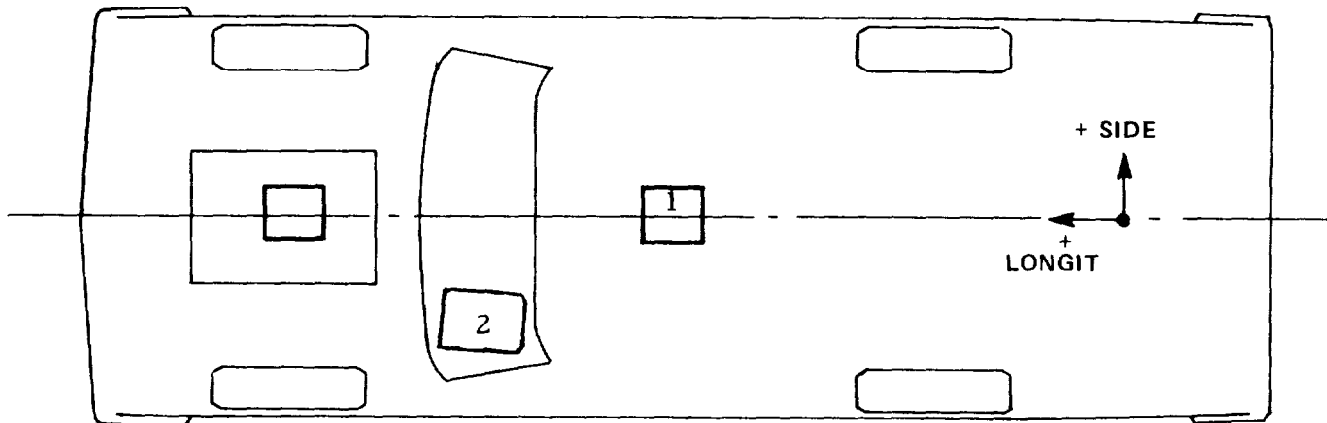
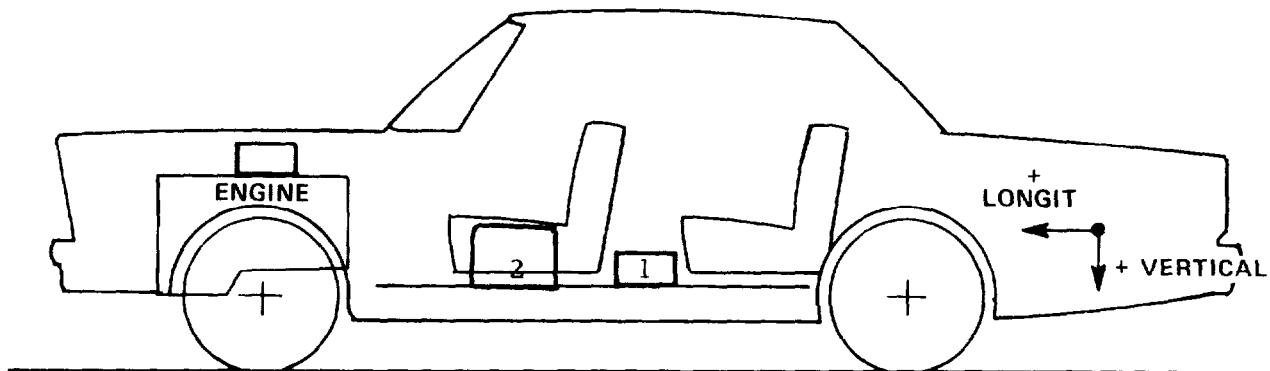
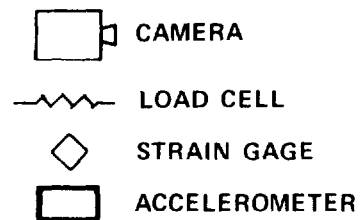


REMARKS

1. There was no North side camera, and only one pit camera.
2. No pole load cells were used for this test.

VEHICLE MOUNTED SENSORS

TEST VEHICLE Base Line 3



REMARKS

1. No. 1 accelerometer package was the standard triaxial sensors which were turned 90° toward the pole.
2. No. 2 accelerometer package was a triaxial unit mounted under the driver's seat on the floorpan and in line with the impact point.
3. There were no accelerometers on the engine.
4. The rear bench seat was removed for the test.

VEHICLE IMPACT TEST ~ DATA SUMMARY

VEHICLE TESTED Mod. 3, Modified 1966 Ford Sedan, DATE 2-18-69

NOMINAL TEST CONDITIONS 20 mph, 90° Side Pole Impact

VEHICLE WEIGHT 3594 LBS CAL TEST NO 6

MEASURED VEHICLE IMPACT VELOCITY (MPH)

ROAD TRIP SWITCHES 17.4 ± 0.5 *

FILM DATA 17, REBOUND 3

COMPARTMENT ACCELEROMETERS 25 **

MEASURED VEHICLE IMPACT ANGLE N. A. DEGREE

IMPACT POINT ON VEHICLE Right Front Door, 6 Inches Forward of Door Center

TOW ROAD CONDITIONS N. A.

AMBIENT TEMPERATURE N. A. °F

CHANNELS RECORDED ON FM TAPE None

POST TEST VISUAL INSPECTION

FINAL REBOUND DISTANCE 70 INCHES

FINAL CRUSH DISTANCE 14 INCHES

REMARKS

1. Pole penetrated slightly into the vehicle roof.
2. Windshield was cracked on both the driver and passenger sides.
3. There was no noticeable buckling of the reinforcing strut between "B" posts.
4. The wraparound effect of the total car appeared to be less than the standard vehicle test.

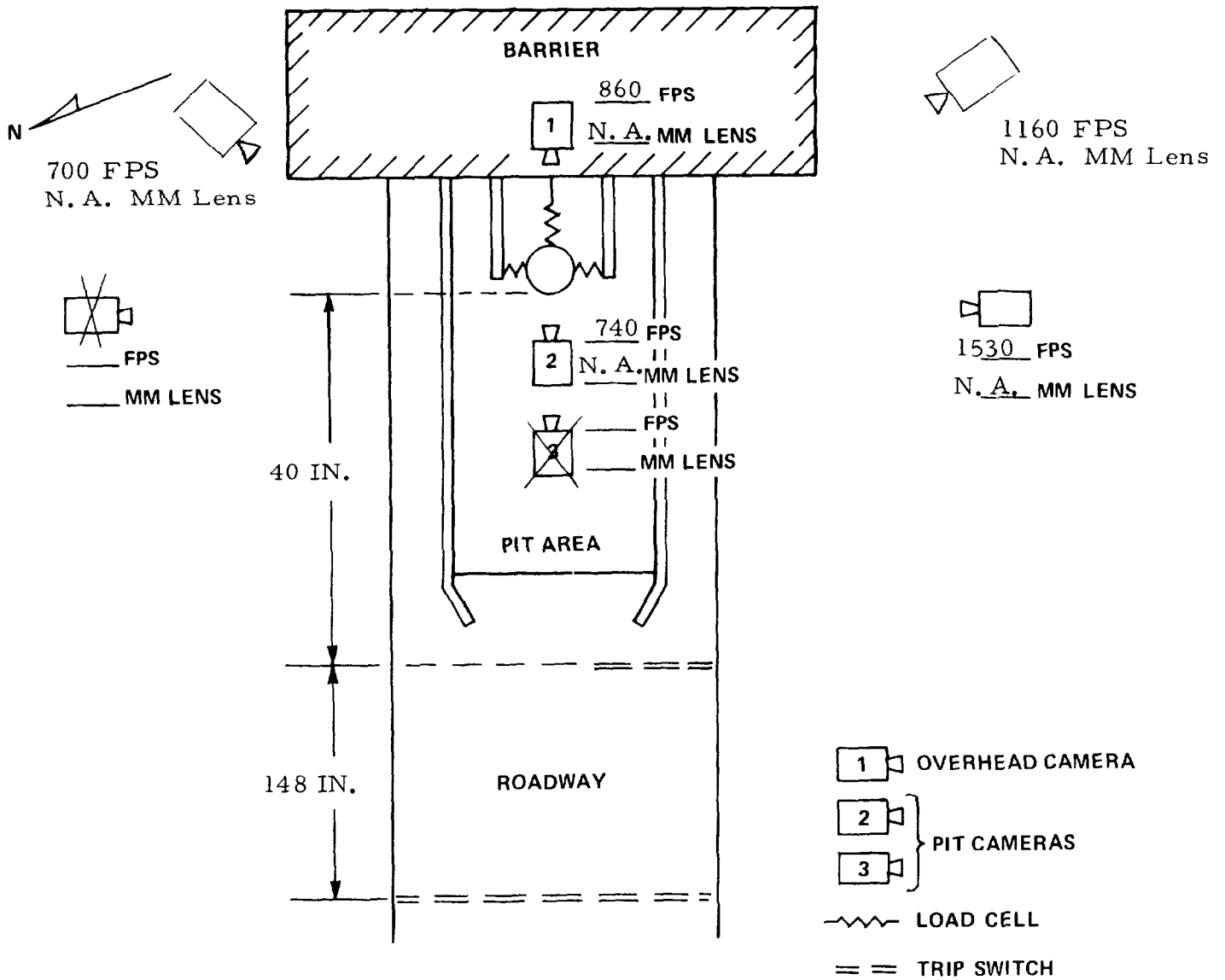
* MOST ACCURATE MEASURE OF VEHICLE VELOCITY

** INCLUDES REBOUND VELOCITY

N. A. = Not Available

TEST SITE LOCATION OF SENSORS AND CAMERAS

TEST VEHICLE Mod. 3

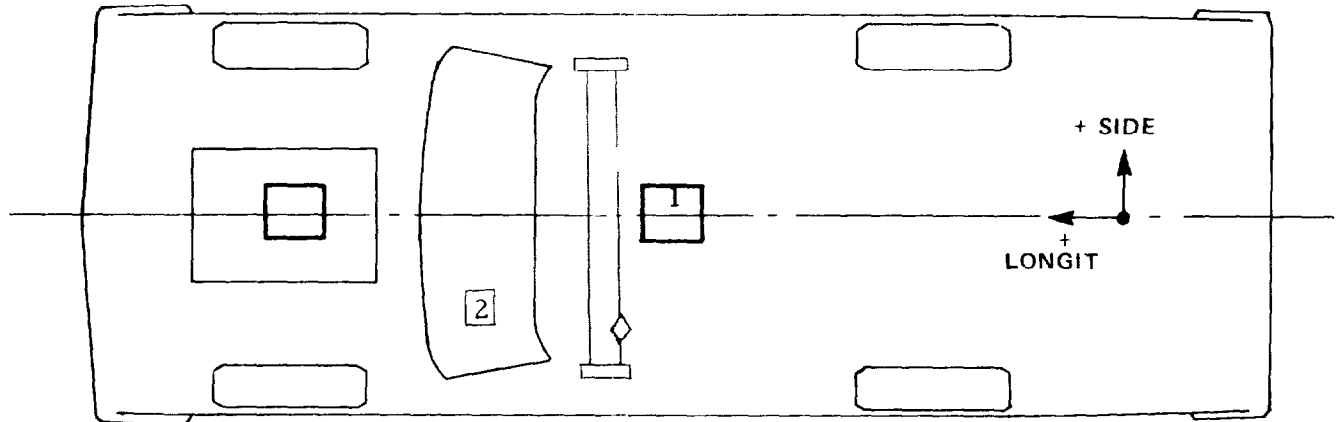
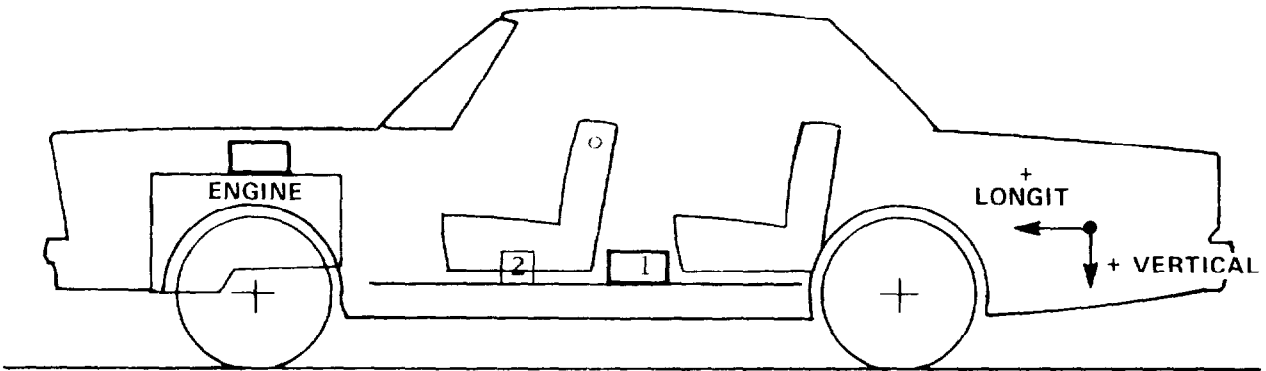
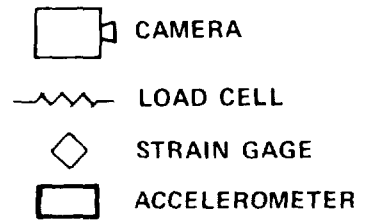


REMARKS.

1. There was no north side camera, and only one pit camera.
2. No pole load cells were used for this test.

VEHICLE MOUNTED SENSORS

TEST VEHICLE Mod. 3



REMARKS

1. No. 1 accelerometer package contained the standard triaxial sensors.
2. No. 2 accelerometer package was a triaxial unit mounted under the driver's seat on the floorpan.
3. There were no accelerometers on the engine.
4. Two strain gauges were mounted on the lateral strut between the "B" posts.
5. The rear bench seat was removed for the test.

VEHICLE IMPACT TEST ~ DATA SUMMARY

VEHICLE TESTED D-2, Modified 1966 Ford Sedan, DATE 4/11/69

NOMINAL TEST CONDITIONS 20 MPH, 90° Side Pole Impact

VEHICLE WEIGHT 3524 LBS CAL TEST NO 12

MEASURED VEHICLE IMPACT VELOCITY (MPH)

ROAD TRIP SWITCHES 20.5 ±0.5 *

FILM DATA 20.6, REBOUND 2.3

COMPARTMENT ACCELEROMETERS 20.41 **

MEASURED VEHICLE IMPACT ANGLE 87 DEGREE

IMPACT POINT ON VEHICLE Front-Right Door, 4 Inches Forward of Door Center

TOW ROAD CONDITIONS Dry - Very Good

AMBIENT TEMPERATURE 50°F

CHANNELS RECORDED ON FM TAPE Triaxial Accelerometers, Driver's Seat
Side Accelerometer, Passenger Compartment
Side Accelerometer, "B" Post Top
Side Accelerometer, "B" Post Bottom
Road Trip Switches

POST TEST VISUAL INSPECTION

FINAL REBOUND DISTANCE 59 INCHES

FINAL CRUSH DISTANCE 22 INCHES

REMARKS

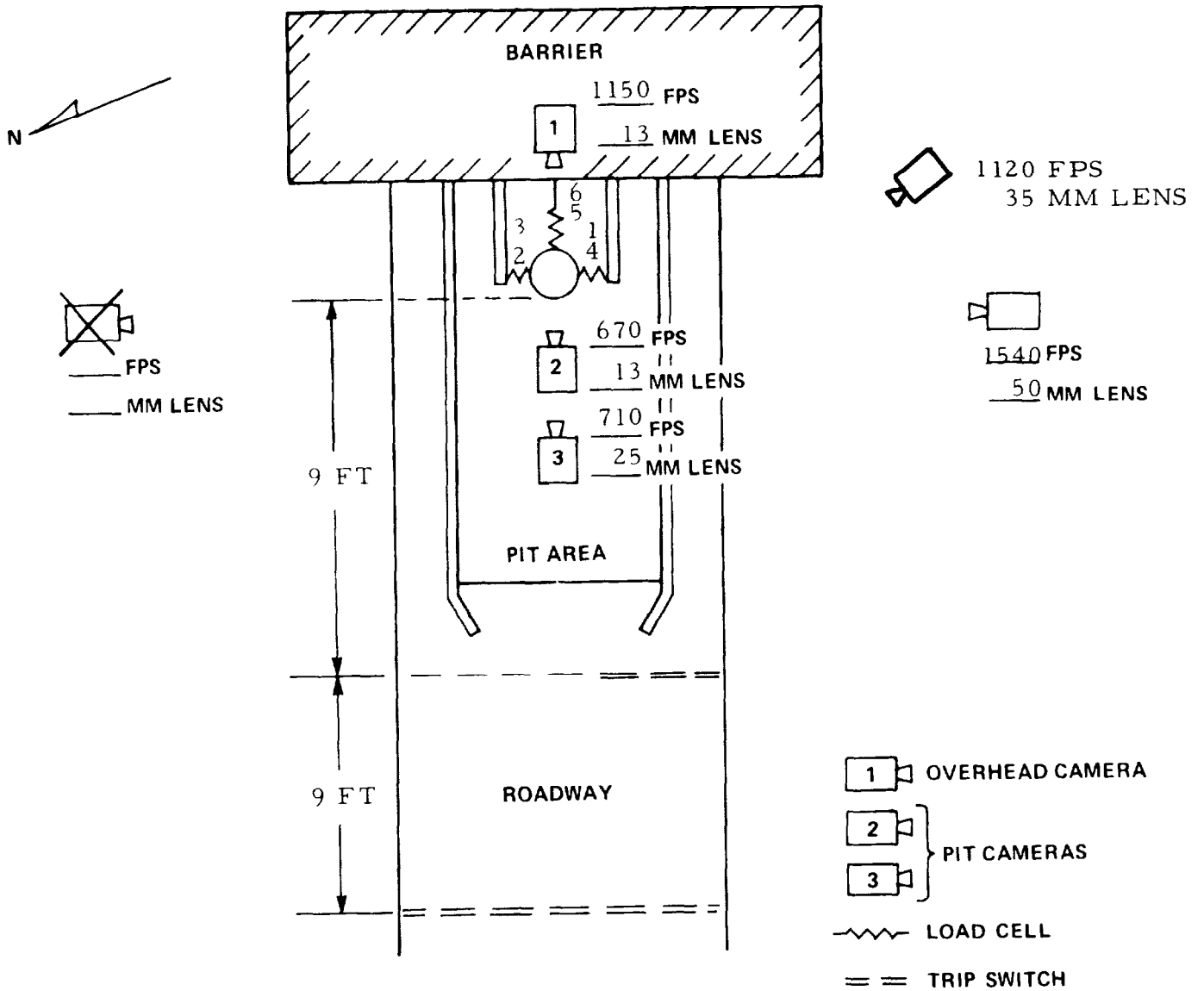
1. Interior Horizontal Brace Between "B" Posts Was Not Bent.
2. "B" Post On Left Side Was Bowed Out And Still Attached At Its Top And Bottom.
3. Both Right Side Door Latches Were Still Engaged.
4. Left Side Main Frame Rail Was Not Noticeably Bent.
5. Total Car Contained A Slight "U" Shape Around Pole.
6. Engine Appeared To Be Displaced Approximately 1-1/2 Inches At Its Front.

* MOST ACCURATE MEASURE OF VEHICLE VELOCITY

** INCLUDES REBOUND VELOCITY

TEST SITE LOCATION OF SENSORS AND CAMERAS

TEST VEHICLE D-2

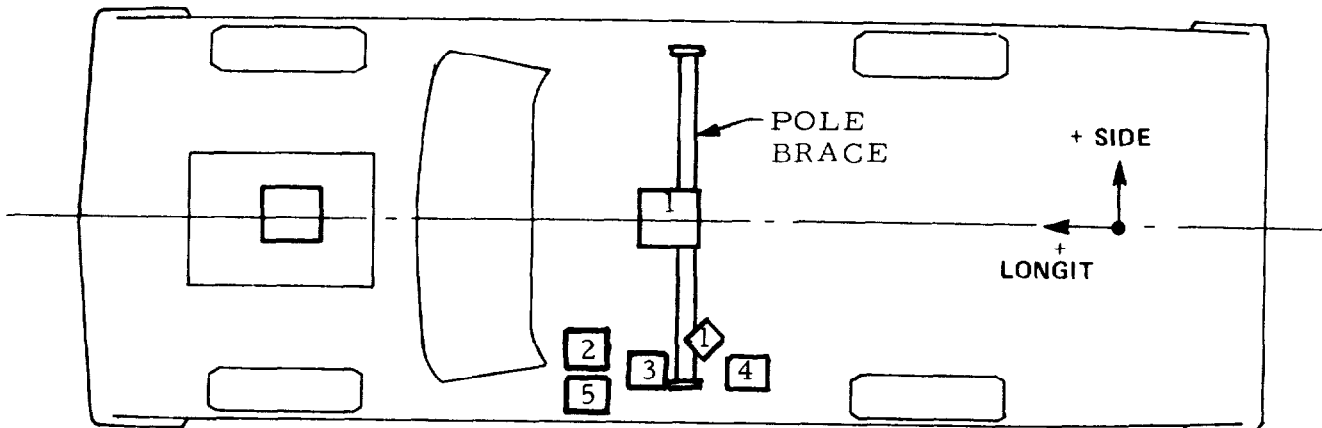
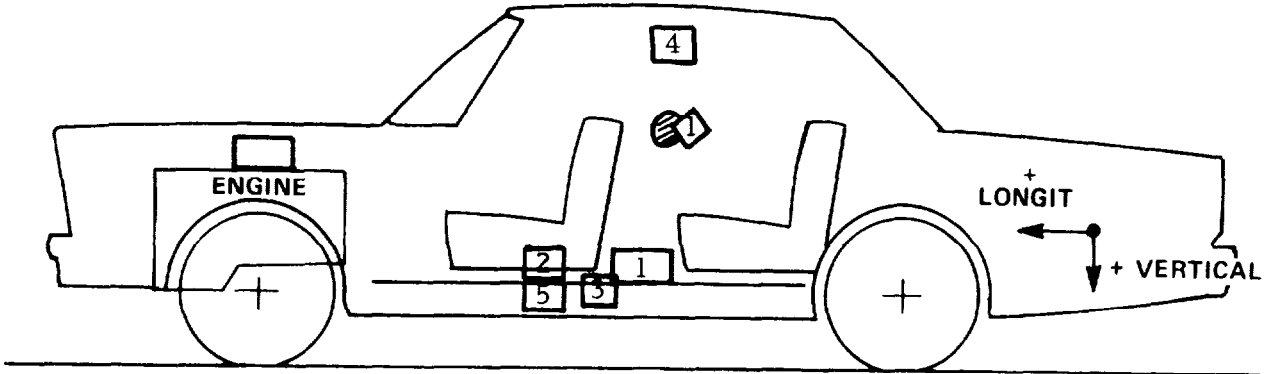
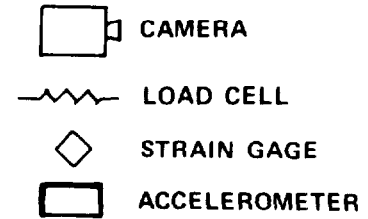


REMARKS

1. No Camera Coverage From North Side.
2. Load Cells Nos. 2, 5 And 4 Were Mounted At The Top Of The Pole.
3. Camera Coverage Was Excellent.

VEHICLE MOUNTED SENSORS

TEST VEHICLE D-2



REMARKS

1. No. 1 Accelerometer Was Oriented Along The Side Axis Only.
2. No. 2 Triaxial Accelerometer Package Was In Line With Pole Impact.
3. No Accelerometers On Engine Block.
4. No. 1 Strain Gauges Were Mounted On Horizontal Brace.
5. No. 3 Accelerometer Was Mounted At Bottom Of "B" Post.
6. No. 4 Accelerometer Was Mounted At Top Of "B" Post.
7. No. 5 Accelerometer Was Mounted On Side Frame Rail.
8. There Were No On-Board Cameras Or Load Cells.

VEHICLE IMPACT TEST ~ DATA SUMMARY

VEHICLE TESTED Mod. 3A(1), Modified 1966 Ford Sedan, DATE 7/15/69

NOMINAL TEST CONDITIONS 20 MPH, 90° Side Pole Impact

VEHICLE WEIGHT 3692 LBS CAL TEST NO 17

MEASURED VEHICLE IMPACT VELOCITY (MPH)

ROAD TRIP SWITCHES 21.7 ± 0.5 *

FILM DATA 20, REBOUND 3

COMPARTMENT ACCELEROMETERS 23 **

MEASURED VEHICLE IMPACT ANGLE 94 DEGREE

IMPACT POINT ON VEHICLE Right Front Door, 4 Inches Forward of Door Center

TOW ROAD CONDITIONS Dry, Very Good

AMBIENT TEMPERATURE 84 °F

CHANNELS RECORDED ON FM TAPE None

POST TEST VISUAL INSPECTION

FINAL REBOUND DISTANCE 47 INCHES

FINAL CRUSH DISTANCE 19 INCHES

REMARKS

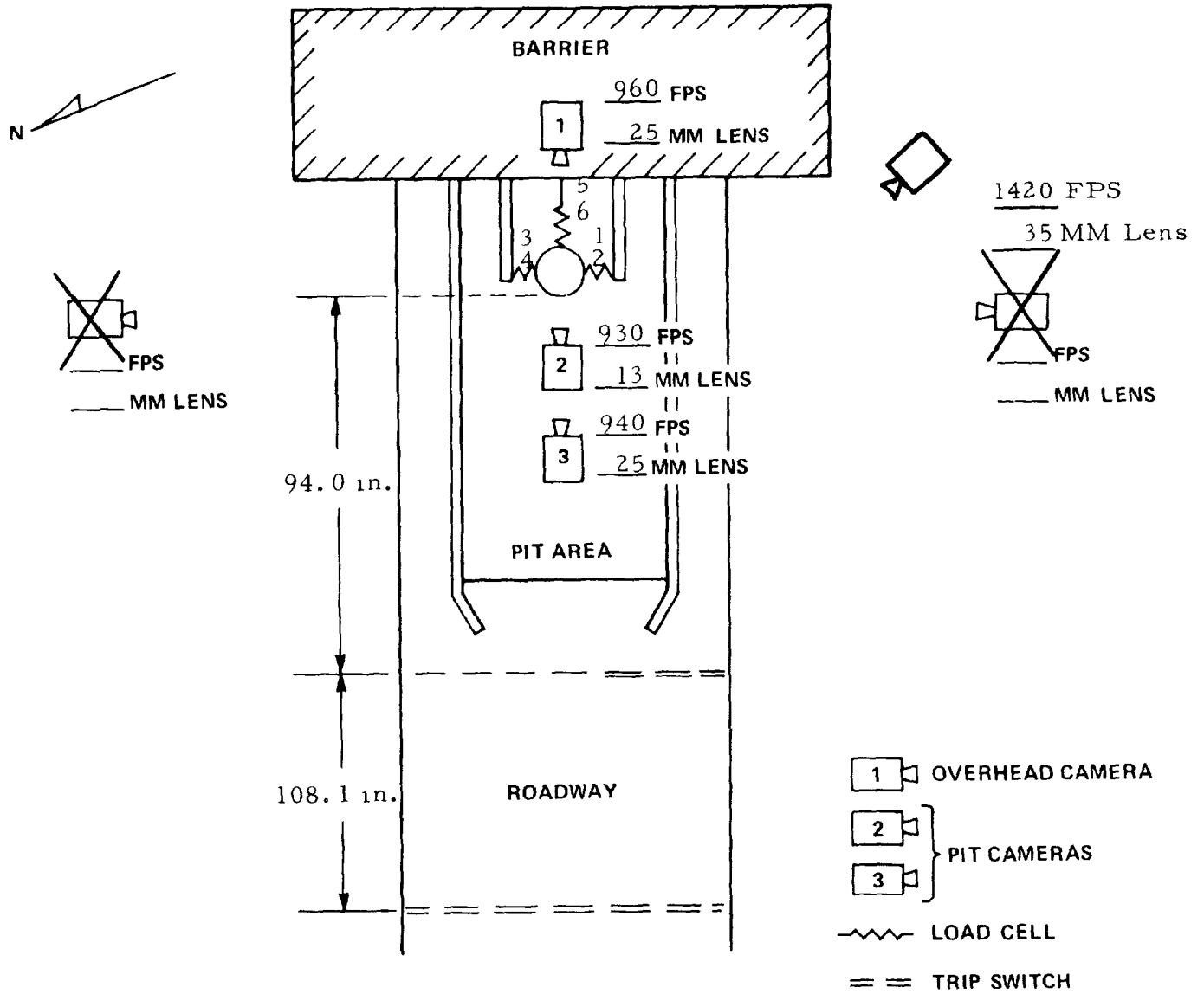
1. The vertical I-beam support behind the "B" post (on impact side) yielded inward 7 inches and was rotated approximately 90 degrees.
2. The horizontal I-beam reinforcement behind the door was pivoted inward about its forward connection and bent slightly.
3. The bowed roof reinforcements did not appear to have yielded.
4. The forward and aft knee braces between the modified side rails under the floorpan yielded slightly.
5. The left side vertical I-beam support at the "B" pillar did not appear bent.

* MOST ACCURATE MEASURE OF VEHICLE VELOCITY

** INCLUDES REBOUND VELOCITY

TEST SITE LOCATION OF SENSORS AND CAMERAS

TEST VEHICLE Mod. 3A(1)

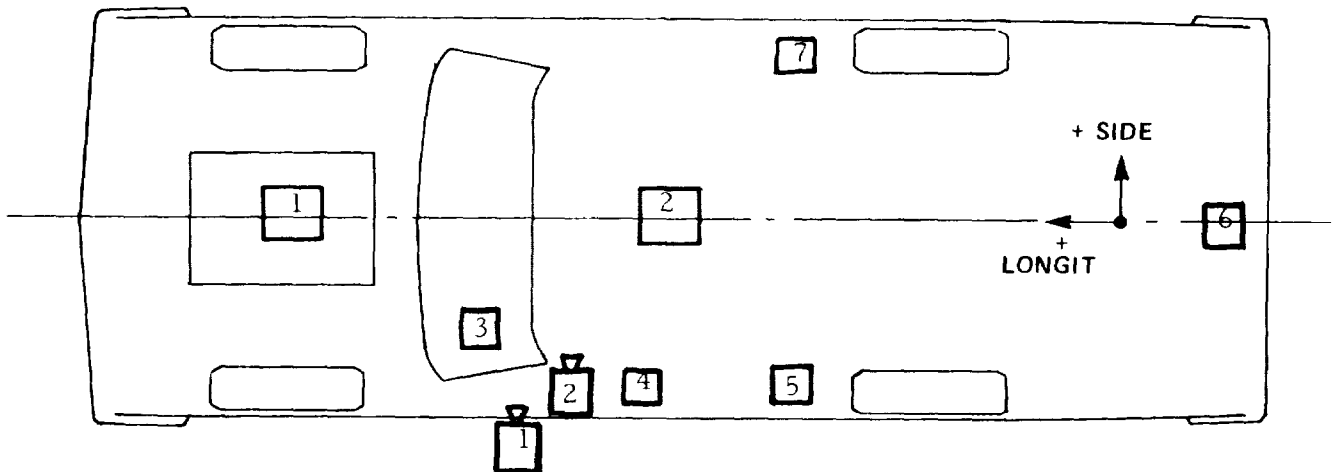
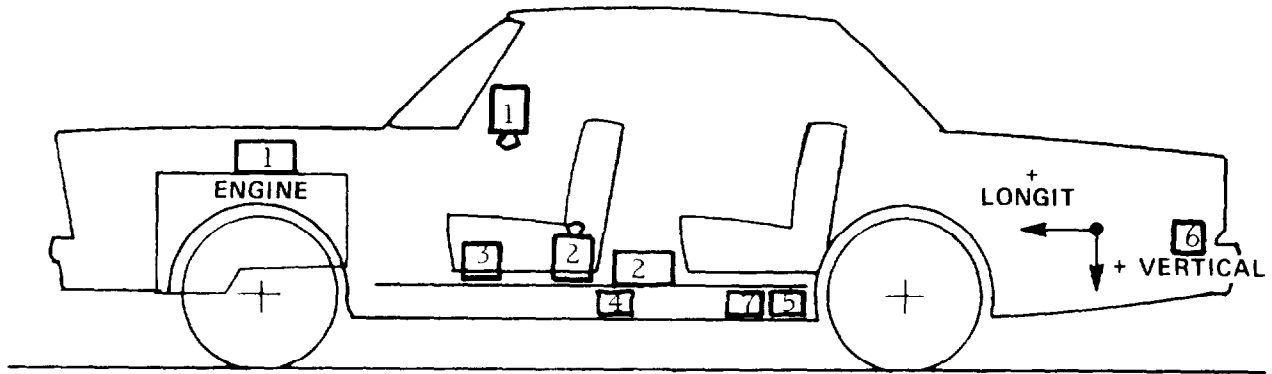
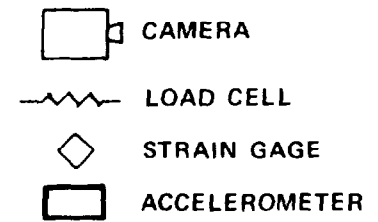


REMARKS

1. Camera coverage was not obtained from the north and south sides.
2. Load cells Nos. 3, 5 and 1 were at the top of the pole.
3. Camera coverage from the four stationary cameras was excellent.

VEHICLE MOUNTED SENSORS

TEST VEHICLE Mod. 3A(1)



REMARKS

1. No. 1 accelerometer on engine was oriented along the side axis only.
2. No. 2 accelerometer in compartment was oriented along the side axis only.
3. No. 3 accelerometer was mounted under left front seat.
4. No. 4 accelerometer was mounted on the left side frame, near "B" post.
5. No. 5 accelerometer was mounted on the left side frame, slightly aft.
6. No. 6 accelerometer was mounted on the rear frame.
7. No. 7 accelerometer was mounted on the right side frame, slightly aft.
8. No. 1 camera viewed the reinforcing structure behind the impacted door.
9. No. 2 camera viewed the overhead reinforcing tubes.
10. Both front and rear passenger seats were removed.

VEHICLE IMPACT TEST ~ DATA SUMMARY

VEHICLE TESTED Mod. 3A(2), Modified 1966 Ford Sedan, DATE 8-28-69

NOMINAL TEST CONDITIONS 20 mph, 90° Side Pole Impact

VEHICLE WEIGHT 3876 LBS CAL TEST NO 20

MEASURED VEHICLE IMPACT VELOCITY (MPH)

ROAD TRIP SWITCHES 20.5 ±0.5 *

FILM DATA 21, REBOUND 3

COMPARTMENT ACCELEROMETERS 30 **

MEASURED VEHICLE IMPACT ANGLE 90 DEGREE

IMPACT POINT ON VEHICLE Right Front Door, 1 Inch Aft of Door Center

TOW ROAD CONDITIONS Dry, Very Good

AMBIENT TEMPERATURE 79 °F

CHANNELS RECORDED ON FM TAPE Side Accelerations From the Following Sensors:
Left Side Rail Fwd., Left Side Rail Aft, Driver's Seat, Right Side Rail Aft,
Pass. Compartment, and Engine.

POST TEST VISUAL INSPECTION

FINAL REBOUND DISTANCE 43. INCHES

FINAL CRUSH DISTANCE 15. INCHES

REMARKS

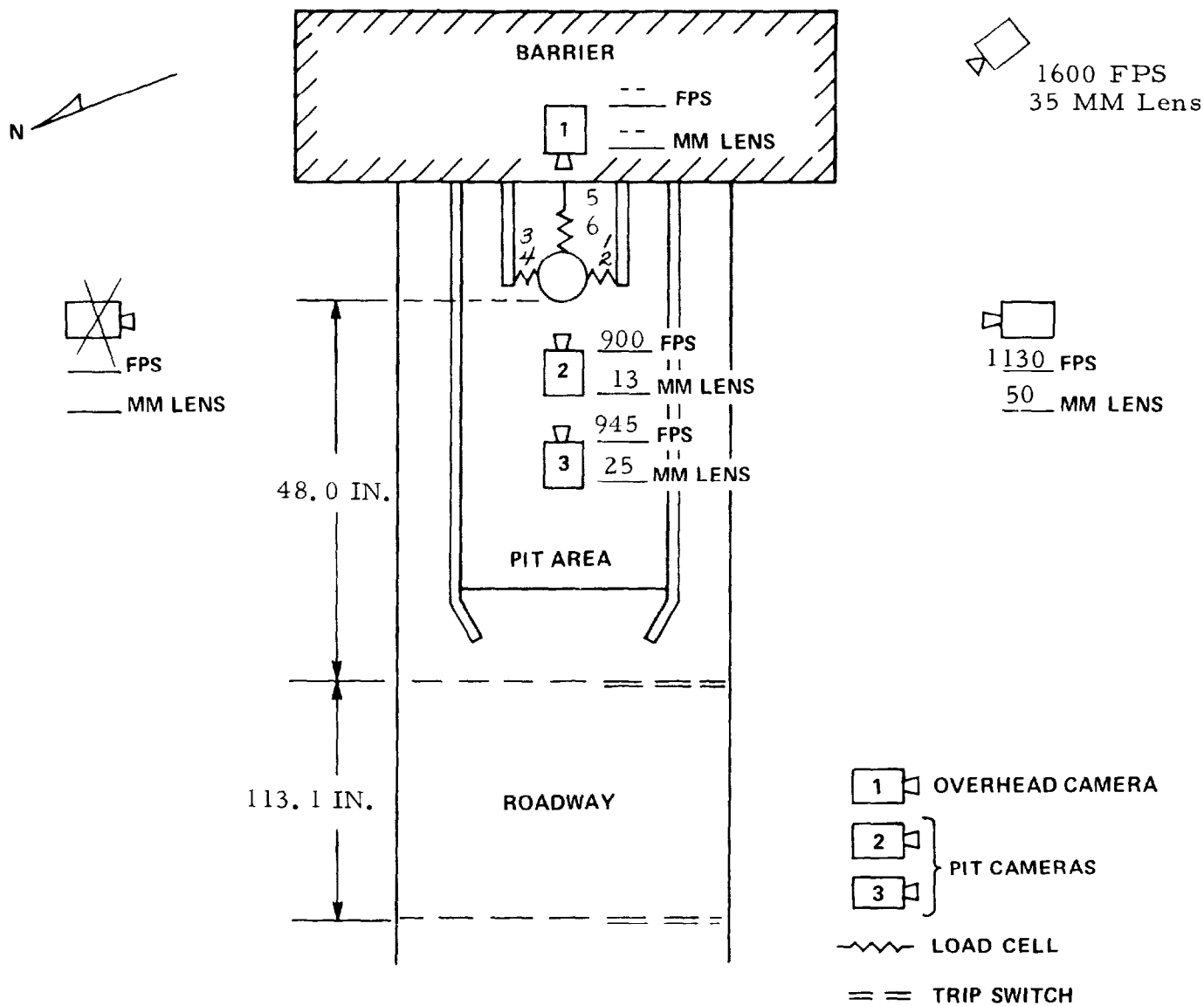
1. The rebounding vehicle was stopped by the modified frame underneath contacting the towing rail.
2. The 3 x 3 vertical box beam support behind the "B" post (On Impact Side) yielded inward - good plastic hinge at center.
3. The horizontal 4 inch "I" section behind the door yielded slightly between the door and dash panel.
4. The forward and aft knee braces between the modified side rails under the floorpan yielded slightly.
5. The left side modified "B" pillar did not appear bent.
6. The bowed structure inside of the roof, connecting the side "B" pillars, did not appear bent.

* MOST ACCURATE MEASURE OF VEHICLE VELOCITY

** INCLUDES REBOUND VELOCITY

TEST SITE LOCATION OF SENSORS AND CAMERAS

TEST VEHICLE Mod. 3A(2)

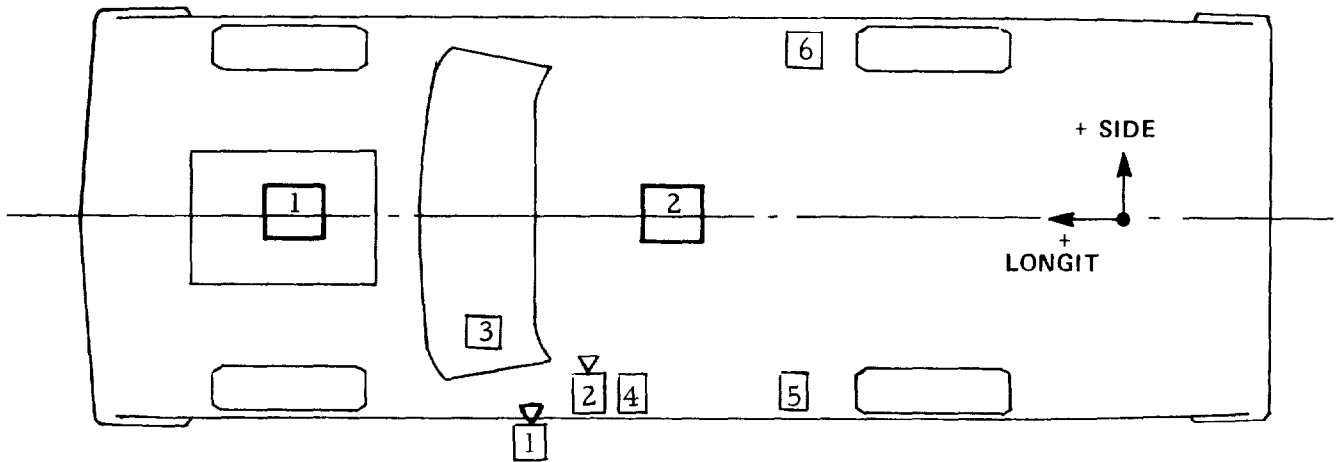
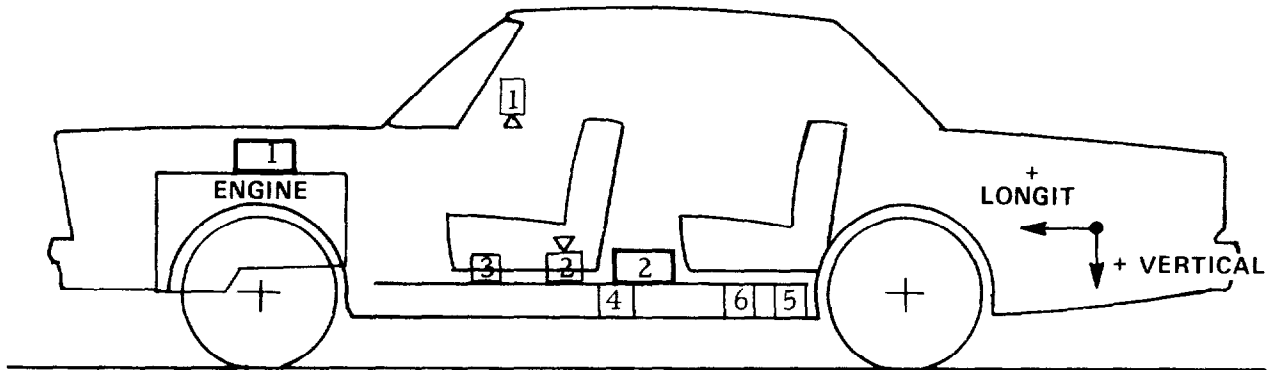
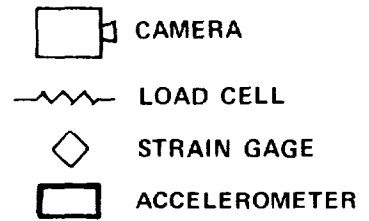


REMARKS

1. The overhead camera film contained no timing pulses, so it could not be used.
2. Load cells Nos. 3, 5 and 1 were at the top of the pole.
3. Camera coverage was not obtained from the north side.

VEHICLE MOUNTED SENSORS

TEST VEHICLE Mod. 3A(2)



REMARKS

1. Camera No. 1 viewed the reinforcing structure behind the impacted door. Frame rate - approx. 600 fps.
2. Camera No. 2 viewed the overhead reinforcing tubes.
3. No. 1 accelerometer on engine was oriented along the side axis only.
4. No. 2 accelerometer in compartment was oriented along the side axis only.
5. No. 3 accelerometer was mounted under left front seat.
6. No. 4 accelerometer was mounted on left side frame near "B" post.
7. No. 5 accelerometer was mounted on left side frame, slight aft.
8. No. 6 accelerometer was mounted on right side frame, slightly aft.
9. Both front and rear passenger seats were removed.